UNIVERSITY OF MICHIGAN
ENGINEERING RESEARCH INSTITUTE
ELECTRONIC DEFENSE GROUP

ERRATA
Technical Report No. 64
(2262-113-T)

Page 16 Last line - Change "M_y/H_s" to "M_x/H_x".

Page 34 Line 2 - Change "$M_y \simeq M_z$" to "$M_z \simeq M_s$"

Page 37 Table 3, line 1 - Change "$\int \frac{d\Omega}{d\pi}$" to "$\int \frac{d\Omega}{4\pi}$".

Page 37 Table 3, line 2 - Change "$\int \frac{d\Omega}{d\pi}$" to "$\int \frac{d\Omega}{4\pi}$".

Page 52 Line 7 - At end of line 7 add " X ".

Page 97 Paragraph 2, line 7 - At end of line 7, add""extremum of Eq. D-3".

Page 108 Eq. D-6 and in expression for N_γ and f_γ, for "--- $\sum_{nm} N_\gamma BA_\theta \frac{\partial(\Delta\theta_n)^2}{\partial N_\gamma}$"
read " --- $\sum_{nm} BA_\theta (\Delta\theta_\gamma)^2$ (four places).

Page 116 Eq. F-3, Matrix of C - Change lower right hand element from "0" to "1".

Page 116 Eq. F-8, matrix of $(CC')^{-1}$ - Change lower right hand element from "0" to "1".

ENGINEERING RESEARCH INSTITUTE
UNIVERSITY OF MICHIGAN
ANN ARBOR

REVERSIBLE SUSCEPTIBILITY IN FERROMAGNETS

Technical Report No. 64
Electronic Defense Group
Department of Electrical Engineering

by
Dale M. Grimes

Approved by: H. W. Welch, Jr.

Project 2262

TASK ORDER NO. EDG-6
CONTRACT NO. DA-36-039 sc-63203
SIGNAL CORPS, DEPARTMENT OF THE ARMY
DEPARTMENT OF ARMY PROJECT NO. 3-99-04-042
SIGNAL CORPS PROJECT NO. 194B

Submitted in partial fulfillment of the requirements for the
Degree of Doctor of Philosophy in the University of Michigan

April 1956

TABLE OF CONTENTS

LIST OF TABLES

LIST OF ILLUSTRATIONS

ACKNOWLEDGMENTS

Many people have aided the author during the course of both theoretical and experimental investigations described in this thesis. Mr. Ralph Olson assisted in setting up the experimental apparatus, in recording data, in calculating the finished data, and in drawing up the final graphs. Mr. D. W. Martin was instrumental in setting up much of the early experimental apparatus and in helping to establish some of the earlier techniques. He also aided in the formulation of Appendix C. Mr. P. E. Nace was an invaluable aid in criticizing the ideas presented and in proofreading the manuscript. Professor E. Katz and Dr. L. W. Orr assisted during the early stages of the work. Professor H. W. Welch, Jr., was a continuing source of aid and encouragement.

In addition, the author would like to thank each member of his doctoral committee for their helpful comments.

ABSTRACT

The purpose of this study is to investigate theoretically the variation of the low-frequency reversible susceptibility exhibited by a ferromagnet as a function of the internal magnetization level for small alternating fields both parallel with and normal to a static magnetic biasing field assuming firstly that the susceptibility has its origin in domain-wall motion and secondly that it has its origin in domain rotation. An understanding of this variation is of interest for the insight gained into the methods of magnetization processes as well as for the design of variable-inductance magnetic-core devices. Experimental data are reported and compared with the results of the theory.

To calculate these susceptibilities, a distribution function $f(\theta)d\theta$ equal to the fraction of all atomic magnetic moments in the system of interest which makes an angle between θ and $\theta + d\theta$ with respect to the applied biasing field must be known. This involves an effective "history" field which cannot be known. However, such an expression can be developed in terms of a totallized magnetic field equal to the sum of the biasing, demagnetizing and history fields. The inherent assumptions are that the material is polycrystalline and nonoriented, that each atomic magnetic moment is oriented along some "easy" crystallographic direction, that the localized demagnetizing fields act to randomize the particular "easy" direction occupied, and that each cation possesses a magnetostatic energy proportional to the cosine of the angle between its moment and the field direction.

On the basis of the above assumptions, an expression for the magnetization M is derived in terms of the totallized magnetic field H. This is done for magnetization along the [100] and the [111] directions and for isotropy. These correspond respectively to a total of six, eight and an infinite number of easy crystallographic directions.

For the case of parallel fields and magnetization by wall motion, the reversible susceptibility is assumed to be the derivative of the magnetization with respect to the totallized field. For transverse fields and magnetization by wall motion the reversible susceptibility is derived by assuming that the total magnetic field and the moment of the polycrystalline specimen are always aligned.

For the case of magnetization by domain rotation, it is assumed that the Landau-Lifshitz differential equation is applicable to each crystallite. The susceptibility parallel or transverse to the field is calculated by setting the proper component of the alternating field equal to zero.

The unknown totallized field can be eliminated between the susceptibilities and the magnetization since all are functions of $f(\theta)d\theta$.

Experimental data, which are reported for three ferrite specimens, are found to lie between the expected theoretical curves for the different magnetization types. The expected curves for the cases of domain-wall movement and domain rotation are sufficiently different to allow an approximate experimental separation of the contribution to the susceptibility from each type.

It is concluded that the theory here presented gives rise to a new technique for the separation of the contribution to the measured susceptibility from each mechanism. Using this technique, it was found that the relative importance of the two mechanisms depends upon the ferrite composition.

REVERSIBLE SUSCEPTIBILITY IN FERROMAGNETS

1. SCOPE OF PAPER

This paper is concerned with the reversible susceptibility as measured on material which possesses a permanent magnetic moment in the absence of an external magnetic field. The variation of the low-frequency reversible susceptibility exhibited by such ferromagnetic materials as a function of the internal biasing level for small alternating fields both parallel with and normal to a static magnetic biasing field is developed on a theoretical basis. This knowledge is useful to the engineer so that he can adequately consider it when designing a variable inductance and to the physicist so that he can obtain a better understanding of the processes by which the moment of a magnet is altered.

Experimental data were taken to check the theory. It is concluded that the theory represents a useful approximation to the true state inside a ferromagnet. The calculation of the precise state would require methods presently unavailable.

Although the theory is considered applicable to all ferromagnetic materials, the experimental work here reported was carried out using the ferromagnetic oxides commonly called ferrites. The theoretical calculations were carried out only for cubic and for isotropic symmetries.

A total of thirteen ferrites, representing what was believed to be widely different values of the usual magnetic parameters of magnetostriction and anisotropy, were measured. Of the thirteen a total of three with

quite different resulting susceptibility-magnetization curves were chosen for a detailed study. The results obtained using the final three specimens are included in this paper.

The theory was developed assuming firstly that the susceptibility had its origin in domain-wall movement and secondly that the susceptibility had its origin in domain rotation. The difference between the two types of behavior is large enough to allow an approximate experimental determination of the relative contribution to the susceptibility from each mechanism.

2. MAGNETIC PROPERTIES OF MATERIALS. INTRODUCTORY REMARKS

The theory of magnetic materials is intimately connected with the atomic theory. A result of the Pauli exclusion principle, when applied to atoms in a gas, is that no two of the electrons surrounding any nucleus can have the same quantum numbers. In other words, if any two electrons possess the same orbital quantum numbers about the same nucleus they must have their spin moments oriented in opposite directions. If, solely for simplicity, we assume that the ultimate source of the magnetic moment lies with the electron spin itself rather than any orbital motion of the electrons, and if we also assume that all electrons occupy the lowest possible orbital energy state, then a nucleus surrounded by an even number of electrons in an S state[5] carries no magnetic moment as a result of unbalanced spins; that is, for every spin moment oriented in one direction there is an equal one oriented in the opposite direction. For an odd number of electrons there must be a net unbalanced magnetic moment.[1,2]

When a magnetic field H is applied to a material whose net atomic spin magnetic moment is zero, the time-rate of change of the magnetic field sets up an electromotive force. This force in turn sets up an atomic current which can be considered from either a classical or a quantum-mechanical point of view.[1,2,5] From the point of view of classical theory it can be considered as an adjustment of the electronic orbitals. From the quantum-mechanical point of view it can be considered as a shifting of the elec-

tronic energy levels.[1,2] This current, according to Lenz's law, creates an effective magnetic field directed in the opposite sense to the H. This field, which originates with the material, can be considered in terms of a magnetic moment per unit volume to which it is numerically equal. The moment per unit volume is defined to be the magnetization M. Since no resistance exists on the atomic scale the "currents" continue indefinitely. Since the magnetization and the applied field are oppositely directed, the susceptibility, which is defined to be the ratio, is negative. Material with a negative susceptibility is defined to be diamagnetic.

Let us now consider a material in the gaseous state in which each nucleus is surrounded by a cloud of electrons with a net spin unbalance. Materials with an odd number of electrons are automatically included. As in the case of diamagnetic material, from the Lenz' law concept there appears a negative susceptibility. However, the unbalanced magnetic moments will tend to align themselves with the applied field and will produce a magnetization in the same direction as the applied field. Since this magnetization is larger than the diamagnetic magnetization and is aligned with the field, materials with a net unbalanced moment possess a positive susceptibility. Gaseous materials with a small positive susceptibility are defined to be paramagnetic.

For many elements, the entrance into a chemical compound alters the electronic structure of the atom to be more nearly that of the noble gases. They therefore carry a small or zero net unbalanced moment. However, certain elements have unfilled inner shells which carry an unbalanced magnetic moment and which enter only weakly into the chemical binding. The elements of the most interest here fall into three groups: those with partially filled 3d shells; those with partially filled 4f shells; and those with partially filled 5f shells. Some metals for which the interaction

between moments, defined as spin-spin interactions, are known to be important are chromium[39], manganese[39], iron, nickel, cobalt, gadolinium[38], and dysprosium.[40]

Solids containing these elements exhibit, at elevated temperatures, magnetic properties very similar to those of a gaseous paramagnet. As these solids are cooled, many will undergo magnetic transitions of some sort. Many oxides exhibit, below the transition temperature, a susceptibility which decreases with decreasing temperature[3] in contradiction to the accepted theory of paramagnetic behavior. For the metals iron, cobalt and nickel, the room-temperature susceptibility is many orders of magnitude larger than for paramagnets.[4] Many complex iron-oxide compounds (the ferrites) also possess very large room-temperature susceptibilities.

It is not possible even approximately to predict these behaviors on the basis of classical electromagnetic field theory alone. It is possible to explain them qualitatively from the quantum theory. The overlapping wave functions of the different atoms give rise to an exchange energy. This exchange energy, which provides the covalent binding of solids, also acts to create an interaction between magnetic moments.

The result of this energy is that, for example, in metallic manganese and iron the net unbalanced moment of each atom feels an effective magnetic field which originates at least predominantly with the unbalanced spins of nearest-neighbor atoms. This effective field is commonly called the exchange field[2] and for the case of iron acts to align the spins of nearest-neighbor atoms parallel with each other. In the case of manganese the exchange field attempts to order the spins of nearest-neighbor atoms antiparallel with each other. The former case is defined to be ferromagnetism, the latter antiferromagnetism. The effective exchange field is, at least in most instances, very large compared with the field pro-

duced by any available laboratory magnet. It is so large that any increase in the magnetic moment on the atomic scale because of an applied field can be ignored. Since the magnetic energy per gram atom is given by $\mu_o \vec{M} \cdot \vec{H}$ and the thermal energy by $\frac{3}{2}RT$, where R is the gas constant, and since the magnetic ordering will cease for $\frac{3}{2}RT \approx \mu_o HM$, an approximate measure of the effective exchange field can be obtained by determining the temperature at which the ordering disappears. This temperature is defined as the Curie temperature. It is found that for the case of iron the exchange field is of the order[6] of 10^8 ampere-turns per meter.

An array of parallel spins in two dimensions is depicted in Fig. 1. Each A is surrounded by nearest-neighbor B's and vice versa. Fig. 1 also represents the case of a two-dimensional antiferromagnet. The direction of the arrows indicate the direction of the atomic moment. Note that all A's are oriented in one direction, all B's in the opposite direction. Just as in this two-dimensional case an antiferromagnet can be broken into sets of interpenetrating sublattices. Each sublattice contains parallel spins but the spins of the different sublattices are oriented antiparallel. Note that if the net spin on A were different from that on B a resultant net M would exist. Also if the symmetry were such that there were more B-sites than A-sites a net unbalanced moment would exist. The latter case exists and is the usual explanation of the spontaneous moment of the ferrites.[7]

To find the configuration of the moments for the case of the ferromagnets, it is necessary to minimize the sum of all energies in the system.[6] These energies are the magnetostatic energy, the anisotropy energy, the magnetostrictive energy and the exchange energy. A more precise treatment of these effects is left to appendices A and D. Qualita-

tively, it can be seen that the magnetostatic energy acts to decrease the net moment, the exchange energy acts to align all moments, and the anisotropy energy acts to keep all material aligned along certain preferred crystallographic directions.

The result of these effects is that certain volumes of the material have their moments aligned parallel with each other by the exchange field. A volume so oriented is defined to be a domain. Each domain, in the absence of any macroscopic magnetic field, is very nearly aligned along some crystallographic "easy" direction. The boundaries between domains are defined to be domain walls. For cubic symmetry, and if the easy direction is the [100] direction, 90 and 180 degree walls are possible. (See Fig. 2).

An applied field must be considered small when added to the exchange field. Thus, no net change in local moment can be expected when the field is applied. However, the magnetostatic energy will be altered in such a way as to demand that the net number of moments oriented favorably with respect to the applied field increase at the expense of those not so favorably oriented.

This magnetostatic-energy alteration can be accomplished as well as the requirement of minimization of the sum of exchange and anisotropy energies by assuming that the domain walls move in such a manner as to increase the volumes of domains oriented favorably with respect to the applied field.[8] (See Fig. 3). It is also possible that the moments of the domains rotate[9] against the anisotropy torque to become more nearly aligned with the field. (See Fig. 3). It is not possible <u>a priori</u> to predict the most likely mechanism by which the moment will change. However, if the easy direction is the [111] direction and if only easy direc-

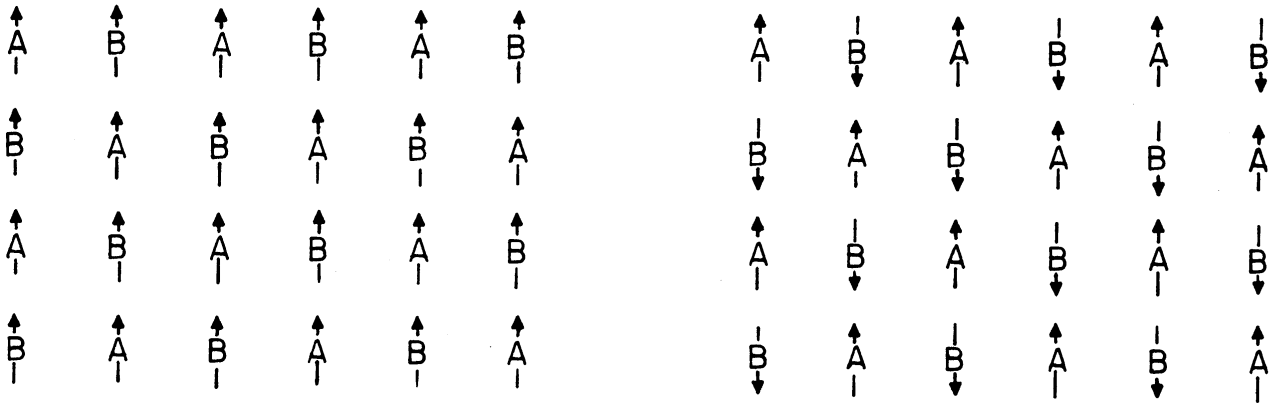

FIG 1. MAGNETIC ORDERING.

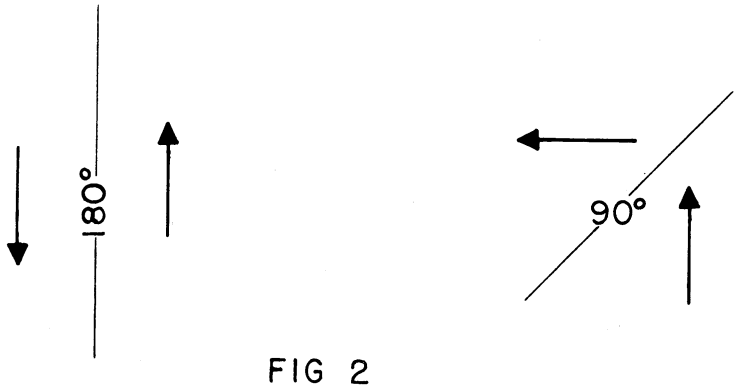

FIG 2

POSSIBLE SINGLE CRYSTAL DOMAIN WALL CONFIGURATIONS.
[100] CUBIC SYMMETRY.

tions are occupied the largest possible macroscopic M would be, for a nonoriented polycrystal, 0.867 M_s, where M_s is the value of the spontaneous moment.

The usual experimental result for the variation of the moment of a polycrystalline material as a function of applied field is shown in Fig. 4. A material which has not been subjected to an applied field after being cooled from above its Curie temperature would occupy the point J. When a field is applied the virgin curve JC is traced. When the field is subsequently reduced to zero the material retains a value of magnetization M_r as shown at the point E. To reduce the magnetization level to zero again it is necessary to apply a field $-H_c$ to the specimen. The value M_r is defined as the remanence and the field H_c as the coercive force. The value of magnetization at the point C is the saturation or spontaneous moment. The loop CEGAC is known as the hysteresis loop. The slope of the M-H curve at the point J, starting from the virgin material, is known as the initial susceptibility. Consider, in traversing the loop, the applied field, H_{ap}, to be stopped at such a time that the material occupies the position B. If H_{ap} is slightly decreased the top curve BI is traced. If H_{ap} is then returned to its original value, the lower curve from I toward B will be traversed for the small-signal case. For a given ΔH_{ap}, the slope of a straight line drawn through the points B and I is known as the incremental susceptibility. The limiting value of the incremental susceptibility as ΔH_{ap} goes to zero is defined to be the reversible susceptibility.

A major unsolved problem of ferromagnetism is the precise description of Fig. 4 in terms of a mathematical theory. The magnetization cannot be given as a unique function of H_{ap} alone and is indeed an infinite-valued function of H_{ap} depending upon the history of the material.

FIG. 3

ILLUSTRATION OF POSSIBLE MAGNETIZATION MECHANISMS

FIG. 4

AN ILLUSTRATIVE M-H LOOP

If the magnetization is changed by domain-wall movement the derivation of such a history-dependent function would require as many coupled differential equations as domain walls. The situation is no better for the variation of the magnetic moment by the rotation of the moment of entire domains.

Since a direct analytical approach seems impractical, some type of statistical method seems demanded if such a function is to be derived.

For convenience in making this discussion more quantitative, consider an infinite cylinder of nonoriented polycrystalline material. The radius of the cylinder may or may not also be infinite. Consider an external field H_{ap} to be applied along the length of the cylinder. The resulting equation

$$M = M_s \frac{\int_0^{\pi} f(\theta) \sin\theta \cos\theta \, d\theta}{\int_0^{\pi} f(\theta) \sin\theta \, d\theta} \qquad (1)$$

now describes the magnetization if $f(\theta)\, d\theta$ is a distribution function equal to the number of atoms whose magnetic moment is oriented at an angle between θ and $\theta + d\theta$ with respect to the applied field. M_s is the maximum value of magnetization. The M-H loop and its ramifications, such as the reversible susceptibility, can be calculated from Eq. 1 if $f(\theta)\, d\theta$ is known as a function of the field H_{ap} and the history of the material. Although the problem is now no closer to being solved than without Eq. 1 it has been reformulated to a question of the determination of a distribution function.

This distribution function can be easily calculated for the case of a paramagnetic gas in thermal equilibrium.[1] However, this in-

volves a system of smallest units which are maintaining equilibrium by continually exchanging energy. For the usual statistical mechanical system, the time average of any quantity for any system in an ensemble is the same as the ensemble average over the systems at a given time.[10] This is based upon the so-called "ergodic" argument. In the case of the ferromagnet the thermal disorder effect upon the domains is considered small enough to be negligible. The thermal effect is considered to affect the magnetic parameters such as M_s, the anisotropy coefficients and the magnetostriction but not the disordering of the domains. The disorder must be considered to arise from the presence of localized strains or magnetic poles in the material. Each atomic moment is not continually exchanging energy but rather occupies some metastable minimum energy in the presence of random but fixed forces which vary throughout the material. Any attempt to consider this problem must consider a "snapshot" of the material and the resulting properties computed as an average over the system rather than a time average of the system as it goes through all possible configurations.

Each atomic magnetic moment, then, sits in some metastable position; the particular position depends upon the history of the material[12] and may exist because of nucleation energies[37] or because of wall "snags"[32]. These positions depend upon the positions occupied by neighboring spins. Therefore the energy of each atomic moment is not necessarily independent of the spatial coordinates.

The result is a history dependence of the function $f(\theta)\, d\theta$ that is not present when a thermal disorder is considered. This dependence upon history is responsible for the hysteresis and is not at all negligible, as is obvious from Fig. 4.

3. THE ORIGIN AND FREQUENCY DEPENDENCE OF THE INITIAL SUSCEPTIBILITY

3.1 The Initial Susceptibility

As mentioned in Chapter 2, the spontaneous moment of the ferrites exists as the difference of two oppositely oriented moments. The spontaneous moment of the ferromagnetic metals exists with all moments oriented in parallel. It will be assumed throughout the rest of this paper that the equations for ferrimagnetism in terms of the measured parameters are the same as the equations for ferromagnetism. This is to be assumed even though it has been amply demonstrated that a real difference between the two cases exists in many properties, such as* the g-values[13], and the variation of the susceptibility with temperature in the paramagnetic region.[7]

It was also mentioned in Chapter 2 that there are two possible mechanisms by which the magnetization can be altered in the presence of a magnetic field many orders of magnitude smaller than the exchange field. These mechanisms were seen to be (1) the movement of the boundary between regions of material whose magnetic moments are oriented in different directions, and (2) the rotation of domains as a whole to more nearly align themselves with the applied field. In addition the change in magnetization can be regarded as consisting of the sum of both reversible and irreversible effects[14] of either type. Once initiated, irreversible movements are no longer controllable and go to completion at a

---

* For a definition of the g factor see reference 39, p. 143.

certain minimum rate while dissipating some finite amount of energy. The reversible processes, if carried out sufficiently slowly, are reversible not only in the sense of continued oscillation about the same equilibrium point but also in the thermodynamic sense of no energy dissipation for sufficiently slow movements. At a finite frequency the energy dissipation is nonzero, but the reversibility in the sense of magnetic movements about the same equilibrium point remains and the process is still controllable by the applied field.

In addition to the magnitude of the reversible susceptibility, the loss factor, or its inverse, the magnetic Q, is of interest as well as the variation of both as a function of the gross magnetization level for each of the two different sources of reversible magnetization.

It is obvious that an additional field ΔH_{ap} could be applied at an arbitrary angle with respect to the gross applied field H_{ap}, which is here defined to be the biasing field. With superposition assumed, the resulting susceptibility is a linear combination of the susceptibility parallel with and normal to the biasing field. It is therefore of interest to investigate each of the above mentioned factors both parallel with and normal to the biasing field.

3.2 Susceptibility Due to Domain Rotation

A direct consequence of the application of Newton's law to rotating systems is that the time rate of change of angular momentum is equal to the applied torque; furthermore L, the angular momentum per unit volume, is related to M, the magnetic moment per unit volume, by the magneto-mechanical factor γ, i.e., $M = \gamma L$. This equation is the sum of similar equations valid for the individual electrons. γ can be calculated in terms of fundamental atomic constants for magnetization by elec-

tron spin. It is given by $\frac{ge}{2m}$ where $\mu_o\gamma$ is equal to 221 $\frac{\text{kilocycle meter}}{\text{ampere second}}$ for g = 2. Now the total torque per domain must equal the sum of the torques for each electronic moment; thus for a rotating magnetic moment,

$$\frac{\partial M}{\partial t} = \gamma\mu_o \left[M \times H'\right] . \qquad (2)$$

H' is the sum of all fields affecting the domain.

It is to be noted that this equation contains no damping term. If it were literally true, a domain once set in motion by the application of an external field would oscillate forever. This cannot represent a physical situation, as was recognized and corrected by Landau and Lifshitz[9] who introduced an additional term perpendicular both to the moment M and to the direction-of-motion vector (M X H'). This phenomenological term can be written as $-\frac{\lambda}{M_s^2}\mu_o \left[M \times (M \times H')\right]$. The M_s^2 in the denominator is entered to require the constant term λ to be independent of the spontaneous moment.

With the addition of the damping term, the differential equation is

$$\frac{\partial M}{\partial t} = \gamma\mu_o(M \times H') - \frac{\lambda}{M_s^2}\mu_o \left[M \times (M \times H')\right] . \qquad (3)$$

Let it be assumed that the material has its spontaneous moment oriented in the z-direction, and let the applied ΔH be given by

$$H_\Delta = H_\Delta \cos\theta_o z + H_\Delta \sin\theta_o x = H_z \hat{z} + H_x \hat{x}$$

where $\hat{z}$ and $\hat{x}$ represent unit vectors in the z-and x-direction respectively; then to first order the resulting susceptibility as measured by M_x/H_s is given by

$$\chi_r = \frac{M_s \sin \theta_o}{H'} \quad , \tag{4}$$

where H' is the effective magnetic field consisting of the sum of all internal and applied fields. For the demagnetized case the applied field is zero so that H' represents the effective internal field.

Now calculate the value of the initial susceptibility in terms of the magnetic parameters, and set this result equal to Eq. 4 with a zero applied field to obtain an approximate expression for H'. The procedure is to consider the energy of the system in the presence of a small signal, assuming the rotational mechanism, and solve for the equilibrium condition. Consider the total energy of the system to consist of two terms, one due to the magnetostatic energy and the other due to the anisotropy energy U_{an}.[15] Then

$$U = U_{an} - M_s H' \cos (\theta_o - \theta) \ .$$

Taking variations with respect to θ gives

$$\frac{dU}{d\theta} = 0 = \frac{dU_{an}}{d\theta} - M_s H' \sin (\theta_o - \theta) \ . \tag{5}$$

Thus it follows that

$$H' = \frac{dU_{an}/d\theta}{M_s \sin (\theta_o - \theta)} \quad \text{and} \quad M = M_s \cos (\theta_o - \theta).$$

For ease in calculations assume the domains to be initially oriented in the [001] direction and to turn in the xz-plane. Therefore the anisotropy energy, which can be written as (See Appendix A)

$$U_{an} = K_1 (\ell_x^2 \ell_y^2 + \ell_y^2 \ell_z^2 + \ell_z^2 \ell_x^2) \tag{6}$$

where the ℓ_x represents the direction cosine of the magnetic moment to the x-axis, becomes

$$U_{an} = K_1 \sin^2 \theta \cos^2 \theta = \frac{K_1}{8} (1 - \cos 4\theta)$$

$$\frac{dU_{an}}{d\theta} = (K_1/2) \sin 4\theta.$$

Solving for H' gives

$$H' = \frac{K_1 \sin 4\theta}{2M_s \sin (\theta_o - \theta)} .$$

Finally solving for χ_o^r gives

$$\chi_o^r = \left.\frac{dM}{dH'}\right]_{\theta=0} = \left.\frac{\frac{dM}{d\theta}}{\frac{dH'}{d\theta}}\right]_{\theta=0} = \frac{M_s^2 \sin^2 \theta_o}{2K_1} \qquad (7)$$

It is also through this mechanism that the magnetostriction and the elastic constants would enter, since they act to build up an effective anisotropy of the form[6]

$$\Delta K_1 = 9/4 \left[(c_{11} - c_{12})\lambda_{100}^2 - 2c_{44} \lambda_{111}^2\right] \qquad (8)$$

where the λ's represent the magnetostriction in the [100] and [111] direction respectively, and the c_{ij}'s represent the elastic moduli.

Eq. 4 gives the susceptibility resulting from the equation of motion, and Eq. 7 gives the same susceptibility based upon magnetic parameters.

Setting these two equations equal and solving for the effective anisotropy field H_{an}[16] gives

$$H_{an} = \frac{2K_1}{M_s \sin \theta_o} \qquad (9)$$

Eq. 3 then describes the motion of large groups of dipoles whose motion gives rise directly to an externally measurable susceptibility.

3.3 Susceptibility Due to Wall Motion

The development of a differential equation of motion describing the behavior of a domain wall arises from the application of Eq. 3 to the moments in a domain wall. The resulting equation can be written for a 180° wall as:[17,8,18] (See Appendix A).

$$m\ddot{x} + \beta\dot{x} + \alpha x = 2M_s H_z \qquad (10)$$

m is the effective mass of the domain wall;

β is the damping or dissipative term affecting the wall;

α represents the restoring force on the wall;

x is the direction in which the wall moves;

z is the direction of application of the field H_z.

It is to be noted that the magnetization increase, ΔM, resulting from the wall movement through a distance x is directly proportional to x and to M_s, or $2CxM_s = \Delta M$, where C is a constant with dimension $(\text{length})^{-1}$.

Eq. 10 is of the form of a Hooke's law equation with added damping and inertial terms. In well annealed and well formed material the restoring constant α can be considered to have its origin predominantly in internal strains which arose because of the magnetostrictive forces resulting from the presence of the spontaneous moment, absent when the material was annealed.[18] In imperfectly annealed or formed material, residual strains and local impurities must be considered as well as the

magnetostatic energy. For certain geometries the magnetostatic forces predominate.[19]

The β term can be derived directly from Eq. 3 by applying it to the motion of individual cations in the domain wall. The mass term is based upon increased exchange energy due to a distortion of the moving wall also described by Eq. 3. β is derived from the second term of Eq. 3 and m from the first term. The details of this procedure are carried out in Appendix A.

As for the case of rotational susceptibility, the initial susceptibility for wall motion can be derived in terms of the magnetic and elastic parameters of the system. Becker[20] assumed the internal strains to be sinusoidal in nature with a maximum amplitude of σ_i. For 90^o walls he obtained the expression for the susceptibility:

$$\chi_o^w = \frac{16}{3} \frac{M_s^2}{\lambda_{100}\sigma_i} .$$

If the only strains present are due to magnetostriction, then

$$\sigma_i = \lambda_s E$$

where

λ_s represents the saturation magnetostriction, and

E represents the Young modulus.

Substituting this into the equation for the initial susceptibility one obtains

$$\chi_o^w = \frac{8\pi M_s^2}{9 \lambda_s^2 E} \qquad (11)$$

as derived by Kersten.[18]

Solving for the initial susceptibility from Eq. 10, and remembering that $2CxM_s = \Delta M$ yields:

$$\chi_o^w = \frac{2\ CM_s^2}{\alpha} \quad \text{for } 90^o \text{ walls.}$$

Combining the two equations and solving for α leads to

$$\alpha = \frac{9\ EC\lambda_s^2}{4\pi} \tag{12}$$

In summary, the differential equation (3) describes the motion of the magnetic moment in the permanently magnetized system, even for the case of wall motion when applied to the spins in a domain wall. However, it is assumed that these wall moments contribute relatively little to the measured susceptibility. The source of the susceptibility is the movement of these spins in such a manner as to produce a movement of the boundary between regions magnetized in different directions. This motion is describable by an equation of the form of Eq. 10.

3.4 The Separation of the Magnetization Mechanisms

The experimental determination of one or the other magnetization mechanism is difficult because of the similarity of the results. Many attempts have been made to differentiate between them on the basis of the different frequency dependence of the two types.[21,22,23,24,25,27] The initial zero-frequency susceptibility is an easily measurable quantity of a ferromagnet. It is possible to combine this zero-frequency susceptibility and its frequency dependence in such a fashion that a factor dependent only upon M_s and other constants of the system results. For the case of magnetization by rotation and by highly damped wall motion

the product of the first power of the susceptibility and the frequency ω_a at which the imaginary portion of the susceptibility is a maximum gives:[21,23,26]

$$\text{Rotation} \quad \omega_a \chi_o^r = \frac{2\gamma\mu_o M_s}{3} \tag{13}$$

$$\text{Viscous Damped wall motion} \quad \omega_a \chi_o^w = \frac{4M_s{}^2 C\mu_o}{\beta} \tag{14}$$

(See Eqs. B6 and B13.)

For slightly damped wall motion, the product of $\omega_a{}^2 \chi_o$ gives

$$\text{Inertial damped wall motion} \quad \omega_a{}^2 \chi_o^w = \frac{4M_s{}^2 C\mu_o}{m} \tag{15}$$

(See Eq. B14)

It is apparent from the form of Eq. 13 that a plot of log ω_a versus log χ_o should yield, if M_s is varied, a straight line of unit slope. The same would also be true of Eq. 14 if M_s/β remained constant. A series of experiments have been carried out on nickel-zinc ferrite[21,26] for which a plot of log ω_a versus log χ_o yields a straight line of unit slope. This has been interpreted as a substantiation for the domain-rotation phenomena.

Domain arrangements should be sensitive to strain, as can be seen from Eq. 11. However, the initial susceptibility and peak frequency of the nickel-zinc ferrites are relatively insensitive to strain. This argument has been used to try to demonstrate rotation.[28] Rado has first measured the frequency spectrum of some ferrites, then pulverized them to a particle size which is presumed to be small enough so that only single domains could exist and then remeasured the frequency spectrum.

By doing this process the low-frequency dispersion was eliminated. He therefore concluded that the magnetization mechanism responsible for this dispersion was wall motion.[23,24] Unpublished work of Epstein shows that nickel-zinc ferrites which have a high density exhibit frequency characteristics expected from wall motion.

The situation is still not clear.

One of the objectives of the present paper is the development of a new technique for the determination of the magnetization mechanism and to use this technique on several different types of ferrites.

4. THEORY OF MAGNETIZATION CONSIDERING THE AVERAGING PROCESS OVER A POLYCRYSTAL

4.1 The Calculation of $f(\theta)\, d\theta$.

As mentioned in Chapter 2, the M-H loop and its ramifications can be quantitatively described if a function $f(\theta)\, d\theta$, equal to the number of magnetic ions which have their moments oriented at an angle between θ and $\theta + d\theta$ with respect to the applied magnetic field is known. The present problem is, in essence, two fold. The first part is the calculation of $f(\theta)$. The second is the calculation of the susceptibilities in terms of $f(\theta)$.

In an ordinary statistical mechanical problem the smallest units considered are assumed to be constantly exchanging energies with other similar particles in such a manner that the energy held by one unit is independent of the energy held by its momentary nearest neighbor. In such a problem the time average of the thermodynamic variables are taken equal to an ensemble average over many systems. If similar arguments are to be applied to a ferromagnet with the smallest unit considered to be the atoms furnishing the moment, only a system average can be considered since each atom must contain a random but fixed energy in the presence of a static magnetic field. For the ordinary system, say a gas, the thermodynamic quantities are calculated assuming that equilibrium exists when defined as a minimization of the free energy, i.e., when the most probable state exists. When a ferromagnetic material is considered this state certainly does not exist, as is made obvious by the presence of hysteresis with res-

pect to H_{ap}. The material must be considered to occupy some state of locally minimized free energy, thus a steady state. The particular steady state occupied must depend upon local potential minima in the form of wall "snags" or nucleation energies or both. Thus $f(\theta)$ must be a function both of the applied field H_{ap} and of the history of the material.[29] The problem can be handled if this history effect is considered as an effective field which acts in addition to the applied field. For this case the magnetization and the different susceptibilities can be calculated in terms of the total field, and then this total field eliminated between the susceptibilities and the magnetization. Appendix C considers the question in more detail. The following discussions assume such a relationship exists.

Many attempts to derive an expression for $f(\theta)$ have been made. Gans[36] lists his result and states that it is "not without foundation." Brown utilized Heisenberg's model of domains of fixed and equal volume and derived expressions for $f(\theta)$ as a function of anisotropy type.[11] He later derived the same expression for the case of no anisotropy with a model allowing wall movement.[29] Appendix D gives a derivation using the same mathematics as Brown, but using a model based upon the spins of individual atoms. This model makes it possible to take into account the anisotropies and wall motion. The result is that:

$$f(\theta)\, d\theta = \exp\,(AH_t \cos\theta)\, d\theta \qquad (16)$$

where θ is the angle between the magnetic moment of a given domain and H_{ap}, where A is a constant, and where H_t is H_{ap} plus any effective history field H_h and demagnetizing field -NM.

The magnetization M as a function of H_t results from substituting Eq. 16 into Eq. 1. The necessary symmetry conditions must be considered

depending upon the anisotropy type. The resulting equations for M/M_s for an anisotropy condition such that the easy directions are along [111] and [100] and a similar quantity for isotropic material are given in Table 1. The equations are derived in Appendix E.

Table 1. Magnetic Moment and Wall-Motion Susceptibility

Anisotropy Type	M/M_s	χ^w_{rp}/χ^w_o	χ^w_{rt}/χ^w_o
[100]	$G(\eta) = \frac{1}{4\pi}\int \frac{\sum \ell_i \sinh\eta\ell_i \, d\Omega}{\sum \cosh\eta\ell_i}$	$\frac{3\, dG(\eta)}{d\eta}$	$\frac{3\, G(\eta)}{\eta}$
[111]	$E(\eta) = \frac{3\sqrt{3}}{\eta^2}\int_0^{n/\sqrt{3}} u \tanh u \, du$	$\frac{3\, dE(\eta)}{d\eta}$	$\frac{3\, E(\eta)}{\eta}$
isotropic	$L(\eta) = \text{ctnh}\eta - \frac{1}{\eta}$	$\frac{3\, dL(\eta)}{d\eta}$	$\frac{3\, L(\eta)}{\eta}$

In addition to the assumptions going into the derivation of $f(\theta)\, d\theta$, for the case of the [111] and [100] orientations, it is assumed that all material in the system has its magnetic moment oriented along an easy direction.[11,12,30] The derivation of the susceptibilities from the magnetization assumes that none of the material deviates in direction from these easy directions, i.e., the effective anisotropy fields are infinite. This therefore implies magnetization by wall motion as opposed to magnetization by rotation for the small-signal susceptibility. The rotation of domains from one easy direction to another for the change in gross magnetization is not ruled out but presumably such a thing would not be possible for a vanishingly small applied signal.

The situation is a little more complex for the case of assumed

isotropy, for here the concept of wall motion ceases to be defined. Indeed no walls should exist for zero anisotropy material. This seems difficult to reconcile with the concept of effectively infinite anisotropy fields. (See Appendix D). However, for the [100] anisotropy there are six possible directions of magnetization, and for the [111] anisotropy there are eight possible directions of magnetization. The isotropic case can be considered as the extension to an infinite number of possible directions, each with an effective infinite anisotropy field. Although the physical formulation remains a little nebulous, mathematically passing to the limit allows working with $L(\eta)$ as opposed to $E(\eta)$ or $G(\eta)$. Further, as given in Appendix E, the expansion of the three functions for small values of η gives identical series to the seventh power of η. At high values of η the applied field becomes of the same order of magnitude as the anisotropy field, thus the assumptions of strict [111] or [100] anisotropy cease to be valid. It is to be expected that the isotropic assumptions should remain a fair approximation for all values of M.

4.2 Reversible Susceptibility Assuming Wall Motion

The equations describing the variation of the reversible susceptibility with M, assuming effectively infinite anisotropy fields, are derived in Appendix E and are listed in Table 1. For completeness, the derivation for isotropic material will be described here. From Table 1, $M = M_S L(\eta)$, where $\eta = A(H_b + H_h - NM)$, A is a constant, H_b is the applied biasing field, H_h the effective history field, and -NM the effective demagnetizing field. The parallel reversible susceptibility is the susceptibility seen by a vanishingly small magnetic field applied opposite to the direction of the last change in H. The latter criterion is to assure the constancy of H_h. The parallel susceptibility is therefore given by:

$$\chi^{w}_{rp} = \frac{\partial M}{\partial H} = \frac{dM}{d\eta}\,\frac{\partial \eta}{\partial H_b} = AM_s\,\frac{dL(\eta)}{d\eta} = AM_s\left[\frac{1}{\eta^2} - \operatorname{sech}^2\,\eta\right] \quad (17)$$

Defining χ^{w}_{o} as the value of χ^{w}_{rp} when $\eta = 0$, and noticing that $\lim_{\eta \to 0} \frac{dL(\eta)}{d\eta} = \frac{1}{3}$, it follows that:

$$\chi^{w}_{rp} = 3\chi^{w}_{o}\,\frac{dL(\eta)}{d\eta} \quad (18)$$

where

$$\chi^{w}_{o} = (1/3)\,AM_s\ .$$

(Note that $H_{ap} = H_b + \Delta H_b$)

To calculate the reversible susceptibility normal to the applied field refer to Fig. 5. In a polycrystalline material the field and resultant magnetization are assumed always to be aligned on a macroscopic scale, thus:

$$\chi^{w}_{rt} = \frac{dM}{dH_b} = \frac{M}{H_t} = \frac{M_s L(\eta)}{\eta/A} = 3\chi^{w}_{o}\,\frac{L(\eta)}{\eta} \quad (19)$$

Values of χ^{w}_{rp}, χ^{w}_{rt} and M are listed in Table 2 for material with [100], [111] and isotropic orientations. Figures 6 (parallel) and 7 (transverse) depict the variation of the susceptibilities with magnetization. Figure 8 shows a comparison of the parallel and transverse curves for isotropic material.

The foregoing paragraphs assume that the small changes in H_b occur slowly enough so that the material remains always in an equilibrium position. It is also of interest to estimate the variation of these curves from the predicted values as the frequency is increased, and to consider the possible variation in the phase angle between the applied H and resultant M, or its inverse tangent, the magnetic Q. To do this Eq. 10 must be

FIG. 5 RELATIONSHIP FOR DETERMINING TRANSVERSE REVERSIBLE SUSCEPTIBILITY

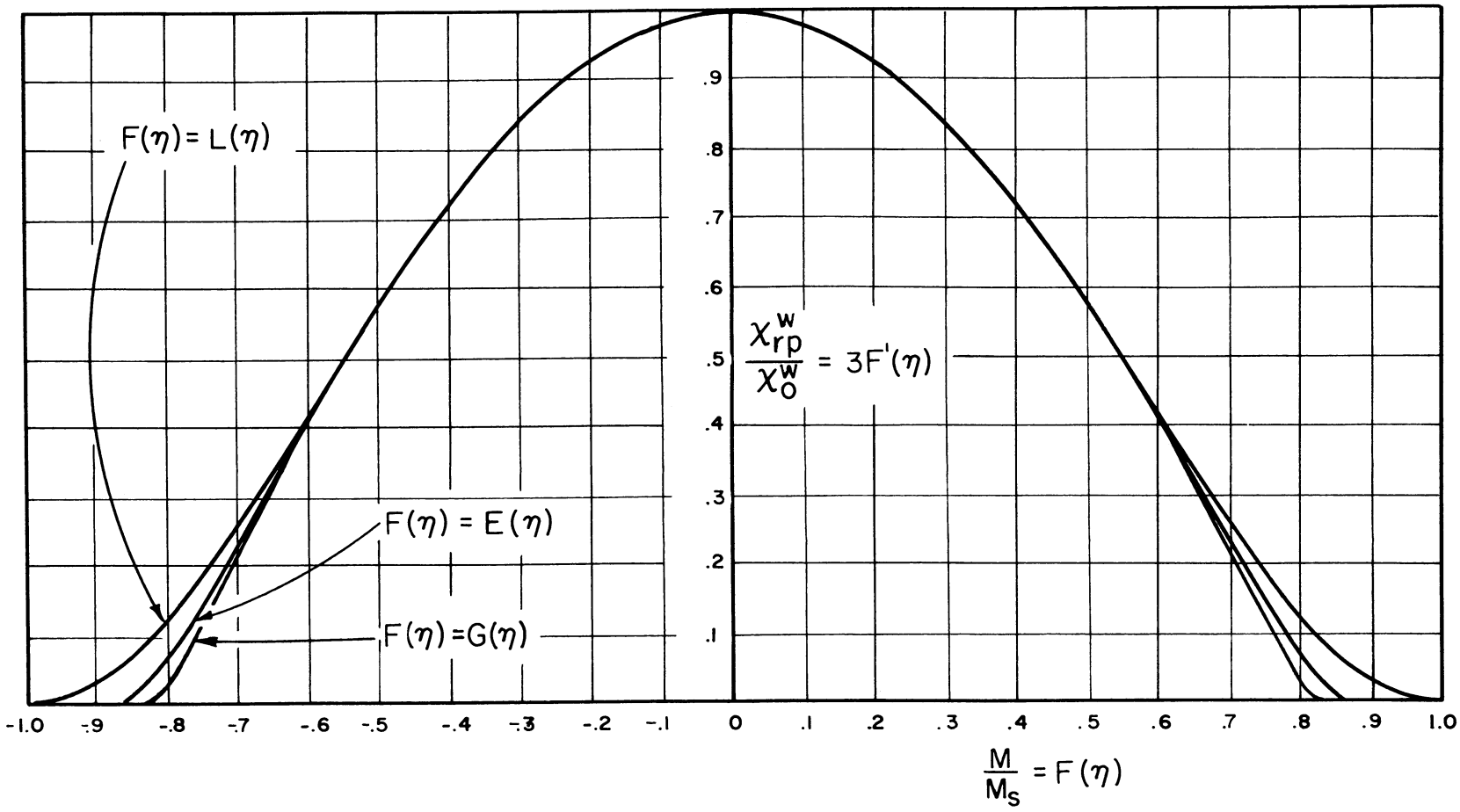

FIG 6

THEORETICAL PARALLEL REVERSIBLE
SUSCEPTIBILITY VS MAGNETIZATION

FIG 7

THEORETICAL TRANSVERSE REVERSIBLE SUSCEPTIBILITY VS MAGNETIZATION

FIG 8

THEORETICAL SUSCEPTIBILITIES
WALL MOTION

ISOTROPIC MATERIAL

considered. Since α arises from local magnetic fields which may have their origin in many different processes, it must be expected that α will be a function of the angle between the applied biasing field H_b and the reversible field H_r. Just what function of this angle that α must be remains obscure, but α_p for parallel fields must surely be equal to or greater than α_t for transverse fields.

The coefficient β of Eq. 10 depends upon many parameters of the system but not upon the angle between fields. The magnetic Q^W, from Eq. 10 for $\omega^2 << \alpha/m$, is given by:

$$Q^W = \frac{\alpha}{\omega\beta} \quad , \tag{20}$$

where ω is 2π times the applied frequency.

Thus it is to be expected that the Q^W measured parallel with the applied field be equal to or larger than the Q^W measured normal to the applied field for a specified value of M.

4.3 Reversible Susceptibility Assuming Domain Rotation

To calculate the reversible susceptibility as a function of the magnetization when its origin lies with domain rotation, consider the Landau-Lifshitz differential equation, Eq. 3, as applied to a specific domain. If the direction of orientation of the magnetic moment of the domain is chosen to be the z-axis there will exist three susceptibilities, which can be described as χ_x, χ_y and χ_z. The subscript indicates the axis along which the susceptibility is to be measured. If the resulting susceptibility is written using matrix notation a nondiagonalized matrix results. If, on the other hand, the susceptibilities are written in terms of $\chi_+ = \chi_x + i\chi_y$, $\chi_- = \chi_x - i\chi_y$, and χ_z the resulting matrix is diagonal. If the time dependent quantities all vary as $\exp(j\omega t)$, and if

only the terms to first order in the ratio of M or H along the x- or y-axis to M or H along the z-axis are kept,[31] ($M_z \simeq M_z$) (See Appendix B) one obtains:

$$\chi_+ = \frac{\gamma\mu_o M_s}{\gamma\mu_o(H_{an} + H_t) - \frac{ij\omega}{1 - i\epsilon}}$$

$$\chi_- = \frac{\gamma\mu_o M_s}{\gamma\mu_o(H_{an} + H_t) + \frac{ij\omega}{1 + i\epsilon}} \qquad (21)$$

$$\chi_z = 0$$

where

H_{an} is the effective anisotropy field acting on the domain;

H_t is the sum of applied, history and demagnetizing fields;

i is the imaginary operator providing spatial rotation;

j is the imaginary operator providing time dependence;

γ is the gyromagnetic constant;

$\epsilon = \lambda/\gamma\mu_o M_s$.

Eq. 21 gives the susceptibilities for each domain. Since the measuring field will be applied to a macroscopic sample consisting of many such domains it is necessary to reformulate the susceptibilities in terms of the angle between the moment of the domain and the applied biasing field. To do this consider the system q' to be a macroscopic system whose z-axis is the direction of the biasing field. Let the system k' be that system which has for its z-axis the direction of the moment of the domain. Using matrix notation

$$M_{k'} = \chi_{k'} H_{k'} \qquad (22)$$

TABLE 2 Tabulated Magnetic Moment and Wall-Motion Susceptibility

The Susceptibility and Magnetization for Isotropic Material, [111] Oriented Material and for [100] Oriented Material. Wall Motion.

η	$L(\eta)$	$3L'(\eta)$	$3L(\eta)/\eta$	$E(\eta)$	$3E'(\eta)$	$3E(\eta)/\eta$	$G(\eta)$	$3G'(\eta)$	$3G(\eta)/\eta$
.00	.000	1.000	1.000	.000	1.000	1.000	.000	1.000	1.000
.45	.148	.960	.987	.148	.960	.987	.148	.960	.987
.65	.211	.920	.974	.211	.920	.974	.211	.920	.974
.82	.262	.878	.959	.262	.878	.959	.262	.878	.959
.96	.302	.840	.944	.302	.840	.944	.302	.840	.944
1.09	.338	.801	.930	.338	.801	.930	.338	.801	.930
1.22	.371	.761	.912	.371	.761	.912	.371	.761	.912
1.35	.403	.719	.896	.403	.719	.896	.403	.719	.896
1.47	.431	.680	.880	.431	.680	.880	.431	.680	.880
1.60	.460	.640	.863	.460	.640	.863	.460	.640	.863
1.73	.487	.600	.845	.487	.600	.845	.483	.600	.880
1.86	.512	.561	.826	.511	.537	.824	.508	.560	.819
2.01	.539	.519	.804	.538	.516	.803	.536	.520	.800
2.15	.562	.481	.784	.560	.480	.781	.558	.485	.779
2.31	.586	.441	.761	.585	.435	.760	.580	.445	.753
2.49	.612	.400	.737	.610	.390	.735	.603	.405	.727
2.68	.636	.360	.712	.634	.354	.710	.624	.365	.699
2.90	.661	.329	.684	.658	.309	.681	.647	.320	.669
3.15	.686	.280	.653	.682	.267	.650	.669	.276	.637
3.44	.711	.240	.620	.706	.225	.616	.691	.233	.603
3.82	.739	.200	.580	.731	.177	.574	.717	.183	.563
4.32	.769	.160	.534	.757	.135	.526	.744	.135	.517
4.98	.799	.120	.481	.782	.096	.471	.767	.085	.462
5.35	.813	.105	.456	.793	.078	.445	.777	.066	.436
6.10	.836	.081	.411	.809	.054	.398	.790	.043	.389
7.10	.859	.059	.363	.824	.036	.348	.801	.026	.338
8.10	.877	.046	.325	.833	.024	.309	.809	.017	.300
9.20	.891	.035	.291	.841	.015	.274	.814	.012	.265
11.00	.909	.025	.248	.848	.009	.231	.819	.007	.223
13.00	.923	.018	.213	.853	.006	.197	.823	.004	.190
15.00	.933	.013	.187	.857	.003	.171	.825	.002	.165
20.00	.950	.007	.143	.861	.001	.129	.828	.001	.124
30.00	.967	.003	.097	.864	.000	.086	.830	.000	.083
75.00	.987	.001	.040	.866	.000	.035	.831	.000	.033
∞	1.000	.000	.000	.867	.000	.000	.831	.000	.000

where $\chi_{k'}$ represents the nondiagonalized susceptibility **matrix** in terms of x, y, z. If the matrix A rotates a given quantity from the q' to the k' coordinate system, then $M_{k'} = \chi_{k'} H_{k'} = \chi_{k'} A H_{q'}$. The observed moment $M_{q'}$ is thus given by

$$M_{q'} = A^{-1} \chi_{k'} A H_{q'} . \tag{23}$$

The transformation matrix A is the well-known Euler matrix. Although Eq. 23 could be used to evaluate the susceptibilities, in practice it is easier to transform to systems q and k given in terms of x + iy, x - iy, and z. The details of this procedure are left to Appendix F.

Upon solving Eq. 23 for the case of parallel reversible and biasing-fields, the resultant susceptibility is given by (See Appendix G)

$$\chi^r_{rp} = (1/2)\ (1 - \cos^2\theta)\ (\chi_+ + \chi_-) \tag{24}$$

where the r superscript on the χ indicates that the susceptibility is based upon a rotational mechanism, the r subscript indicates the reversible susceptibility and the subscript p indicates that the biasing and reversible fields are parallel. θ is the angle between the z-axes of the q and k systems.

The solution of Eq. 23 with the biasing field in the z-direction of the q coordinate system and the susceptibility measured along either the x- or the y-axis of the q coordinates system, (See Appendix G)

$$\chi^r_{rt} = (1/4)(1 + \cos^2\theta + \sin^2\theta \cos 2\psi)(\chi_+ + \chi_-) \tag{25}$$

Eqs. 24 and 25 assume only that the Landau-Lifshitz differential equation applies to each domain. It is now necessary to determine how

these equations vary as a function of the internal magnetization level. To do this, first assume that $(\chi_+ + \chi_-)$ remains constant as the magnetization is varied. This is, of course, an untenable assumption at the higher field strengths and any results must be considered in that light. The details of averaging Eqs. 24 and 25 over a nonoriented polycrystal are carried out in Appendix H. The results are given in Table 3.

Table 3. Magnetic Moment and Domain-Rotation Susceptibility

Anisotropy Type	M/M_s	χ^r_{rp}/χ^r_o	χ^r_{rt}/χ^r_o	
[100]	$G(\eta)$	$1-H(\eta)$	$1+\frac{1}{2}H(\eta)$	$H(\eta)=\frac{3}{2}\left[\int\frac{d\Omega}{d\pi}\frac{\sum \ell_i^2 \cosh\eta\ell_i}{\sum\cosh\eta\ell_i}-\frac{1}{3}\right]$
[111]	$E(\eta)$	$1-R(\eta)$	$1+\frac{1}{2}R(\eta)$	$R(\eta)=\int\frac{d\Omega}{d\pi}\sum{}'\ell_i\ell_j\tanh\frac{\eta}{\sqrt{3}}\ell_i\tanh\frac{\eta}{\sqrt{3}}\ell_j$
isotropic	$L(\eta)$	$3\frac{L(\eta)}{\eta}$	$\frac{3}{2}\left[1-\frac{L(\eta)}{\eta}\right]$	

where $\chi^r_i=\frac{1}{3}(\chi_+ + \chi_-)$.

The derivation and evaluation of the functions $H(\eta)$ and $R(\eta)$ are given in Appendix H. Table 4 lists in tabular form the variation of the susceptibilities with magnetization. The results are depicted graphically in Fig. 9.

From Fig. 9 note that the value of the susceptibility at a given magnetic field is very nearly independent of the anisotropy type chosen, as was true for the case of magnetization by wall movement. Since the curves are nearly the same for small values of M, and since for the large values

TABLE 4 Tabulated Magnetic Moment and Domain-Rotation Susceptibility

The Susceptibility and Magnetization for Isotropic Material, [111] Material and for [100] Oriented Material. Rotation.

η	$L(\eta)$	$3\frac{L(\eta)}{\eta}$	$\frac{3}{2}\left[1-\frac{L(\eta)}{\eta}\right]$	$E(\eta)$	$1-R(\eta)$	$1+\frac{1}{2}R(\eta)$	$G(\eta)$	$1-H(\eta)$	$1+\frac{1}{2}H(\eta)$
.00	.000	1.000	1.000	.000	1.000	1.000	.000	1.000	1.000
.45	.148	.987	1.006	.148	.987	1.007	.148	.987	1.007
.65	.211	.974	1.013	.211	.973	1.014	.211	.973	1.014
.82	.262	.959	1.020	.262	.958	1.021	.262	.952	1.021
.96	.302	.944	1.028	.302	.943	1.029	.302	.943	1.029
1.09	.338	.930	1.035	.338	.929	1.036	.338	.929	1.036
1.22	.371	.912	1.044	.371	.913	1.044	.371	.913	1.044
1.35	.403	.896	1.052	.403	.896	1.052	.403	.897	1.052
1.47	.431	.880	1.060	.431	.880	1.060	.431	.881	1.059
1.60	.460	.863	1.068	.460	.863	1.069	.460	.864	1.068
1.73	.487	.845	1.077	.487	.845	1.078	.483	.847	1.077
1.86	.512	.826	1.087	.511	.828	1.066	.508	.830	1.085
2.01	.539	.804	1.098	.538	.808	1.096	.536	.811	1.095
2.15	.562	.784	1.108	.560	.788	1.106	.558	.795	1.103
2.31	.586	.761	1.119	.585	.768	1.116	.580	.776	1.112
2.49	.612	.737	1.132	.610	.743	1.129	.603	.755	1.123
2.68	.636	.712	1.144	.634	.717	1.142	.624	.734	1.133
2.90	.661	.684	1.158	.658	.693	1.153	.647	.710	1.145
3.15	.686	.653	1.173	.682	.663	1.169	.669	.685	1.158
3.44	.711	.620	1.190	.706	.635	1.183	.691	.656	1.172
3.82	.739	.580	1.210	.731	.600	1.200	.717	.625	1.188
4.32	.769	.534	1.233	.757	.562	1.219	.744	.593	1.204
4.98	.799	.481	1.259	.782	.523	1.239	.767	.564	1.218
5.35	.813	.456	1.272	.793	.505	1.248	.777	.545	1.228
6.10	.836	.411	1.294	.809	.476	1.262	.790	.522	1.239
7.10	.859	.363	1.318	.824	.448	1.276	.801	.503	1.249
8.10	.877	.325	1.337	.833	.432	1.284	.809	.490	1.255
9.20	.891	.291	1.354	.841	.418	1.291	.814	.485	1.258
11.00	.909	.248	1.376	.848	.403	1.299	.819	.475	1.263
13.00	.923	.213	1.393	.853	.391	1.305	.823	.467	1.267
15.00	.933	.187	1.406	.857	.384	1.308	.825	.464	1.268
20.00	.950	.143	1.428	.861	.375	1.313	.828	.456	1.272
30.00	.967	.097	1.451	.864	.365	1.318	.830	.452	1.274
75.00	.987	.040	1.480	.866	.364	1.318	.831	.449	1.276
∞	1.000	0	1.500	.867	.363	1.319	.831	.449	1.276

* The values in columns six, seven, nine and ten were obtained from Eqs. H-14 and H-15 for the large and small values of η. Values between the extremes were obtained by graphical interpolation.

FIG 9 PARALLEL AND TRANSVERSE SUSCEPTIBILITY DOMAIN ROTATION

the moments cannot be aligned in some easy direction, the isotropic equations will be used throughout.

In addition to the variation of the susceptibility because of averaging over the domains the susceptibility per domain will also vary. According to Eq. 4 the susceptibility along the x-axis is given by

$$\chi_o = \frac{M_s}{H'}$$

where

$$H' = H_{an} + H_t \ . \qquad (22)$$

Thus χ_o can be considered constant for each crystallite and macroscopically constant only so long as the field H_t is much less than the anisotropy field H_{an}. (See Eq. 9). In spite of the vector character of the addition in Eq. 22, when averaged over the polycrystal, an increased value of H_t results in an increased value of H' and a correspondingly decreased value of χ_o. Thus only for large values of the anisotropy constant K_1 can the averaging equations as given be considered a good approximation for values of M different from zero.

If the value of K_1 is increased, according to Eqs. 7 and 11, the relative contribution of wall movement should increase. It remains to be determined experimentally if a region exists where K_1 is sufficiently high so that the averaging equations are valid to large values of M, yet sufficiently low so that rotational phenomena predominate.

The magnetic Q as calculated for low frequencies using Eq. 3 is given by

$$Q^r = \frac{\gamma H'}{\omega \epsilon} (1 + \epsilon^2) \ . \qquad (23)$$

ϵ, which is defined in Appendix B, is proportional to the power loss. If

the fields are sufficiently small so that ϵ can be considered constant, Q depends directly upon the total H, and should thus increase with increasing biasing field. Further, the product $\chi_i^r Q^r$ is independent of H', i.e.,

$$\chi_i^r Q^r = \frac{2\gamma M_s}{3\omega\epsilon} (1 + \epsilon^2) . \qquad (24)$$

Although the effect of the decreasing χ_o^r and the increasing Q^r can be considered to result from the frequency of resonance moving farther away from the measuring frequency as the applied field is increased, it would seem more reasonable to state that the cause of the increased resonant frequency is the same as the cause of the increased Q^r and the decreased χ_o^r.

As the susceptibility approaches zero with a large biasing field, the losses due to the applied field remain while the energy stored goes to zero. Therefore, the Q in completely saturated material must be zero.

4.4 A Comparison of the Susceptibility Variation

Since the form of the averaging equation for the transverse susceptibility in the case of magnetization by wall motion is the same as the form for the parallel susceptibility in the case of magnetization by rotation, Fig. 10 illustrates the susceptibility behavior expected for both transverse fields with wall motion and parallel fields with domain rotation. Fig. 11 and Fig. 12 show the variation of the susceptibility with magnetization as a function of magnetization mechanism for parallel and transverse fields respectively. Figs. 13, 14 and 15 show the expected susceptibility variation with magnetization for both magnetization types for the three anisotropy conditions.

FIG 10 THEORETICAL SUSCEPTIBILITIES, ROTATION
ISOTROPIC MATERIAL

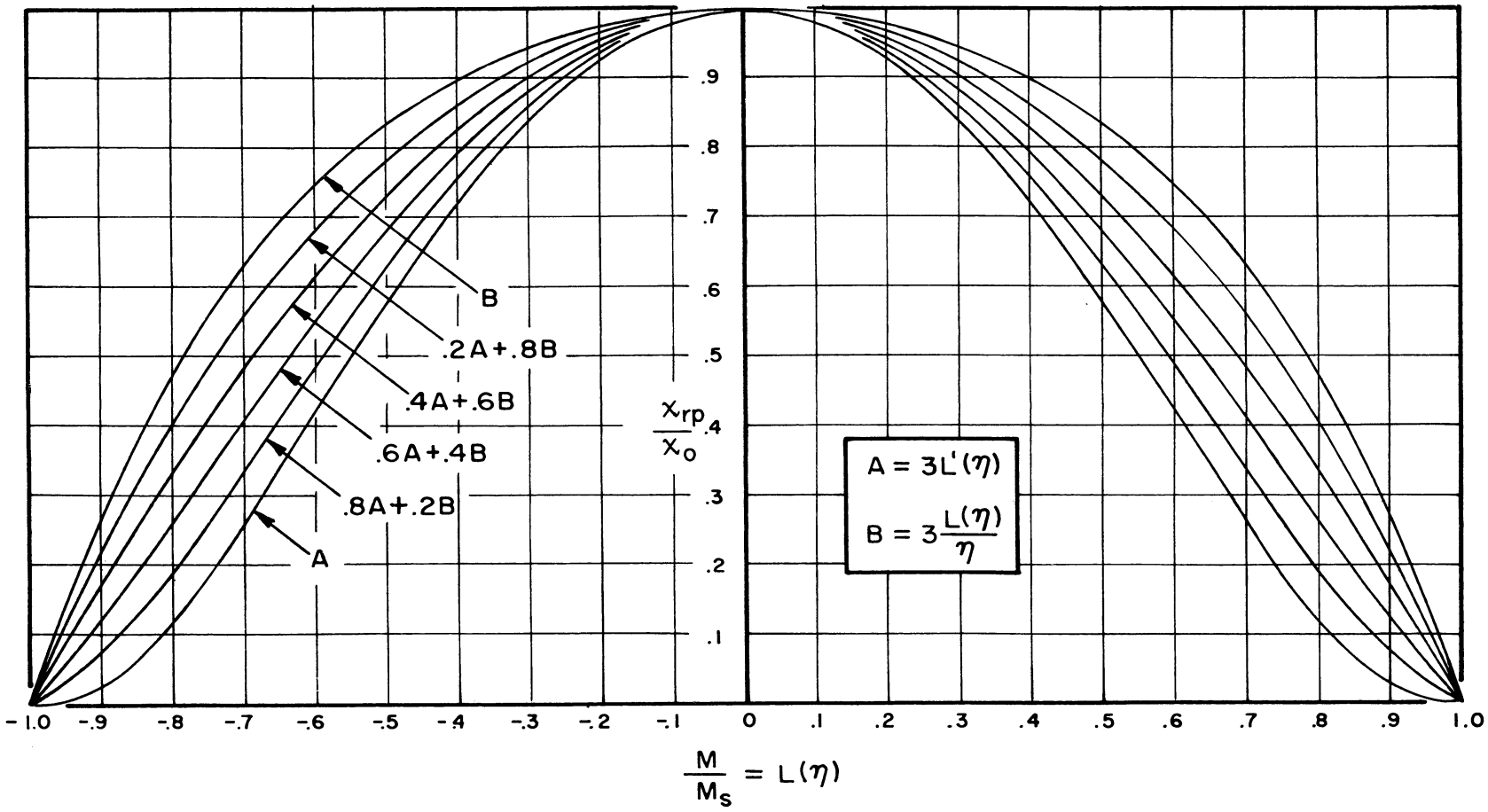

FIG 11. $\frac{\chi_{rp}}{\chi_o}$ VS $\frac{M}{M_s}$ AS A FUNCTION OF PERCENT WALL MOTION

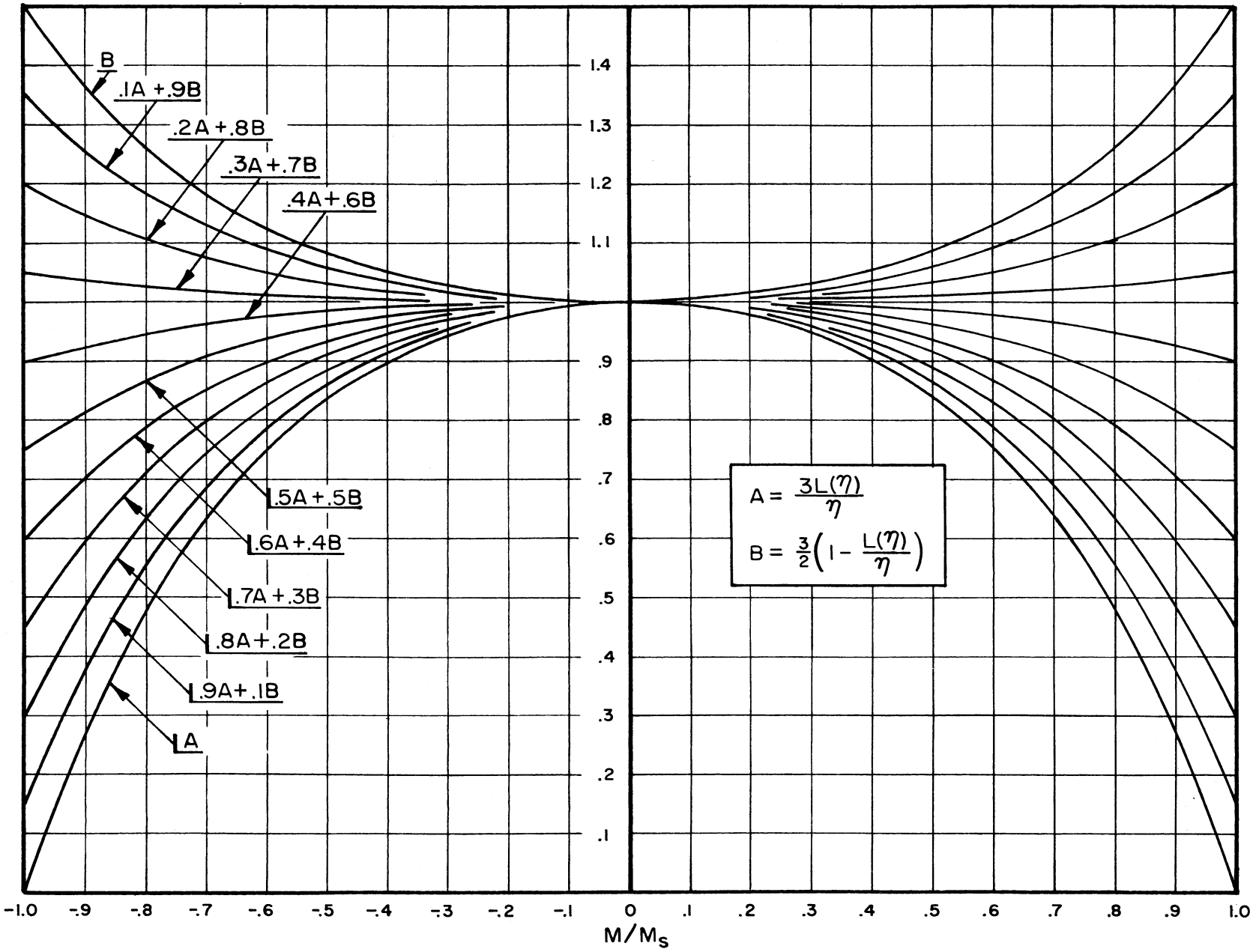

FIG 12. $\frac{\chi rt}{\chi_o}$ VS $\frac{M}{M_s}$ AS A FUNCTION OF PERCENT WALL MOTION TRANSVERSE FIELD

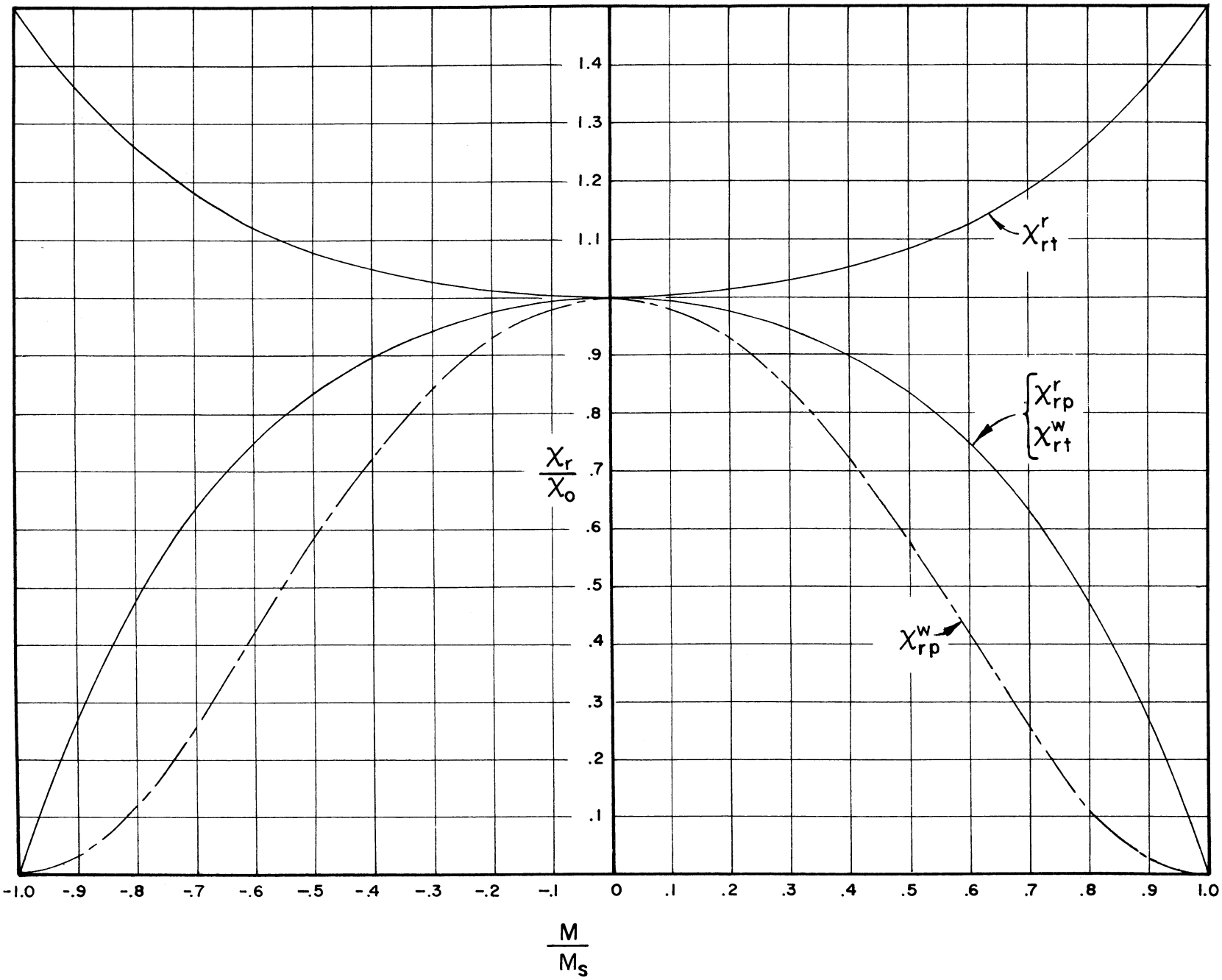

FIG 13. χ_r VS M, ISOTROPIC MATERIAL

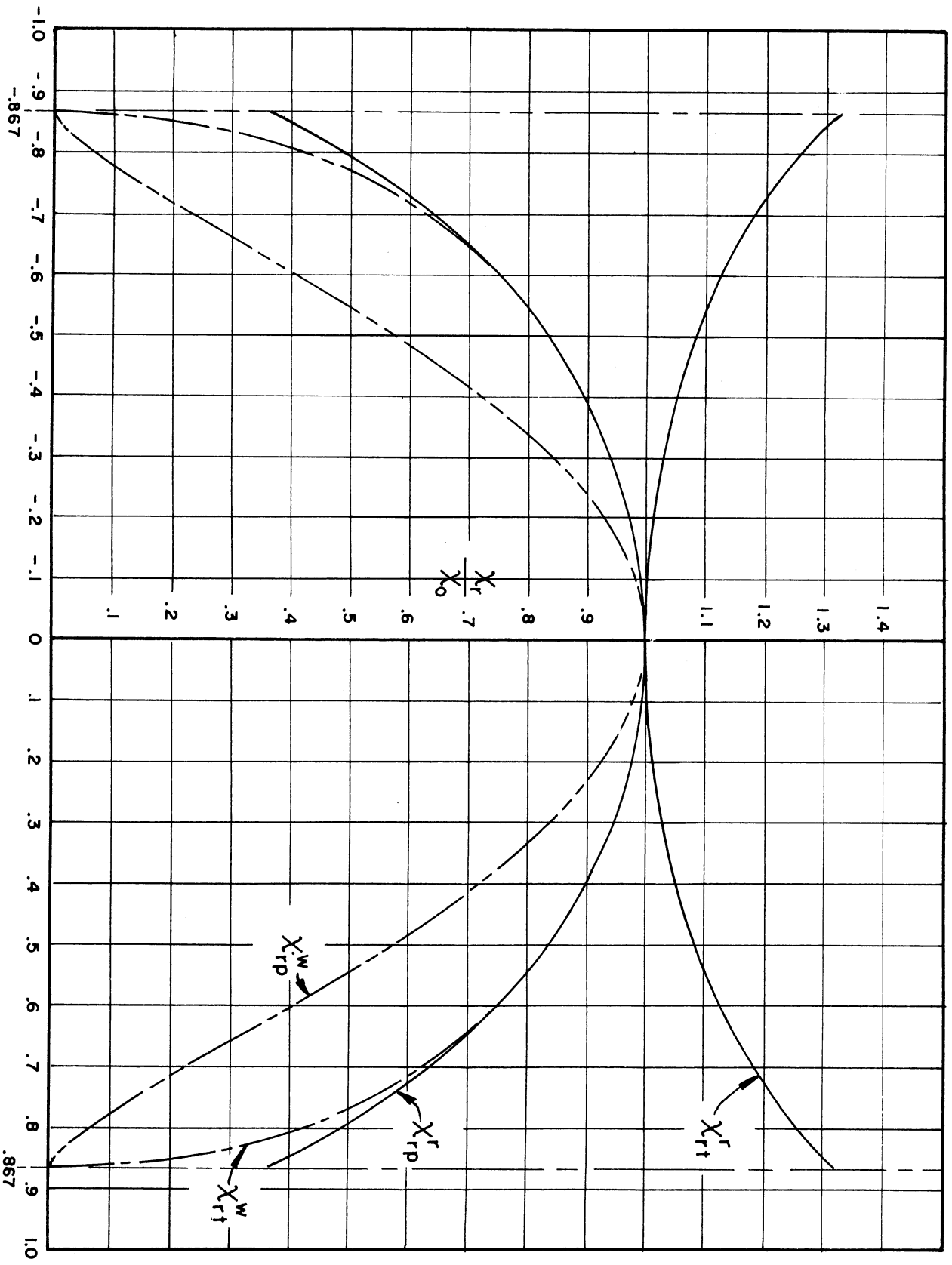

FIG 14. χ_r VS M [111] ORIENTATION

2262 A-G6-183 RC 2-21-55

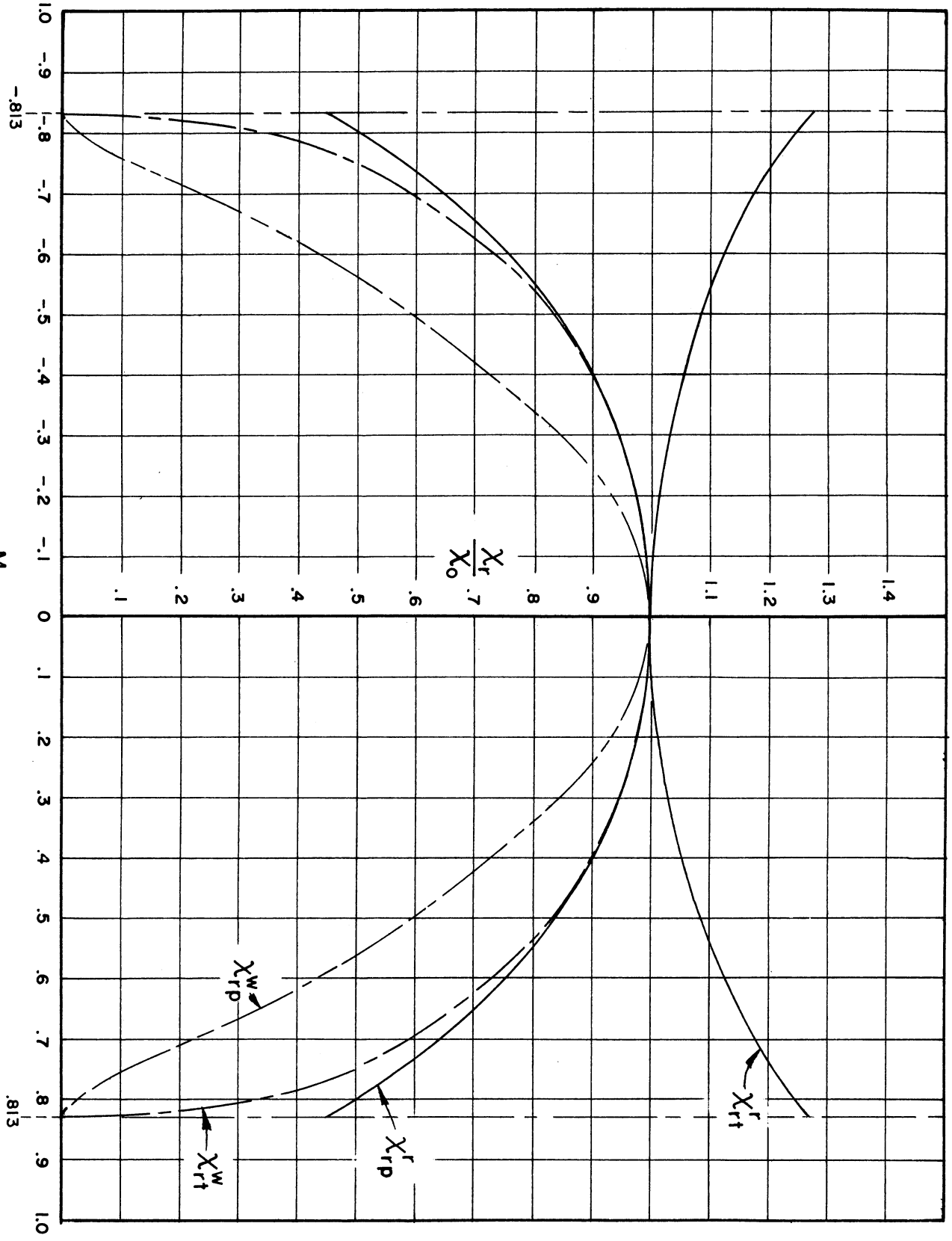

FIG. 15. χ_r VS $\frac{M}{M_s}$, [100] ORIENTATION

2262 A-G6-184 RC 2-21-55

Since the Q depends upon the field H' and not upon M, it is to be expected that for the case of rotation the Q's in the parallel and transverse fields should be equal for a specified value of M. This is in contrast to the case of wall motion where Q_p is expected to be equal to or larger than Q_t.

Note that for the case of domain wall motion the reversible susceptibility equations are related by the equation:

$$\chi^w_{rp} = \chi^w_{rt} + \eta \frac{d\chi^w_{rt}}{d\eta} \qquad (25)$$

independently of the function $f(\theta)d\theta$.

Even if the function $f(\theta)$ as calculated were in error for any feasible function χ^w_{rp} must decrease with increasing M away from an approximately demagnetized state. Thus, from Eq. 25, χ^w_{rt} must decrease with increasing M, though not so rapidly as χ^w_{rp}.

For the case of domain rotation, the reversible susceptibility equations are related by the equation:

$$\chi^r_{rp} = 3\chi_o - 2\chi^r_{rt} , \qquad (26)$$

independently of the function $f(\theta)$. Thus, since any feasible function for $f(\theta)d\theta$ gives rise to a monotonicly decreasing function of the parallel reversible susceptibility with increasing magnetization, the transverse reversible susceptibility must increase with M.

Because of the assumption that all domains remain oriented along crystallographic easy directions, it must be expected that the theory will not be valid for large values of magnetization. If M_s is the maximum possible value of magnetization, it will certainly not be valid for $M > 0.813M_s$

for the case of [100] orientation or for $M > 0.867\ M_s$ for the case of [111] orientation. The reason is that, to obtain values of M larger than these figures indicate, the applied field must be large enough to rotate the static direction of the domain moment out of the assumed easy directions, and thus H_b must be at least approach the value of the effective anisotropy field H_{an}. According to Eq. B-5, the susceptibility χ_o^r must decrease to zero in the case of an infinite applied field. The lower magnetization limit below which the theory is accurate cannot be set so precisely, but will be determined by the effective anisotropy fields. The result is, when the magnetization is altered from saturation in one direction to saturation in the opposite direction, the transverse reversible susceptibility due to domain rotation will have two peaks on different sides of the demagnetized state and the susceptibility due to domain wall motion will have one peak at approximately the demagnetized state. These results are true for all feasible distribution functions $f(\theta)$.

If it is assumed that the function $f(\theta)d\theta$ is known, then a determination of the contribution to the susceptibility from each magnetization mechanism can be measured independently from the parallel and the transverse susceptibility measurements by comparing the experimental curves with Figs. 11 and 12. The result is a new technique for distinguishing between magnetism mechanisms. This method can be applied to individual cores, as contrasted with the necessity for utilizing a family of cores to determine the mechanism from the observed frequency spectra.

The effect of an extreme error in the function $f(\theta)$ can be seen by considering that all of the atomic moments are oriented either parallel or antiparallel with the applied field. For this case it follows that,[32] $M = M_s \tanh \eta$, $\chi_{rp}^w = \chi_o^w \operatorname{sech} \eta$; $\chi_o^w (\tanh \eta)/\eta$; $\chi_{rp}^r = 0$, and

$\chi^r_{rt} = 3/2\ \chi^r_o$. Both of the wall motion susceptibilities are slightly increased, while the rotation equations are strongly altered. The latter results since all domains are oriented parallel with the field, i.e., the z-axis, and the susceptibility in the z-direction of the crystallites was assumed zero in the small-signal solution to the Landau-Lifshitz differential equation.

An indication of how the susceptibility-magnetization curve varies as a function of the precise $f(\theta)$ used can be obtained by considering the anisotropies as variations. The expression for M was identical in all three cases considered to the seventh power of η. Further the expressions for the reversible susceptibility are the same to the sixth power of η for domain wall motion and to the fifth power of η for domain rotation.

5. EXPERIMENTAL METHODS

5.1 Specimen Shape

One phase of the work reported in this paper is the measurement of the reversible magnetic susceptibility and Q both parallel with and normal to an external biasing field to compare with the theory developed in Chapter 4.

If a piece of ferromagnetic material or ferrite is surrounded by air and placed in a magnetic field, the field effective inside the material is, in general, not the same as the external field; that is, the existence of a magnetization alters the effective field. In the event that the material is of the shape of a general ellipsoid, the internal field can be calculated exactly and is given by a term $H = H_{ap} - NM$, where H is the field inside the material, H_{ap} is the applied field as measured in the air, M is the internal magnetization in the material and N is a constant defined as the demagnetizing constant. For general ellipsoids the sum of the N's along each of the axial directions is equal to unity.

In the practical application of ferrites to electric circuits it is quite common to use toroidal samples. The material forms closed flux paths around the toroid and thus has a zero demagnetizing constant. It is not unusual to use a rod of material with a length-to-diameter ratio much greater than one to determine magnetic qualities of a material. Either the rod or the toroid is satisfactory for measuring magnetic qualities along one direction in the macroscopic material. The rod when placed at the center of a solenoid feels an essentially uniform field, while the

toroid feels a field inversely proportional to the distance from the toroidal axis. Transverse field measurements on a rod specimen become impractical, but a toroid is satisfactory since the toroid as a whole can be slipped between the pole faces of an external magnet.

An alternative method would be to have a sphere of material with two orthogonal windings. The sphere would be placed in an external field parallel with the field of one of the windings. This way the and Q of both windings could be measured simultaneously.

5.2 General Procedures

For the investigation here reported a toroidal geometry was used. A toroidal winding measured the χ and Q around the ring. This winding was connected to a Boonton Type 260-A Q Meter. The readings were corrected for the dc resistance of the winding and for the effective area of unit permeability enclosed by the windings. For the parallel-field case the bias field was applied by a second toroidal winding, while for the transverse field case it was applied along the toroidal axis by an external electromagnet. For the parallel-field case it was necessary to isolate the low-impedance biasing circuit from the circuit used for the susceptibility measurement. To do this a parallel L-C circuit resonant at the measuring frequency was placed in series with the biasing circuit. In the parallel-field case, the applied field varies with position but its average value can be accurately calculated, except for small leakage effects, from the current. The sensing winding detects the total change in flux which is in turn proportional to the average induction. The equation $M = (\beta/\mu_o) - H$ gives the resulting magnetization. There is still considerable difficulty in determining the saturation magnetization. The plot of M is still increasing at fields over 16,000 ampere-turns/meter,

at which value leakage is becoming important and ohmic heat excessive. The saturation magnetization was taken to be the value obtained by fitting a Langevin function to the last two points to obtain an estimate of M_s that is believed good within 10 percent. Error in this value affects the normalization of the abscissas of the χ_{rp} vs M curves.

The essential difficulties with the parallel field case arise from the fact that the magnetic field produced at a point within a toroidal winding varies inversely with the distance of the point from the toroidal axis. So the magnetization and susceptibility vary with radius at given applied fields, and the observed values of these quantities are averages over the cross-sectional area. Given the experimental values of the averages, it is not in general possible to solve explicitly for the unaveraged quantities to be compared with theory. Instead the geometrical averages of theoretical curves must be computed, which can then be compared directly with the experimental data. To calculate these averages it is necessary to know how the magnetization varies with position in the sample. The only quantity whose geometrical dependence is known is the applied field H_{ap}; so an additional assumption regarding the relationship between M and H_{ap} must be made before the calculation can be made.

Thus a direct check of the theoretical curves cannot be made on a toroidal sample. However, average χ vs M curves computed under several rather different simple assumptions for the dependence of M on H are found to be similar to unaveraged values[32]. Therefore the unaveraged values will be used in this paper.

In the transverse-field case the applied field is not known from the bias current, here applied to the electromagnet, because of the reluctance and hysteresis of the magnet and the demagnetizing factor of the

specimen to be measured. It is taken as $\frac{1}{\mu_o}$ times the flux density through the hole in the center of the toroid. This value is measured relative to a reproducible starting point by observing, as the magnet current is cycled, the flux changes in a search coil which embraces the hole. The total flux through the core volume is measured using a girdle winding placed snugly about the inner and outer peripheries of the toroid. The difference between the B/μ_o and H_{ap} readings is the apparent magnetization M_a. M_a differs from the true M because of the demagnetizing effect. The true internal field H is the sum of the applied field H_{ap} and the demagnetizing field - NM, i.e., $H = H_{ap} - NM$. Since $M = (B/\mu_o) - H = (\mu_r - 1)H$,

$$H = \frac{H_{ap}}{1 + N(\mu_r - 1)} \qquad \text{and } M = \frac{(\mu_r - 1)\, H_{ap}}{1 + N(\mu_r - 1)} \ .$$

Now $M_a + H_{ap} = M + H$, so that:

$$M_a = \frac{(\mu_r - 1) - N(\mu_r - 1)}{1 + N(\mu_r - 1)} \ H_{ap}. \quad \text{Taking the ratio } M_a/M \text{ gives:}$$

$$\frac{M_a}{M} = (1 - N) \ . \tag{27}$$

The special case where the coil is saturated gives:

$$\frac{M_{as}}{M_s} = (1 - N). \tag{28}$$

Therefore $\frac{M_a}{M_{as}} = \frac{M}{M_s}$ if N is independent of M.

Fig. 16 shows a sketch of the magnet used for the transverse-field measurements. The pole faces were machined flat and parallel with each other. The moving pole face was brought down against the shimmed

FIG 16

MAGNET USED FOR TRANSVERSE FIELD MEASUREMENTS

(HALF SIZE)

ferrite by means of the thread at the top of the center shaft. The circuit used for controlling the magnet current in the transverse-field case and for controlling the biasing current in the parallel-field case is shown in Figure 17. All switches were heavy-duty copper knife switches. The current was maintained steady by a battery bank. The method of operation was as follows. With switch S_a closed, S_b set on zero and S_c open, the potentiometer P was adjusted for zero current through the magnet. For measuring values around the major loop first the proper S_i was closed depending upon the field strength desired. An initial reading was taken at this point on the Q-meter connected to the χ-windings. (See Fig. 18). Following this, switch S_b was thrown to position labeled "read". Fluxmeters were connected to windings labeled H and B in the transverse case; in the parallel case an extra winding wound in the same manner as the χ-winding was used. For the latter case the fluxmeter was connected to the χ -winding and the current through the bias winding was measured. Then another Q-meter reading was taken, the peak switch thrown to the + position, and the fluxmeters or the fluxmeter and ammeter read, depending upon the type of field. The peak switch was opened next and fluxmeters or fluxmeter and ammeter again read. The Q-meter was then observed. Next switch S_b was opened and the fluxmeter deflection noted. The Q-meter was read. Next switch S_a was reversed and the entire process repeated. The result is the χ and Q for a specific field point. To get the entire loop the process was repeated for each of the 24 switch positions S_i.

5.3 The Susceptibility

Using the experimental technique described in Section 5.2 values of the capacitance necessary for resonance and of the effective Q at the points A, B, D, E, F, and H (See Fig. 4) were obtained around the M-H loop.

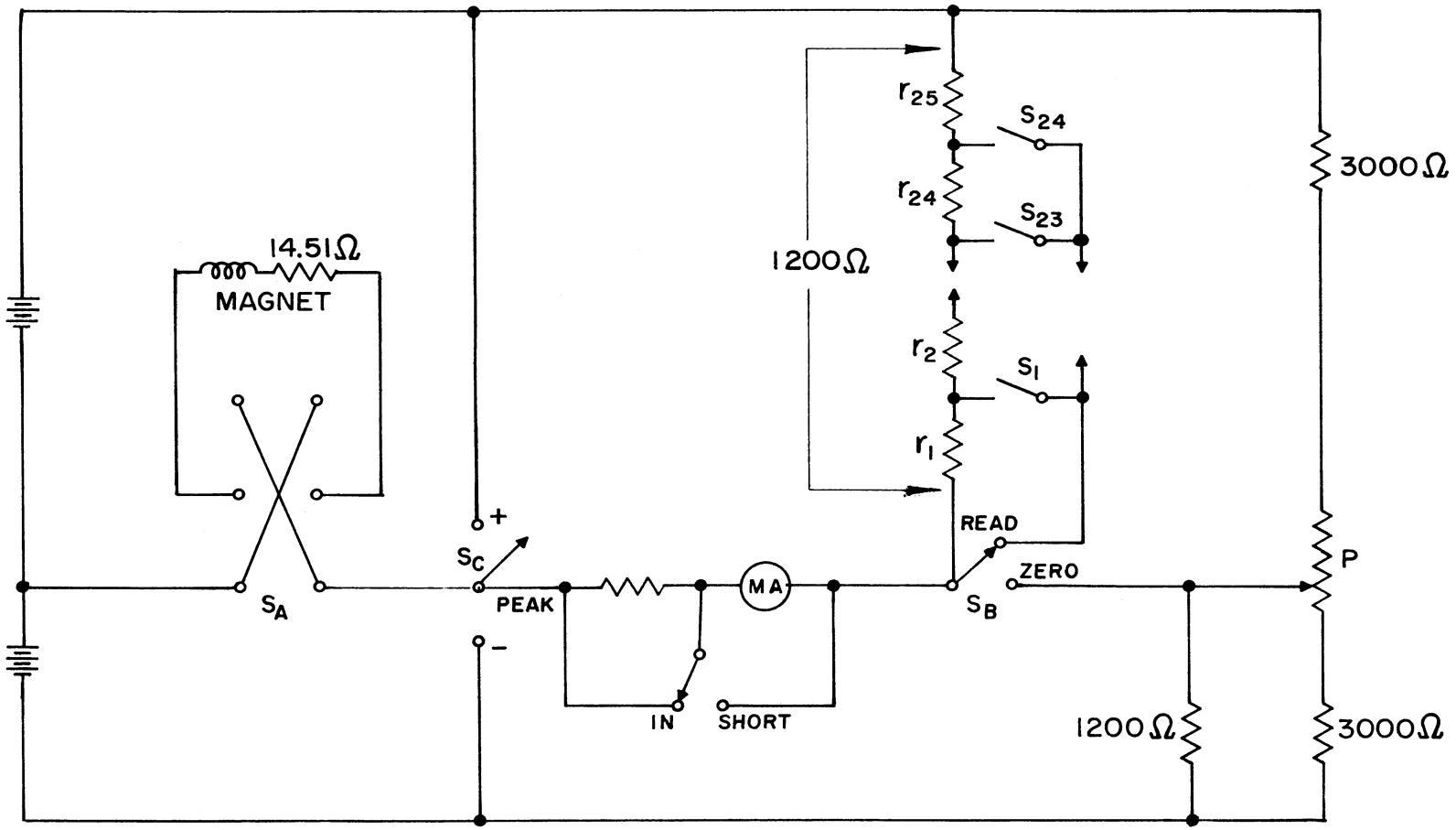

FIG 17

CIRCUIT FOR CONTROLLING THE BIASING MAGNET FIELD

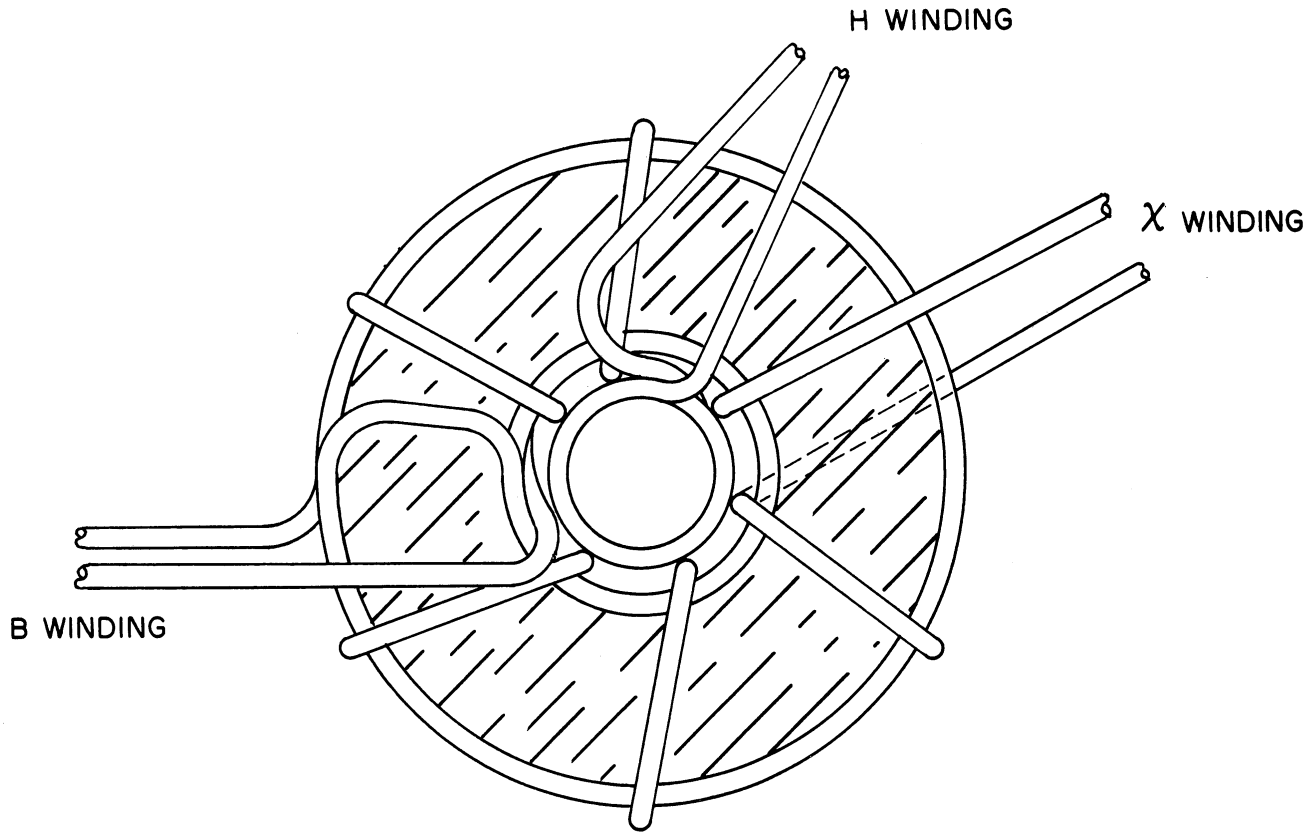

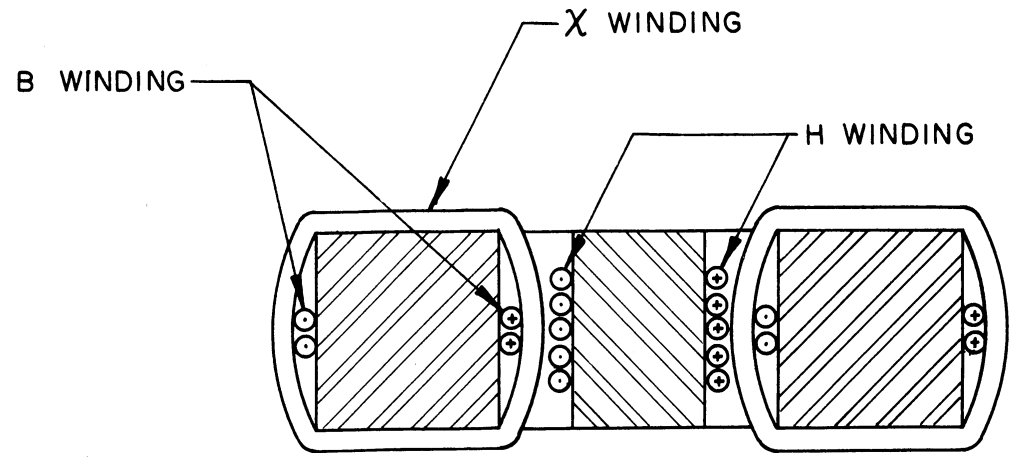

FIG 18

TEST CORE WINDINGS

The condition for resonance of the Q-meter is combined with the known formula for the inductance of a toroid, i.e.,

$$L = \frac{\mu_r \mu_o N^2 t_c \ln \frac{r_{2c}}{r_{1c}}}{2\pi} \tag{29}$$

to yield an expression for the relative permeability (see Fig. 19). Solving for the effective susceptibility,

$$\chi = \frac{2\pi}{\omega^2 \mu_o C N^2 t_c \ln \frac{r_{2c}}{r_{1c}}} - \frac{t_a}{t_c} \frac{\ln \frac{r_{2a}}{r_{1a}}}{\ln \frac{r_{2c}}{r_{1c}}} \tag{30}$$

The second term in a constant for each core and winding.

To correct for drift, an original value of permeability was obtained from the first term of Eq. 30, defined as $\mu_{1\ rem}$. For subsequent readings on the same sample, taken over a period of up to two hours, a drift correction was made using the equation:

$$\mu_i = \mu_{1\ rem} \frac{C_{rem}}{C_i} . \tag{31}$$

C_{rem} is the value of capacitance necessary for resonance at the remanent point taken nearest in time to the point "i" in question, and μ_i represents the first term of Eq. 30.

The susceptibility readings were normalized by dividing through by the value of susceptibility measured when the magnetization was zero.

5.4 The Magnetic Q

The Q-reading taken from the Q-meter must be corrected for two effects; (1) the effective resistance of the winding and (2) the area en-

FIG 19
GEOMETRY FOR COMPUTING $\bar{x}_1$

compassed by the windings not occupied by the ferromagnetic material. In general another correction for the approach of coil self-resonance should be entered. However care was taken throughout to never use readings of capacitance less than 100$\mu\mu$fd. If Q_{ap} is the apparent Q, the Q corrected for the winding resistance Q_c is given by

$$Q_c = \frac{Q_{ap}}{1 - \omega R_w C Q_{ap}} \quad , \tag{32}$$

where as usual ω is the radian frequency, C the capacitance read on the Q-meter and R_w is the measured wire resistance. For the frequencies used, 320 kc and 500 kc, the skin effect is negligible.

To correct for the area of unit-permeability material encompassed by the windings, note that

$$Q_c = \frac{A_w + (1 + \chi_1)A_f}{\chi_2 A_f}$$

where A_w is the effective area of air and wire encompassed. Solving for the Q of the material alone, $Q = \frac{\chi_1}{\chi_2}$; so

$$Q = \frac{Q_c}{\chi + 1 + A_w/A_f} \tag{33}$$

5.5 The Magnetic Moment, Transverse Field

In this case both the effective B and H were read by noting the deflection of fluxmeters. The deflection noted is proportional to the change in flux through an external search coil and to the number of turns on the coil. The fluxmeters were calibrated by the manufacturer and

checked by us for sensitivity. The B-fluxmeter was connected to the B-winding, and the H-fluxmeter to the H-winding. The windings are illustrated in Fig. 18. The assumptions inherent were discussed in Section 5.2. The total change $\Delta M = \Delta B/\mu_o - \Delta H$. Solving for ΔM,

$$\Delta M = \left\{ \frac{S_B \delta_B}{N_B A_f} - \left(1 + \frac{A_w}{A_f} \right) \frac{S_H \delta_H}{N_H A_H} \right\} \frac{1}{\mu_o} \quad , \qquad (34)$$

where:

A_f = area of ferrite in square meters.

A_H = area of the H-winding in square meters.

A_w = area of the unit-permeability material encompassed by the B-windings.

$S_{B,H}$ = sensitivity of fluxmeter in linkages per division, used for B-, H-deflection.

$\delta_{B,H}$ = deflection in divisions of the fluxmeter connected to B-, H-winding.

$N_{B,H}$ = number of turns on the B-, H-winding.

The ΔM measures the change in M in going from the point "i" in question to the remanence point. It should be pointed out that the remanence does not represent the true remanence of the material but rather the remanence in the presence of the remanence field of the magnet. Because of the geometry this is a function of just how the sample is mounted in the magnet. Therefore all readings must be taken for a specific mounting of the sample. It is necessary to find nn apparent remanent moment and an apparent saturation moment. Because of the results expressed in Eq. 28 it is considered that the normalization process can be carried out by dividing by the apparent saturation.

Referring to Fig. 4, two separate sets of readings were taken on each core; one going from point G to C and one going from C to G. The following description will consider only going from G to C. For each switch position "j", values of ΔM for G-H, H-A, A-B and B-C were obtained. The saturation moment was taken as one-half the sum averaged over all points. The effective remanence point was taken as:

$$M_{rem} = \frac{1}{2} \left[\Delta M_{A-B} + \Delta M_{B-C} - \Delta M_{G-H} - \Delta M_{N-A} \right] . \qquad (35)$$

The effective M at any point was found in two ways. For point H, firstly ΔM_{G-H} was subtracted from the effective value of M_s derived as above, and secondly by adding the effective M_{rem} derived as above to the ΔM_{A-H}. Likewise for point B the moment was obtained by subtracting ΔM_{B-C} from M_s and also by subtracting M_{rem} from ΔM_{A-B}. The normalized M so obtained was then assigned to the corresponding switch position "j" for plotting χ and Q as a function of M.

5.6 The Magnetic Moment, Parallel Fields.

The parallel-field magnetization was measured by noting the current through a winding placed outside of the winding labeled χ in Fig. 18 and by noting the deflection of a fluxmeter attached to the χ-winding when the current was changed. The value of H_b averaged over the cross-sectional area was taken as the effective H_b. Since the variation of H_b with r is known, the averaged H_b is given as a simple function of the applied current by:

$$H_b = \frac{N_H I_b}{2\pi \bar{r}_f} \qquad (36)$$

where

$$\bar{r}_f = \frac{r_{2f} - r_{1f}}{\ell n \frac{r_{2f}}{r_{1f}}} .$$

The r's are in meters and H_b is in ampere-turns/meter. The ΔB can be computed from the deflection of the fluxmeter, knowing the sensitivity of the fluxmeter and the cross-sectional area of ferrite and unit-permeability material encompassed by the windings. The resulting equation for the change in magnetization at any point is given by

$$\Delta\bar{M} = \left\{ \left[\frac{S_B}{t_f(r_{2f} - r_{1f})\, N_B} \right] \delta_B - \left[\frac{t_a}{t_f} \frac{N_H}{5(r_{2f} - r_{1f})} \ell n \frac{r_{2a}}{r_{1a}} \right] I_b \right\} \frac{1}{\mu_o} \qquad (37)$$

where in this case the unit of length is the meter, the current is in amperes, S_B is the sensitivity of the fluxmeter, δ_B is the deflection of the fluxmeter, N_B is the number of turns on the winding connected to the fluxmeter and N_H is the number of turns on the winding in which the current is applied.

As was the case for the field parallel with the axis of the toroid, it is necessary to determine the saturation moment and the remanent moment. This measurement is in considerable error because of stray flux at the high field strengths. The technique used here was to fit a Langevin function to the two highest field points, that is to j = 24 and j = 23 and solve for the maximum value of deflection going from point A to point B and from point H to point A. This maximum value was fitted to a Langevin function in both cases. The saturation moment was taken as one-half the sum. The remanence was taken as $M_r = \frac{1}{2}\left[\Delta M_{AB} - \Delta M_{HA}\right]_{j = 24}$. The moment at the point j was taken to be, for points B and F, the change from rem-

anence to the point minus the remanent value, and for points H and H was taken to be the sum of the distance to remanence and the remanent value obtained. Each point was plotted against its corresponding values of χ and Q.

6. EXPERIMENTAL RESULTS

Preliminary measurements were carried out, using the circuitry and the techniques described in Chapter 5, on thirteen ferrites. These ferrites all contained different relative amounts of the metals iron, nickel, zinc and cobalt. It is believed[35], although no measurements were taken, that these ferrites represented widely different values of the magnetostrictive and anisotropic constants. Of these thirteen, three were chosen as being representative of the group and detailed measurements were made on them. The chemical characteristics of each sample will be discussed in turn in Chapter 7. Table 5 lists values of the reversible susceptibility χ_o, the magnetic-Q Q_o, and the coercive force H_c, all measured at zero gross magnetization. In addition the maximum value of the magnetization M_s is listed. Rationalized MKS units are used with the additional definition that

$B = \mu_o(H + M)$.

TABLE 5 Magnetic Parameters of Measured Specimen

f = 500 kc/sec.

Sample	Parallel Field Data				Transverse Field Data		
	χ_o	Q_o	$M_s \times 10^{-4}$	H_c	χ_o	Q_o	$M_s \times 10^{-4}$
F-1-2	388	13.2	31.0	20.6	450	13.5	26.2
F-6-2	48.0	70.9	28.9	130	*50.2	64.6*	23.2
F-10-1	331	48.9	25.8	121	304	50.1	25.2

* f = 320 kc/sec.

The different values of χ_o and Q_o for the parallel and transverse

cases, aside from the inherent experimental error, arise because any hysteresis in the χ versus M curve will affect the parallel and transverse values in different ways. The difference in M_s can, of course, not be real for non-oriented material and is presumed to be due to the effective demagnetizing factor for the transverse-field case as well as the large expected error in the parallel-field case. A demagnetizing factor would make the M_s measured in transverse fields be less than that measured in parallel-fields.

The resulting plots of χ_r and Q as a function of magnetization for the three samples listed in Table 5 are shown in Figs. 20, 21 and 22 for the case of parallel magnetic fields. Figs. 23, 24 and 25 illustrate the same effects for transverse fields. All measurements were taken at 500kc/sec. except Fig. 24, for which the data were taken at 320kc/sec. Figure 23 and 24 also show the variation of the product $\chi_r Q$ as a function of the magnetization M.

The susceptibility results of Figs. 20 through 25 have been summetrized by taking half of the sum of the χ_r at equal values of $\pm$ M. The hysteresis has been measured by taking half the difference of the two readings. A positive hysteresis indicates that the susceptibility for a decreasing moment is larger than that for an equal, increasing moment. The results are plotted in Figs. 26, 27 and 28. Note the change in sign of the hysteresis in transverse fields. Further the magnitude of the hysteresis is less for transverse than for parallel fields.

As was observed previously[32] the zero-field value of susceptibility is a function of the maximum M reached during the cycle. Fig. 29 shows data taken by measuring the impedance of the toroidal sample

at 5 kc/sec. Note that as the maximum field reached was increased, the zero moment susceptibility decreased and moved to a larger magnitude of M.

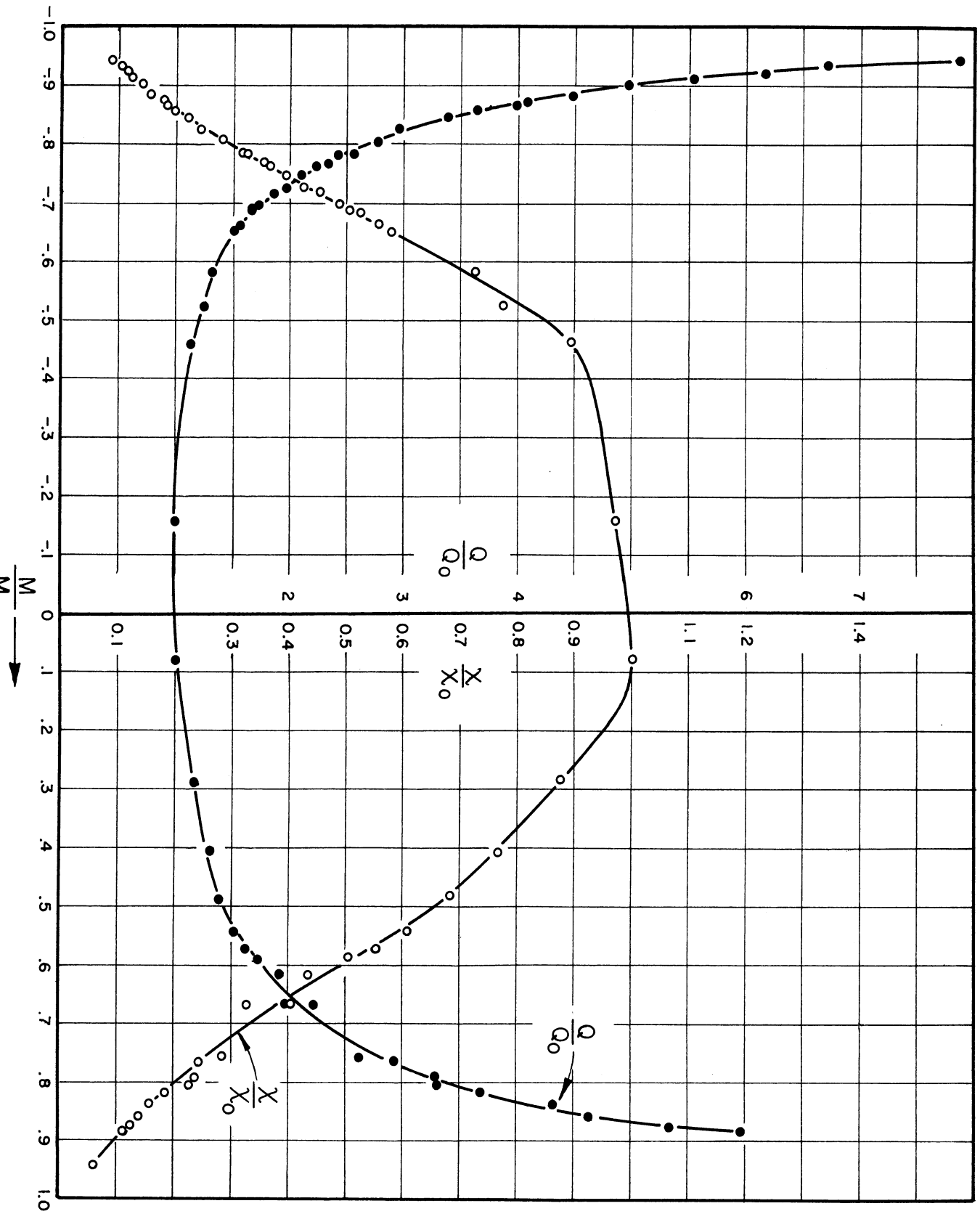

FIG 20 PARALLEL FIELD SUSCEPTIBILITY, CORE F-1-2

2262 A-G6-187 RC 2-27-55

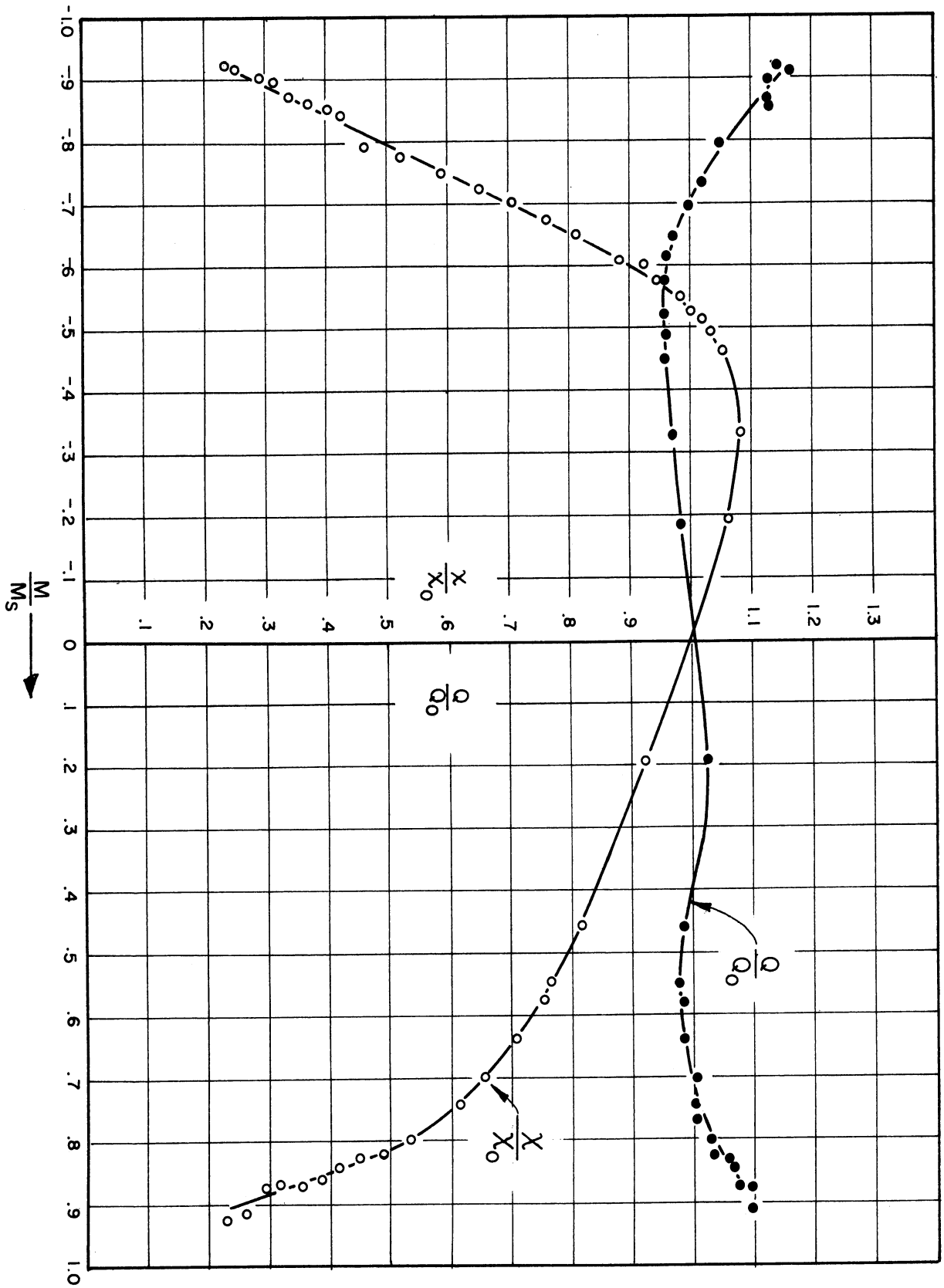

FIG 21 PARALLEL FIELD SUSCEPTIBILITY, CORE F-6-2

2262 A-G6-189 RC 2-28-56

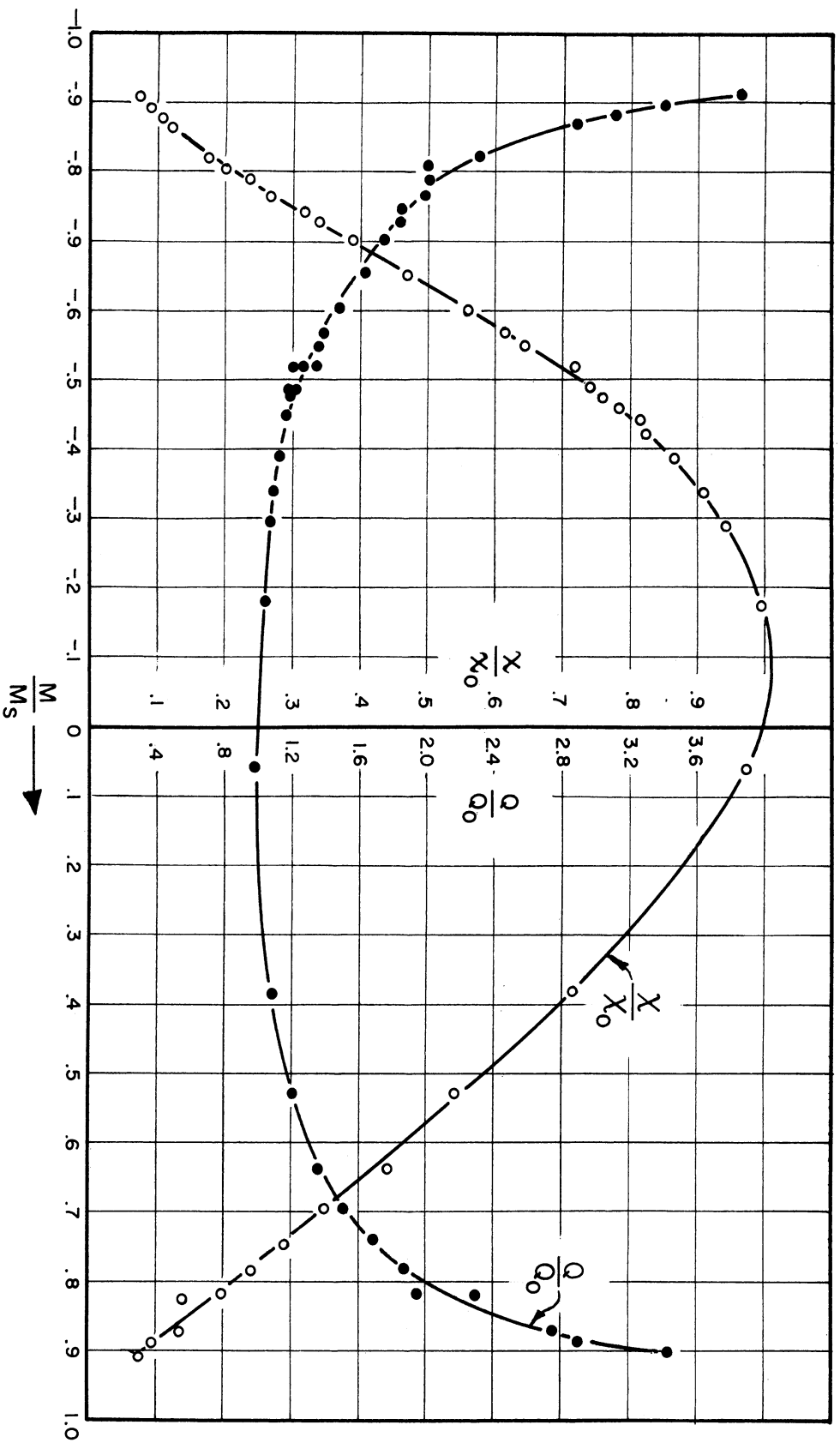

FIG 22 PARALLEL FIELD SUSCEPTIBILITY, CORE F-10-1

2262 A-G6-188 RC 2-28-55

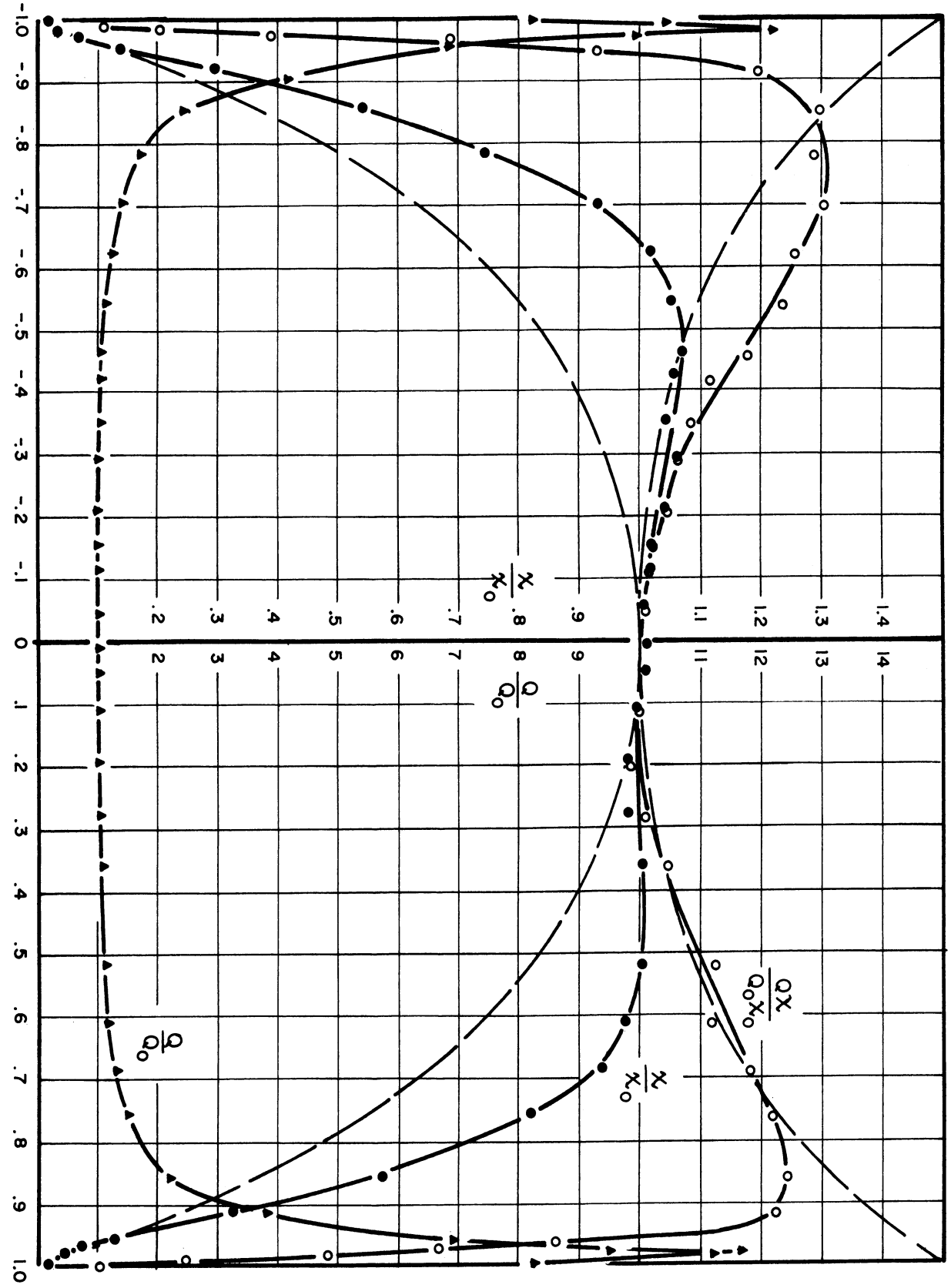

FIG 23 TRANSVERSE FIELD SUSCEPTIBILITY, CORE F-1-2

2262 A-G6-176 RRC 11-15-55

FIG 24 TRANSVERSE FIELD SUSCEPTIBILITY, CORE F-6-2

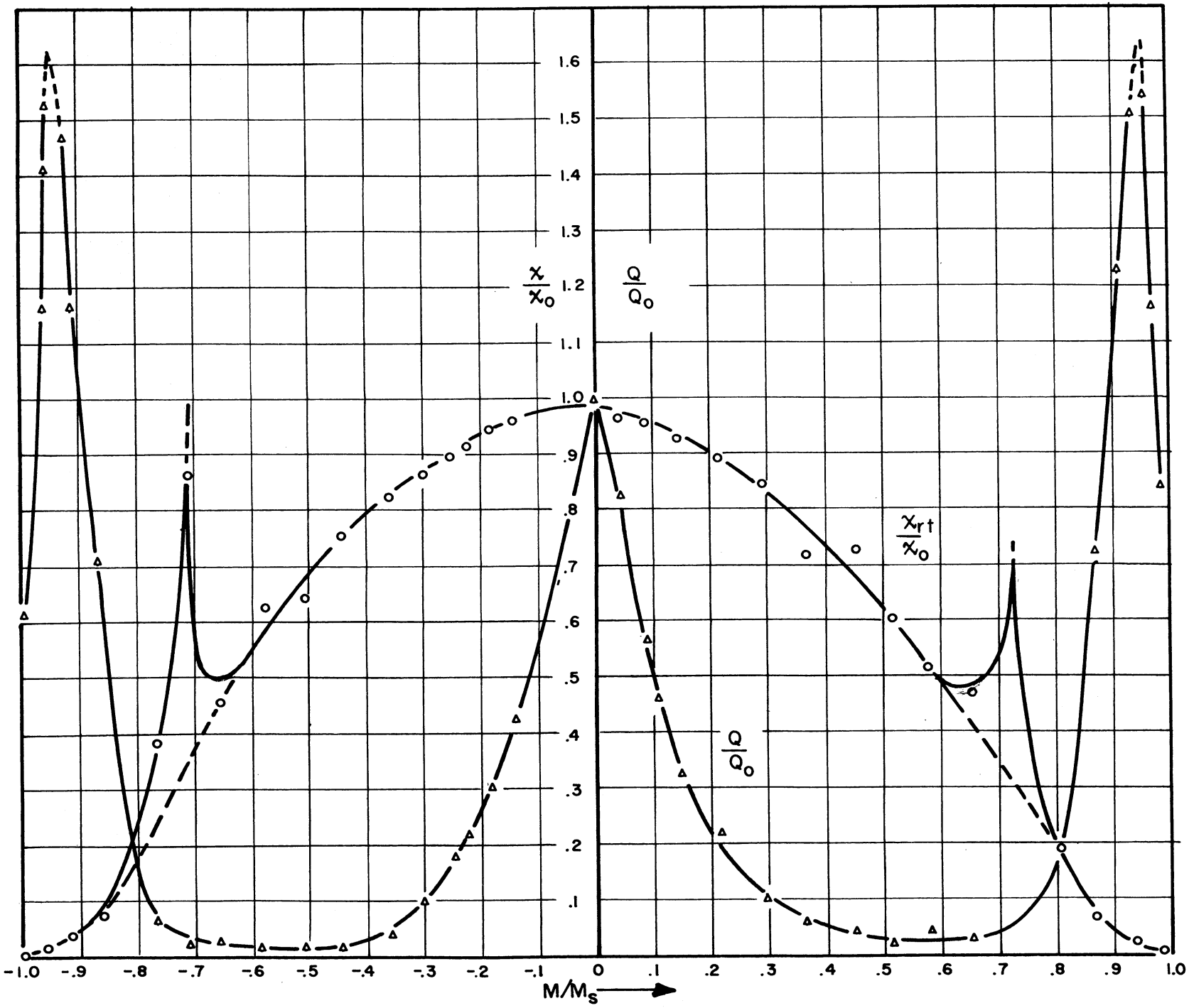

FIG 25 TRANSVERSE FIELD SUSCEPTIBILITY, CORE F-10-1

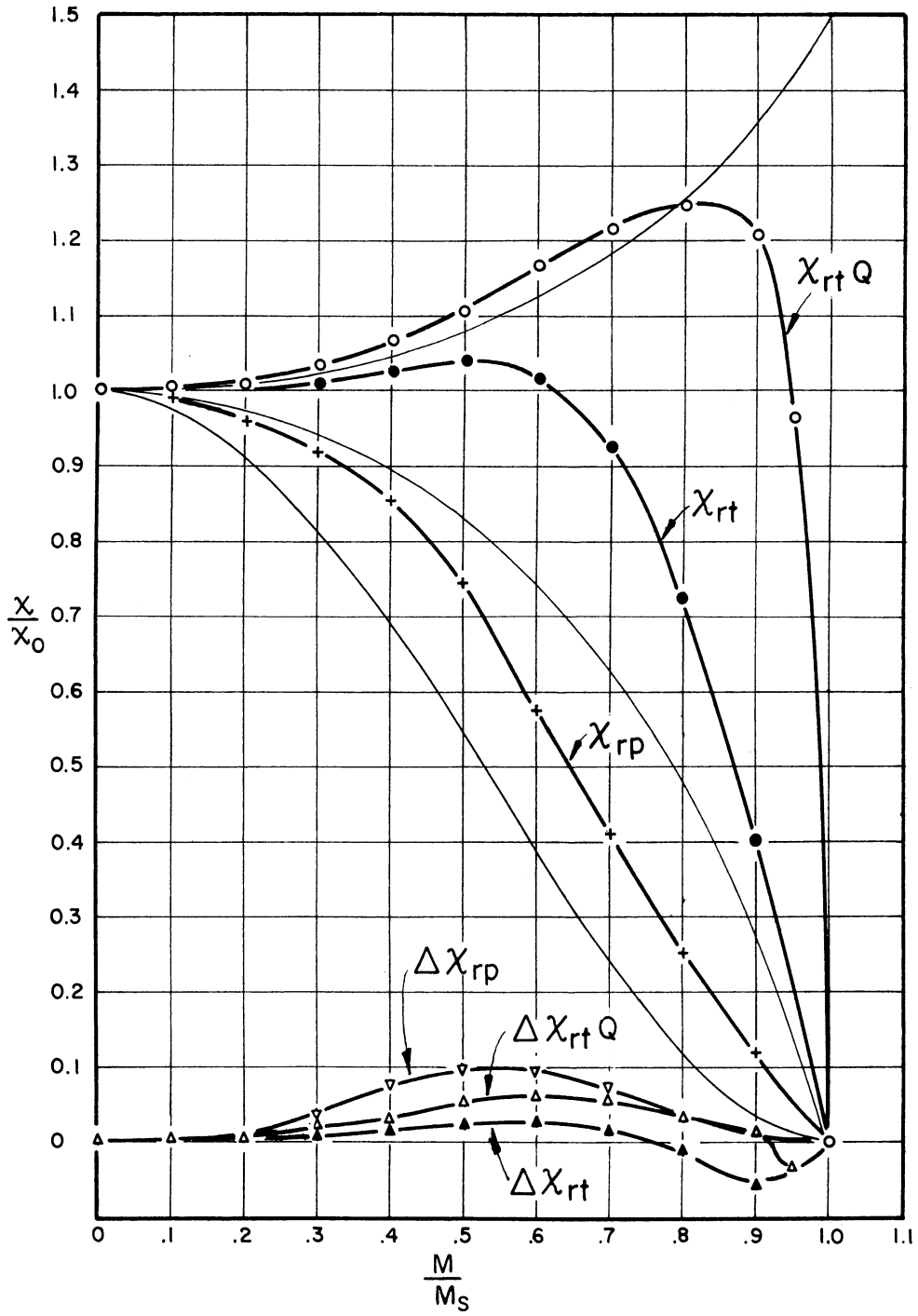

FIG 26

SYMMETRIZED REVERSIBLE SUSCEPTIBILITIES

F-1-2

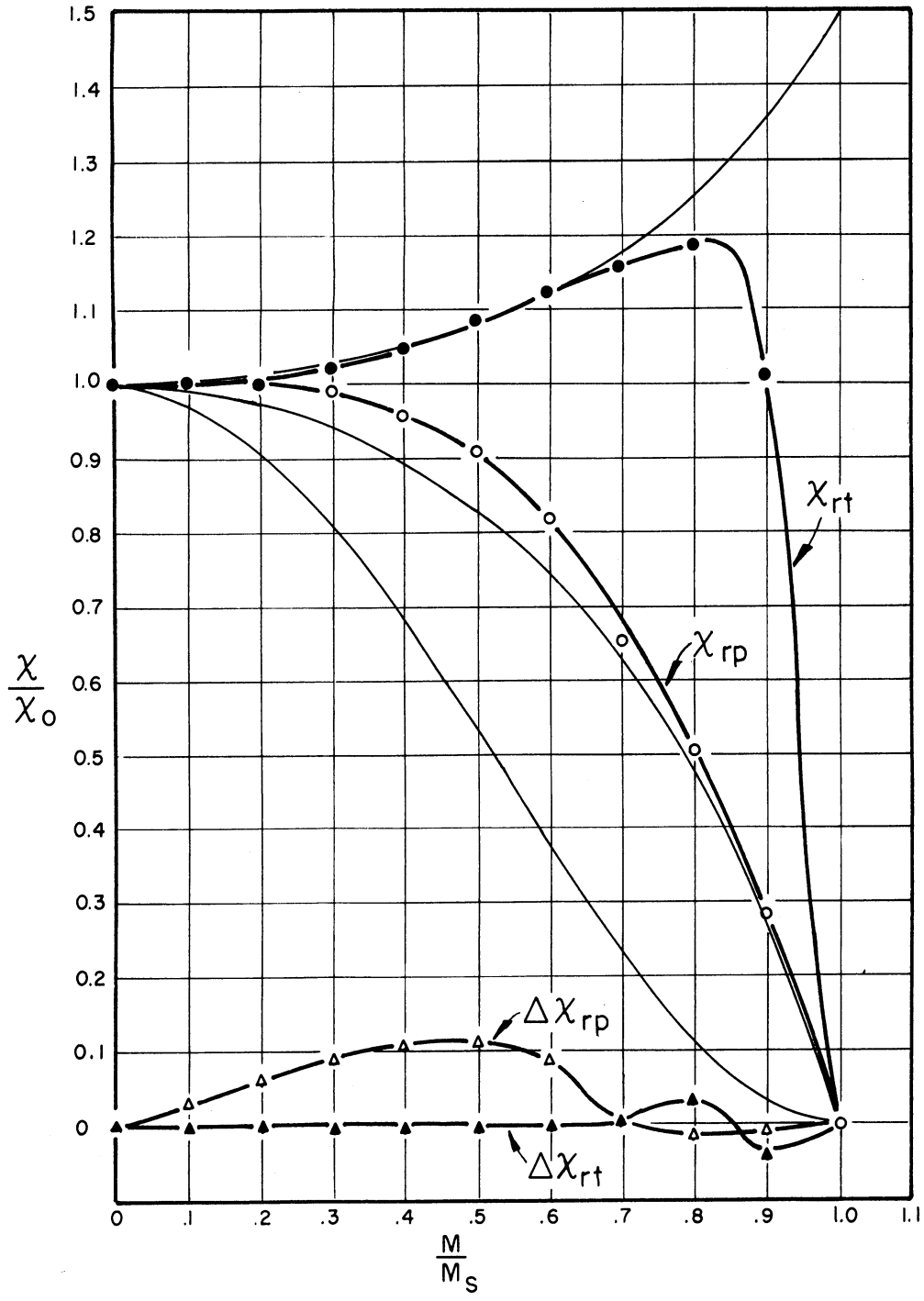

FIG 27
SYMMETRIZED REVERSIBLE SUSCEPTIBILITIES

F-6-2

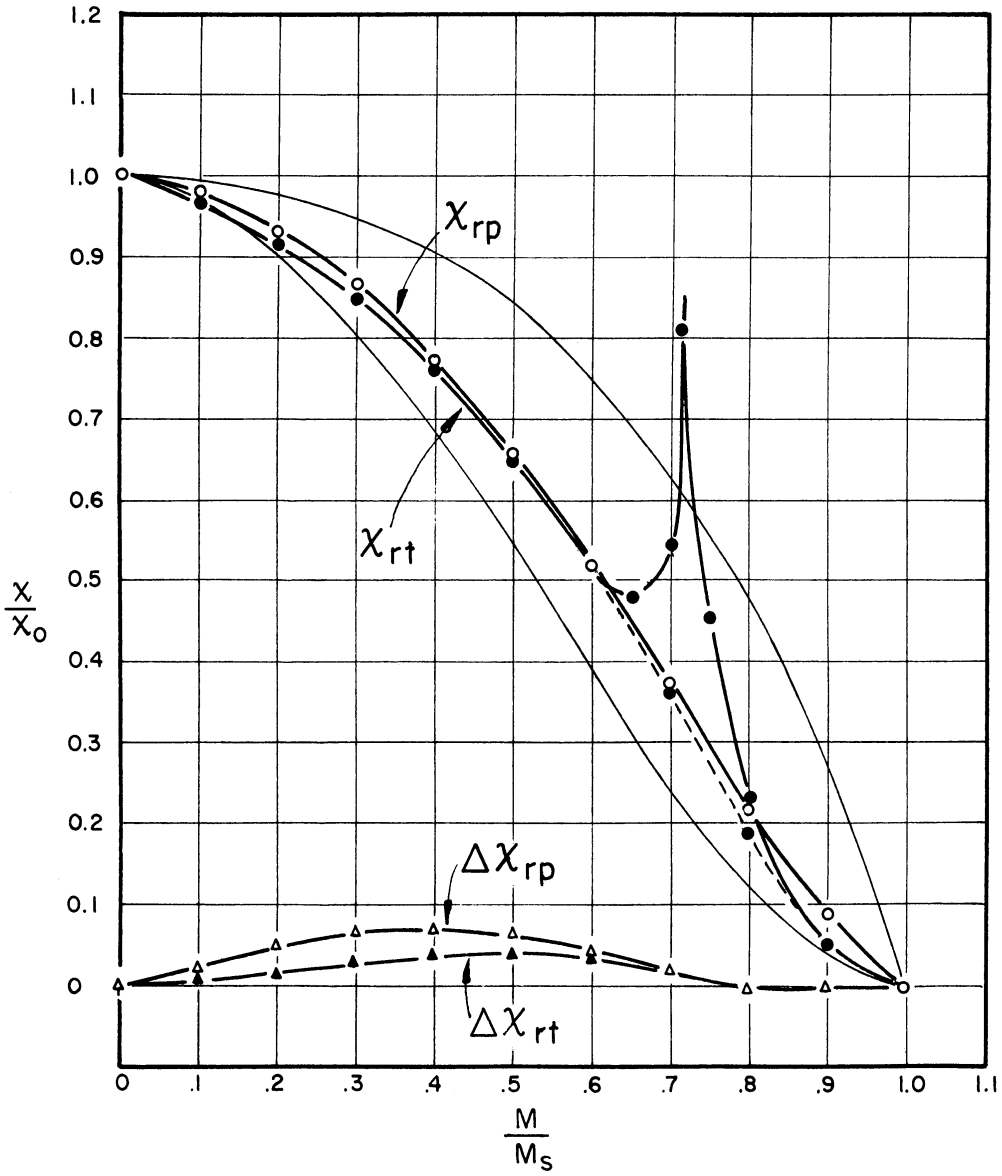

FIG 28

SYMMETRIZED REVERSIBLE SUSCEPTIBILITIES

F-10-1

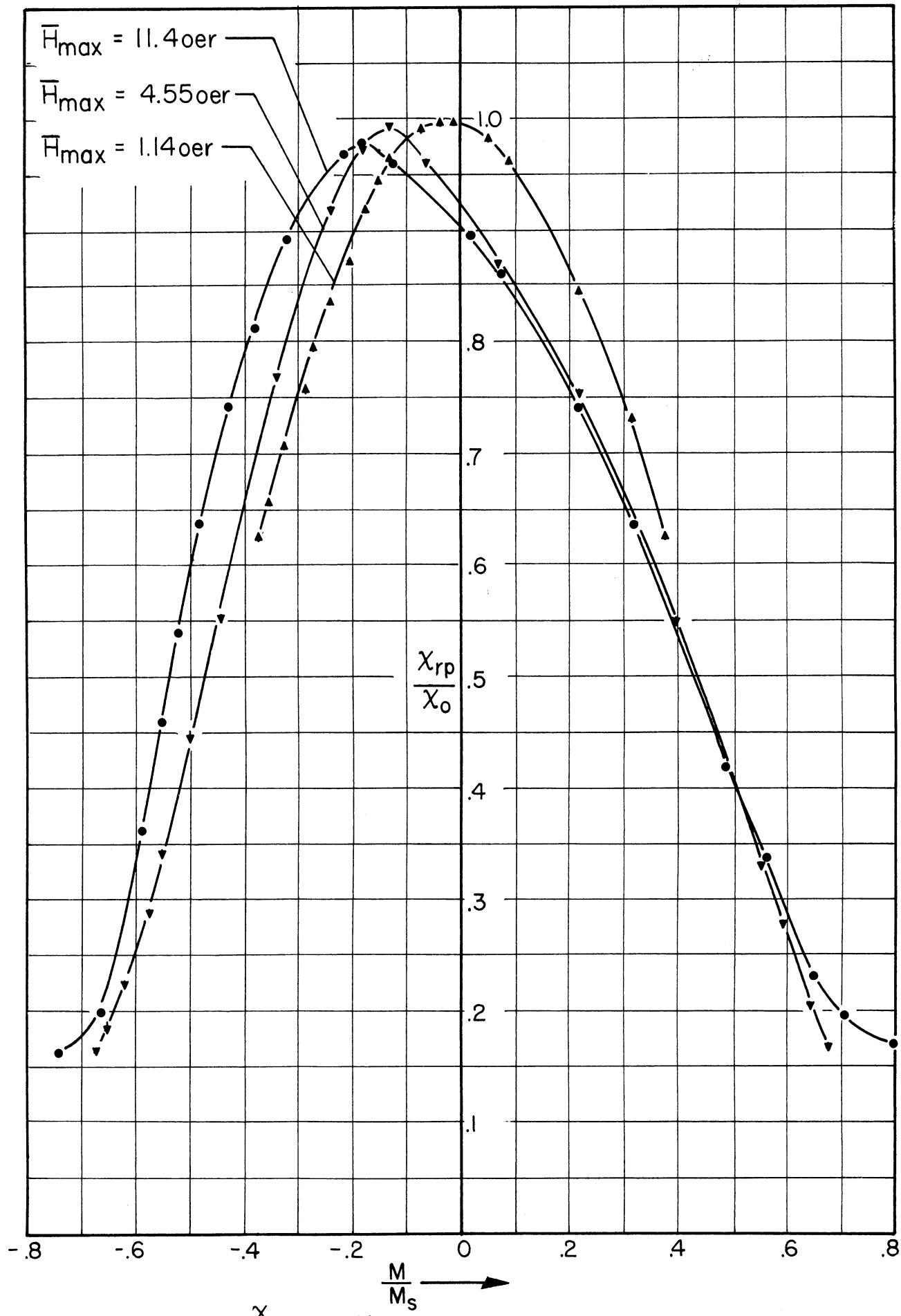

FIG 29 $\frac{\chi_{rp}}{\chi_o}$ VS $\frac{M}{M_s}$ AS A FUNCTION OF MAXIMUM H, GC-E-3

7. INTERPRETATION OF RESULTS

The interpretation of the experimental results involves the remaining hysteresis in the measured curve of susceptibility versus magnetization. Fig. 29, which was taken on a sample measured and reported earlier[32], illustrates the existing hysteresis in parallel field measurements. This can be interpreted in terms of the effect of wall "snags" or nucleation energies in the following manner. Consider that at any point on the loop a fraction D of the material is retained in metastable states by one of the above mechanisms. This fraction D will then contribute little or nothing to the parallel susceptibility and less than the amount expected to the transverse susceptibility for wall motion. Further, this volume D will be oriented, at least predominantly, in the direction of last maximum magnetization. The shifting peak shown in Fig. 29, and whose effects can be seen in each of Figs. 20, 21 and 22, can be understood on the basis of the volume D. As the peak M of the cycle increases, the fraction D which is forced into the metastable positions would evidently also increase. This will obviously shift the susceptibility peak further to the left and diminish its height, as observed. For ease in calculation assume all the material in volume D to be oriented in the direction of the last maximum magnetization. The remainder of the material (1 - D) is taken to be oriented according to Eq. 16. Since the number of atoms with their magnetic moments parallel with the change in biasing field is increased at a specified M over what it would be if D were zero, and, since from the volume D there will be more moments oriented antiparallel

with the change in field, there must be fewer cations with spins oriented normal to the field.

The very extreme case of this model would therefore be with all moments oriented either parallel or antiparallel with the applied field. As discussed in Section 4.4, this results in an increase of both the parallel and normal susceptibilities for the case of magnetization by domain-wall motion. However, for magnetizations up to 0.4 of the saturation value, the maximum expected error for the parallel reversible susceptibility is 16% and for the transverse reversible susceptibility reaches a maximum of only 5%. Because of the extreme model used, it must be assumed that these figures would be much higher than any encountered experimentally.

If the magnetization process is by domain rotation, it would be observable experimentally as an effective difference in the amount contributed to the parallel and transverse susceptibilities from each of the two magnetization mechanisms, the effect of hysteresis on the measurement of domain rotation can be assumed negligible.

In an attempt to eliminate the effect of the hysteresis described above, the experimental curves have been "symmetrized" by computing the susceptibility at each magnetization point as being one-half the sum of that measured at a specific value of magnetization for decreasing M and for increasing M. The amount of hysteresis present is shown by the "antisymmetrized" part, which is one-half of the difference of the susceptibility measured at the two points of equal magnetization.

The symmetrized curves are compared directly with the theoretically expected susceptibility-magnetization curves as shown in Figures 11 and 12. From each figure the contribution to the measured susceptibility from each magnetization mechanism can be read directly. It

is assumed that the total susceptibility is a linear combination of its parts.

The most tenuous point of the entire discussion seems to lie in the symmetrizing technique necessary to eliminate the remaining hysteresis. The error that must be expected will, of course, increase with the size of the antisymmetric susceptibility. This antisymmetric component of the susceptibility has been plotted along with the symmetric component in Figs. 26, 27 and 28.

Errors existing aside from those due to an imprecise knowledge of the distribution function $f(\theta)$ may arise from the imprecise knowledge of the saturation moment and the assumption that the demagnetizing factor (See Eq. 28) is constant.

SAMPLE F-1-2 $\left[Ni_{.4674}Zn_{.5326}Fe_2O_4\right]$

It is generally believed that the initial susceptibility in nickel-zinc ferrites is at least predominantly due to domain rotation.[21,26,27,28] The arguments used are based upon the frequency spectrum of the initial susceptibility and upon the effect of magnetic signals large enough to produce irreversible movements, as outlined in Chapter 3. The anisotropy constant of a nickel-zinc ferrite will, presumably, be smaller than for nickel ferrite alone. The value for nickel ferrite has been given as varying over a wide range[35], but most results give the first-order anisotropy constant to be about -5×10^3 joules/m^3. The calculated polycrystalline magnetostriction of an iron-rich nickel ferrite is on the order of -20×10^{-6}.

Figs. 20, 23 and 26 show the measured susceptibilities, Q's and the products χQ. Fig. 26 is symmetrized for a direct comparison with the theoretical susceptibility curves as depicted in Figs. 11 and

12.

Both the parallel and transverse data show that in this sample about 85 percent of the susceptibility is from rotation and 15 percent is from wall motion. The behavior of the product curve χQ, for low values of M, is higher than the theoretical averaged curve for rotation. The reason for this is not clear, but there seems to be two possibilities. First, the contribution to the Q from the wall movement may increase faster than that from rotation as a function of applied field. Secondly, the assumption of a constant demagnetizing factor may be invalid, producing an error in the magnetization normalization.

SAMPLE F-6-2 $\left[Ni_{.1682}Zn_{.2992}Co_{.5326}Fe_2O_4\right]$

The magnetostriction and anisotropy for core F-6-2 are both expected to be larger than was the case for core F-1-2. Since the measured samples differ from those reported elsewhere[35] no quantitative comparison of the differences can be made. The experimental curves are shown in Figs. 21 and 24. The symmetrized curves are shown in Fig. 27. A major point of interest in Fig. 27 is the relatively large value of the symmetrized function for the parallel-field case at small value of magnetization. (Compare with the same function in Fig. 26.) Fig. 21 also shows a slight dip in the Q for the parallel-field case on either side of the position of the peak low-field Q. The Q remains constant to large values of M in the transverse-field case. The parallel-field data were taken at 500 kc/sec, the transverse-field data were taken at 320 kc/sec. The reason for the frequency difference was to avoid a position of minimum Q in the transverse-field case as described under sample F-10-1.

From the symmetrized curve, Fig. 27, note that the

susceptibility equations fit the theoretical curve for rotation for the transverse-field case at all values of magnetization up to about 0.7 M_s. Further, the parallel-field case lies above the expected curve for all domain rotation. Since the transverse-field case shows about 95% of the susceptibility is due to domain rotation, the increase in the parallel-field case cannot all be due to an error in the effective distribution. (See Eq. 26.) Because of this, and the large value of the antisymmetric susceptibility for small values of M, it must be assumed that the error lies predominantly with the symmetrizing technique.

SAMPLE F-10-1 $\left[Ni_{0.3644}Zn_{0.4400}Co_{0.0316}Fe_{0.1709}Fe_2O_{4+\delta}\right]$

This sample is included to illustrate a sample with an estimated predominant wall movement and to illustrate a resonance found in transverse fields. Sample F-10-1 exhibits a very pronounced drift in susceptibility after the magnetic biasing field has been altered. Points at a value of M less than 0.7 M_s were taken only after a two minute time delay. This drift was not present at larger values of M. The parallel-field susceptibility (Fig. 22) are typical of all material measured to date. The Q increased monotonically from the position of maximum susceptibility.

A comparison of Figs. 22 and 11 show that about 70% of the susceptibility is due to domain wall motion and 30% is due to domain rotation according to parallel-field measurements.

The behavior of the susceptibility of this sample in the presence of a transverse biasing field gave results markedly different from the two previous cases. Note from Fig. 25 that the susceptibility drops rapidly with field and that the Q drops very rapidly to less than

one percent of its initial value. The susceptibility peaks at about 0.7 M_s, then drops rapidly to zero.

This effect is strongly frequency dependent. The same type of behavior occurs at frequencies very roughly odd multiples of the fundamental frequency, but the higher frequencies have dips in Q very much less pronounced than those described here. As the magnetization is varied the frequency of the minimum Q stays the same, within our ability to discriminate on the Q-meter, but the magnitude of the Q varies with the magnetization as shown in Fig. 25. A comparison of other toroids of the same material indicates that the frequency at which the dip occurs is inversely proportional to the thickness of the toroid. This dimensional resonance suggests that the magnetostrictive coupling between the magnetic and elastic lattices is producing standing elastic waves. However, why the effect should appear only in the presence of a transverse biasing field is not clear. Further, at values of M sufficiently high so that magnetization by rotation is assured the effect no longer exists. It is not considered within the scope of this paper to investigate further the effect described here, but merely to report it as found.

Because of this effect it is not considered that the variation of the transverse susceptibility with magnetization is, in this case, a valid method of testing for the magnetization mechanism. Thus only the parallel field measurements can be utilized.

8. CONCLUSIONS

This thesis develops for the first time the expected variation of the susceptibilily and magnetic Q due to domain rotation with the magnetization level in a ferromagnetic material. Experimental measurements are reported on three representative ferrite samples. The proportion of the susceptibility due to each magnetization mechanism is estimated. The curves for rotational susceptibility predict that when the magnetization is changed from saturation in one direction to saturation in the other, that the susceptibility measured normal to that magnetization will go through two maxima. Similar plots for domain-wall motion predict but one peak. The rotational curves, however, contain certain approximations which rule out the possibility of saying if only one peak exists magnetization by wall motion is present. However, if two peaks exist it is possible to state that magnetization by domain rotation is present. These conclusions are not critically dependent upon the character of the particular distribution function, but are valid over a wide variety of distribution functions. The basic premise is that the susceptibility due to domain rotation is zero when measured parallel with the direction of the moment and a maximum when measured normal to it. As the magnetization is increased the fraction of material normal to the measuring field for transverse susceptibility measurements must necessarily increase. It can therefore be stated with certainty that the origin of the susceptibility in core F-6-2 is at least predominantly domain rotation.

The situation is not so clear for cores F-1-2 and F-10-1. For

this case the distribution function $f(\theta)$ must be considered approximately known. Further, it must be assumed that the hysteresis remaining in the plot of χ versus M can be eliminated by the symmetrizing technique utilized in Chapter 5. Only then can a quantitative estimate of the relative contribution of each magnetization mechanism be made.

For core F-1-2, the result of both parallel and transverse measuring fields show that about 80 to 85 percent of the susceptibility has its origin in domain rotation and the remainder in domain-wall movement. For core F-10-1 only the parallel field measurements can be interpreted in terms of domain mechanics. The result is that at least 70 percent of the susceptibility has its origin in domain-wall motion.

It has been previously reported that the origin of the susceptibility in nickel-zinc ferrites was at least predominantly domain-rotation. It has also been reported that magnesium-zinc ferrites exist which have their susceptibility originating at least predominantly with domain-wall movement. Since there seems to be some confusion in the literature regarding the relative importance of the two mechanisms, a new independent technique should be of interest.

These results can be utilized by the engineer in several ways. The question of the best method of varying the inductance of a sample of ferromagnetic material by means of a biasing field can be considered. Care must be taken as to the angle between the fields and as to the mechanism of magnetization if the optimum variable inductance device is to be obtained. An additional result is that the slope of the predicted susceptibilities with field at zero M is zero. Therefore the well known experimental fact that two small signals can utilize the same core material with zero coupling if the signals are applied perpendicular to each other results.

APPENDIX A

DEVELOPMENT OF THE EQUATION OF MOTION FOR THE DOMAIN WALL IN TERMS OF MAGNETIC PARAMETERS[6,27]

The object of this appendix is to start with the differential equation of motion as given by Landau and Lifshitz[9] (Eq. 3), to apply it to magnetic cations situated in a domain wall and to derive from this the terms involving β and m in the differential equation of motion as given in Eq. 10. Before this can be done it is first necessary to develop the structure of a domain wall, i.e., the boundary regions separating two regions whose magnetic moments are oriented in different directions.

It has been experimentally established that the amount of energy necessary to align the spontaneous moment of a ferromagnet in different crystallographic directions is a function of that direction. This energy difference is described by an anisotropy energy. This energy must be expressable in terms of even powers of the direction cosines, ℓ_i. Further the expressions must be homogeneous in each of the three direction cosines for cubic material. The first and second nontrivial terms are $\ell_x^2\,\ell_y^2 + \ell_y^2\,\ell_z^2 + \ell_z^2\,\ell_x^2$ and $\ell_x^2\,\ell_y^2\,\ell_z^2$. Thus the anisotropy energy can be expressed as:

$$U_{an} = K_1(\ell_x^2\,\ell_y^2 + \ell_y^2\,\ell_z^2 + \ell_z^2\,\ell_x^2) + K_2(\ell_x^2\,\ell_y^2\,\ell_z^2). \qquad \text{(A-1)}$$

Where K_1 and K_2 are the first and second order anisotropy coefficients. Only the first term in the expansion will be retained in the present calculation.

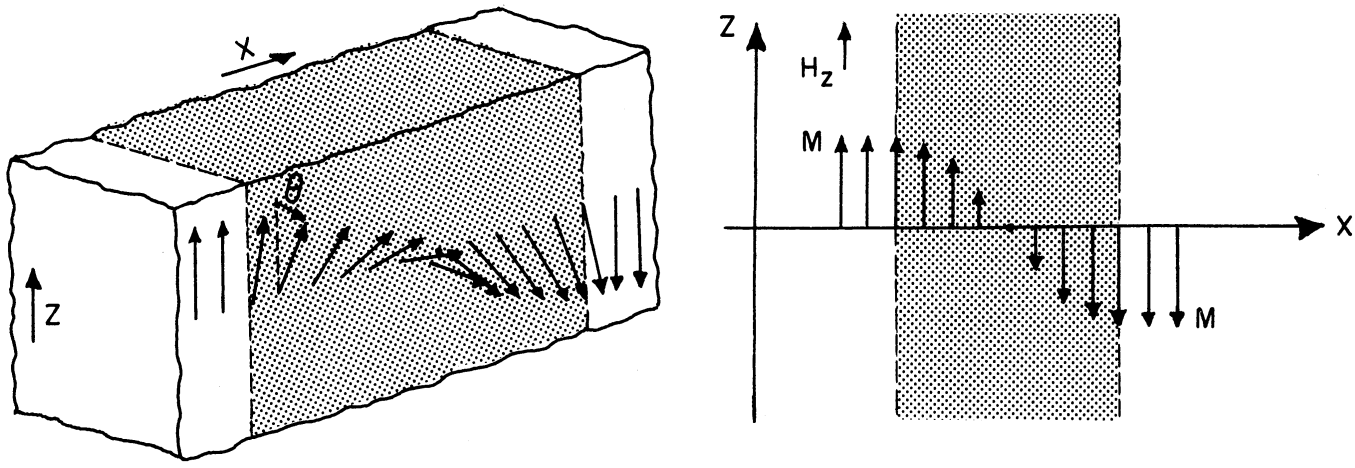

FIG A.I

180° - DOMAIN-WALL STRUCTURE
(AFTER VON HIPPEL, WESTPAL AND MILES)

$$U_{an} = K_1(\ell_x^2\,\ell_y^2 + \ell_y^2\,\ell_z^2 + \ell_z^2\,\ell_x^2) \qquad \text{(A-2)}$$

In addition to the anisotropy energy in ferromagnetic material, there is the force which originally aligns the paramagnetic cations and allows the high values of susceptibility. This force is the exchange force. It has its basis in quantum theory and has no classical counterpart. The resultant exchange energy can be written as

$$U_e = A_e \left[1 - (\Delta\theta)^2\right] \qquad \text{(A-3)}$$

where A_e is the exchange factor if neighboring spins differ in orientation by only a small angle and that angle is given by $(\Delta\theta)$.

If the geometry of Fig. A-1 is assumed, the only variation in the energies is with the variable x, so that

$$\frac{dU_{an}}{dx} = K_1 \frac{\partial g(\theta)}{\partial x}\,dx \quad \text{and} \quad \frac{dU_e}{dx} = A_e \left(\frac{d\theta}{dx}\right)^2 dx \qquad \text{(A-4)}$$

where $g(\theta)$ is the angular dependence of the anisotropy and θ is the angle between the easy direction and the moment of the atom. The effective magnetic moment m per atom is given by

$$m_x = 0, \quad m_y = m \sin\theta, \; m_z = m \cos\theta \; .$$

If it be considered that the change in θ with distance is uniform across the wall of thickness d and that the distance between cations is a, then for an 180° wall $\frac{d\theta}{dx} = \frac{\pi a}{d}$.

For equilibrium to exist the two energies must be equal; so

$$K_1 \int_0^d g(\theta)\,dx = A_e \int_0^d \left(\frac{d\theta}{dx}\right)^2 dx.$$

Therefore,

$$\frac{dx}{d\theta} = \sqrt{\frac{A_e}{K_1 g(\theta)}} \qquad \text{(A-5)}$$

The application of a field H_z produces a torque whose lever arm is proportional to sin θ. According to Eq. 3 this results initially in a precession about the z-axis. However a precession over a finite angle results in an increased exchange energy. For the divergence of B to remain zero a closing field in the x-direction is required, i.e., $H_x = - M_x$. A second precession then occurs about the resultant field of $H_x + H_z$. The field H_x is, for small signals, much larger than H_z. Therefore the resultant motion is in the z-direction with an ensuing movement of the apparent wall.

In order to estimate the effective field H_x, note that the rate of precession of each dipole is given by $\omega = \gamma\mu_o H_x = \frac{d\theta}{dt}$. Now $\frac{d\theta}{dx} v = \frac{d\theta}{dt}$, where v is the velocity of the wall; so it follows that:

$$H_x = \frac{v}{\gamma\mu_o} \frac{d\theta}{dx} = \frac{v}{\gamma\mu_o} \frac{\sqrt{g(\theta)}}{\delta} \qquad \text{(A-6)}$$

where $\delta = \sqrt{A/K_1}$.

The power dissipated per unit volume in the material is given by $-\mu_o \vec{H} \cdot \frac{\partial \vec{M}}{\partial t}$. Upon solving from Eq. 3 and assuming $H_x >> H_z$, $-\mu_o \vec{H} \cdot \frac{\partial \vec{M}}{\partial t} = \lambda H_x^2$. The power generated in the magnetic lattice must equal the power dissipated so that

$$2M_s H_z \mu_o v = \int_{-o}^{d} \mu_o \lambda H_x^2 \, dx = \frac{\mu_o v^2 \lambda}{\mu_o^2 \gamma^2 \delta} \int_o^{\pi} \sqrt{g(\theta)} \, d\theta$$

and

$$v = \frac{2M_s \gamma^2 \mu_o^2 \delta}{\lambda \int_o^{\pi} \sqrt{g(\theta)} \, d\theta} H_z . \qquad \text{(A-7)}$$

Equation A-7 is a relation between the applied field and the velocity of the wall, so the velocity coefficient β of Eq. 10 is given by

$$\beta = \frac{\lambda}{\gamma^2 \mu_o \delta} \int_o^{\pi} \sqrt{g(\theta)}\, d\theta \qquad \text{(A-8)}$$

The wall distortion because of the attempted precession about H_z gives rise to an increase in the energy stored in the wall because of the increased angles between nearest neighbor spins. This added energy is, per unit area, given by

$$-\frac{\mu_o}{2} \int_o^d M_x H_x dx = \frac{\mu_o}{2} \int_o^d H_x^2 \, dx$$

$$= \frac{v^2}{2} \frac{\int_o^{\pi} \sqrt{g(\theta)}\, d\theta}{\gamma^2 \mu_o \delta} .$$

If the coefficient of $(\frac{v^2}{2})$ is set equal to an effective mass m,

$$m = \frac{1}{\gamma^2 \mu_o \delta} \int_o^{\pi} \sqrt{g(\theta)}\, d\theta \qquad \text{(A-9)}$$

Note that $\beta = \lambda m$. Thus the differential equation:

$$2M_s H \mu_o = \beta \dot{x} + m \ddot{x}$$

Because of local strains and magnetostatic energies, as discussed in Section 3.3, a term proportional to the displacement, not derivable from Eq. 3, exists. Thus the final differential equation describing wall motion is:

$$2M_s H \mu_o = \alpha x + \beta \dot{x} + m \ddot{x} \qquad \text{(A-10)}$$

APPENDIX B

FREQUENCY DEPENDENCE OF SUSCEPTIBILITY

B.1 The Landau-Lifshitz Differential Equation

The differential equation of note here is[9]:

$$\frac{\partial M}{\partial t} = \gamma\mu_o \left[M \times H'\right] - \frac{\lambda\mu_o}{M_s^2}\left[M \times \left[M \times H'\right]\right] \qquad \text{(B-1)}$$

Now introduce an operator i which represents a spatial rotation from the x to the y axis. Also define[31]:

$$M_+ \triangleq M_x + iM_y$$

$$M_- \triangleq M_x - iM_y$$

$$\epsilon \triangleq \lambda/\gamma M_s$$

H' is the total field and is the sum of the effective internal field H_{in} and the applied alternating field $H_r = (H_x + H_y)$. The susceptibility to be measured is that resulting from the alternating field H_r. Let all time dependent quantities vary as exp ($j\omega t$) and let the spontaneous moment be oriented in the z direction along with the internal field H_{in}. The latter in essence requires that $H_{in} >> H_r$. Solving (B-1) and neglecting second order terms;

$$j\omega M_s = \gamma\mu_o (M_y H_{in} - M_s H_y) - \frac{\lambda\mu_o}{M_s}(H_{in} M_x - H_x M_s)$$

$$j\omega M_y = \gamma\mu_o (M_s H_x - H_{in} M_x) - \frac{\gamma\mu_o}{M_s}(H_{in} M_y - H_y M_s)$$

Therefore,

$$\frac{dM_s}{dt} = 0 \; ; \; M_z \cong M_s \; .$$

$$j\omega M_+ = - i\gamma\mu_o \, (1 - i\epsilon) \, (H_{in} \, M_+ - H_+ \, M_s)$$

$$j\omega M_- = i\gamma\mu_o \, (1 + i\epsilon)(H_{in} \, M_- \, H_- \, M_s)$$

where:

$$H_+ \triangleq H_x + iH_y$$

Taking the ratios M_+/H_+ and M_-/H_- and setting them equal to χ_+ and χ_- respectively:

$$\chi_+ = \frac{\gamma\mu_o \, M_s}{\gamma\mu_o \, H_{in} - \frac{ij\omega}{1-i\epsilon}} \; ; \quad \chi_- = \frac{\gamma\mu_o \, M_s}{\gamma\mu_o \, H_{in} + \frac{ij\omega}{1+i\epsilon}} \qquad \text{(B-2)}$$

$$\chi_z = 0.$$

The initial polycrystalline susceptibility (See Appendix H) can be taken as:

$$\chi_i^r = \frac{1}{3} \, (\chi_+ + \chi_-)$$

where χ_i is the value of susceptibility when the applied field and internal magnetization are both zero. (This in essence assumes the magnetic moments to be randomly oriented.) Therefore:

$$\chi_i^r = \frac{2\omega_z}{3} \left[\frac{\left[\omega_i^2(1 + \epsilon^2) - \omega^2 \, (1 - \epsilon^2)\right] \omega_i - j\omega\epsilon \left[\omega_i^2(1 + \epsilon^2) + \omega^2\right]}{\omega_i^4(1 + \epsilon^2)^2 - 2\omega_i^2\omega^2 \, (1 - \epsilon^2) + \omega^4} \right] \qquad \text{(B-3)}$$

where:

$$\omega_i = \gamma\mu_o H_{in}$$

$$\omega_z = \gamma\mu_o M_s$$

One of the easiest results of Eq. B-3 to check experimentally is the frequency at which the imaginary portion of the susceptibility peaks. To solve for this analytically from Eq. B-3 proceed in the usual fashion by setting the partial of $Im(\chi_i^r)$ with respect to ω equal to zero and solve for ω. If this frequency is defined to be ω_a the result is[26]:

$$\omega_a = \omega_i (1 + \epsilon^2)^{\frac{1}{2}} = \gamma\mu_o H_{in} \sqrt{1 + \epsilon^2} \qquad \text{(B-4)}$$

It is also of interest to note the zero frequency value of the real part of the susceptibility, χ_o^r. Solving (B-3)

$$\chi_o^r = \frac{2M_s}{3H_{in}} \qquad \text{(B-5)}$$

Therefore the product $\chi_o^r\omega_a$ is given by:

$$\chi_o^r\omega_a = \frac{2\mu_o\gamma M_s}{3} \sqrt{1 + \epsilon^2} \cong \frac{2\gamma\mu_o M_s}{3} \text{ for small } \epsilon. \qquad \text{(B-6)}$$

Thus the product $\chi_o^r\omega_a$ is a constant depending only upon M_s.

B.2 The Harmonic Oscillator Equation

The frequency variation of wall motion is assumed to be describable by the differential equation

$$m\ddot{x} + \beta\dot{x} + \alpha x = 2\mu_o M_s H_z \qquad \text{(B-7)}$$

The magnetization M_z resulting from a wall moving a distance x is $M_z = 2xM_sC$, for 180^o walls. Assuming, as in Section 3.1, a time dependence

exp (jωt) for all time dependent quantities and solving for the initial susceptibility:

$$\chi_i^w = \frac{1 - \frac{\omega^2}{\omega_o^2} - j\frac{\omega}{\omega_1}}{1 - \frac{\omega^2}{\omega_o^2} + \frac{\omega^2}{\omega_1^2}} \chi_o^w \qquad \text{(B-8)}$$

where:

$$\omega_o^2 = \frac{\alpha}{m}$$

$$\omega_1 = \frac{\alpha}{\beta}$$

The zero frequency value of χ_i^w is:

$$\chi_o^w = \frac{4M_s^2 C\mu_o}{\alpha} \qquad \text{(B-9)}$$

It is also of interest to solve for the frequency at which the imaginary portion of the susceptibility will peak. Proceeding in the usual manner the frequency ω_a is found to be:

$$\omega_a^2 = \frac{\omega_o^2}{6}\left[2 - \left(\frac{\omega_o}{\omega_1}\right)^2\right]\left(1 + \frac{4\sqrt{1 - \frac{1}{4}\frac{\omega_o^2}{\omega_1^2} + \frac{1}{16}\left(\frac{\omega_o}{\omega_1}\right)^4}}{2 - \left(\frac{\omega_o}{\omega_1}\right)^2}\right) \qquad \text{(B-10)}$$

The form of Eq. B-10 is quite complex. However, two extremes can be taken — that of very highly damped motion with $\omega_o > \omega_1$ and very lightly damped motion with $\omega_o << \omega_1$.

For the lightly damped motion, with $\omega_o \leq \omega_1$, ω_a can be approximated by:

$$\omega_a = \omega_o \sqrt{1 - \left(\frac{\omega_o}{2\omega_1}\right)^2} \qquad \text{(B-11)}$$

In the limiting case of no damping $\omega_a = \omega_o$. For the highly damped case the peak frequency is given by:

$$\omega_a = \omega_1 \sqrt{1 + 2\left(\frac{\omega_1}{\omega_o}\right)^2} \qquad \text{(B-12)}$$

For the limiting case of zero effective mass $\omega_a = \omega_1$.

The product of the initial susceptibility and the frequency of the peak in the imaginary portion of the susceptibility is, therefore, for the case of highly damped motion:

$$\chi_o^w \omega_a = \frac{4M_s^2 C\mu_o}{\beta} . \qquad \text{(B-13)}$$

The product involves a constant and M_s^2/β.

For the case of lightly damped motion $\omega_a \simeq \omega_o$ and the product $\omega_a^2 \chi_o^w$:

$$\omega_a^2 \chi_o^w = \frac{4M_s^2 C\mu_o}{m} \qquad \text{(B-14)}$$

involves constants and M_s^2/m.

APPENDIX C

CAN THE EFFECT OF SNAGS BE CONSIDERED AS AN EFFECTIVE FIELD?[32]

In Section 4.1 it is observed that if the history could be treated as an effective[32] field, then the total field term H_t could be considered as a parameter and eliminated between the magnetization and the susceptibility. This technique can be explained, if not justified, from two standpoints.

Not for a justification, but for an explanation of the susceptibility, consider what it would be in the absence of wall snags, or wall nucleation energies. Then assume the measured susceptibility to be linearly related to the above described susceptibility. See Fig. C1. The curve χ_R represents the reversible susceptibility in the absence of holes and nucleation energies, i.e., assuming only that the state occupied is the most probable state as given by an
The initial point on the $\hat{\chi}$ curve is given by the slope of the virgin material as a field H_b is applied, and the bottom dashed curve is the measured reversible susceptibility χ_r which is here to be considered linearly related to χ_R.

Assuming Eq. D-7 and isotropy, the fraction of the atomic moments oriented at an angle between θ and $\theta + d\theta$ with respect to the applied field is given by:

$$f(\theta)\, d\theta = \frac{\exp(\eta \cos\theta)\, d\theta}{\frac{1}{\eta}(e^{\eta} - e^{-\eta})} \qquad (C\text{-}1)$$

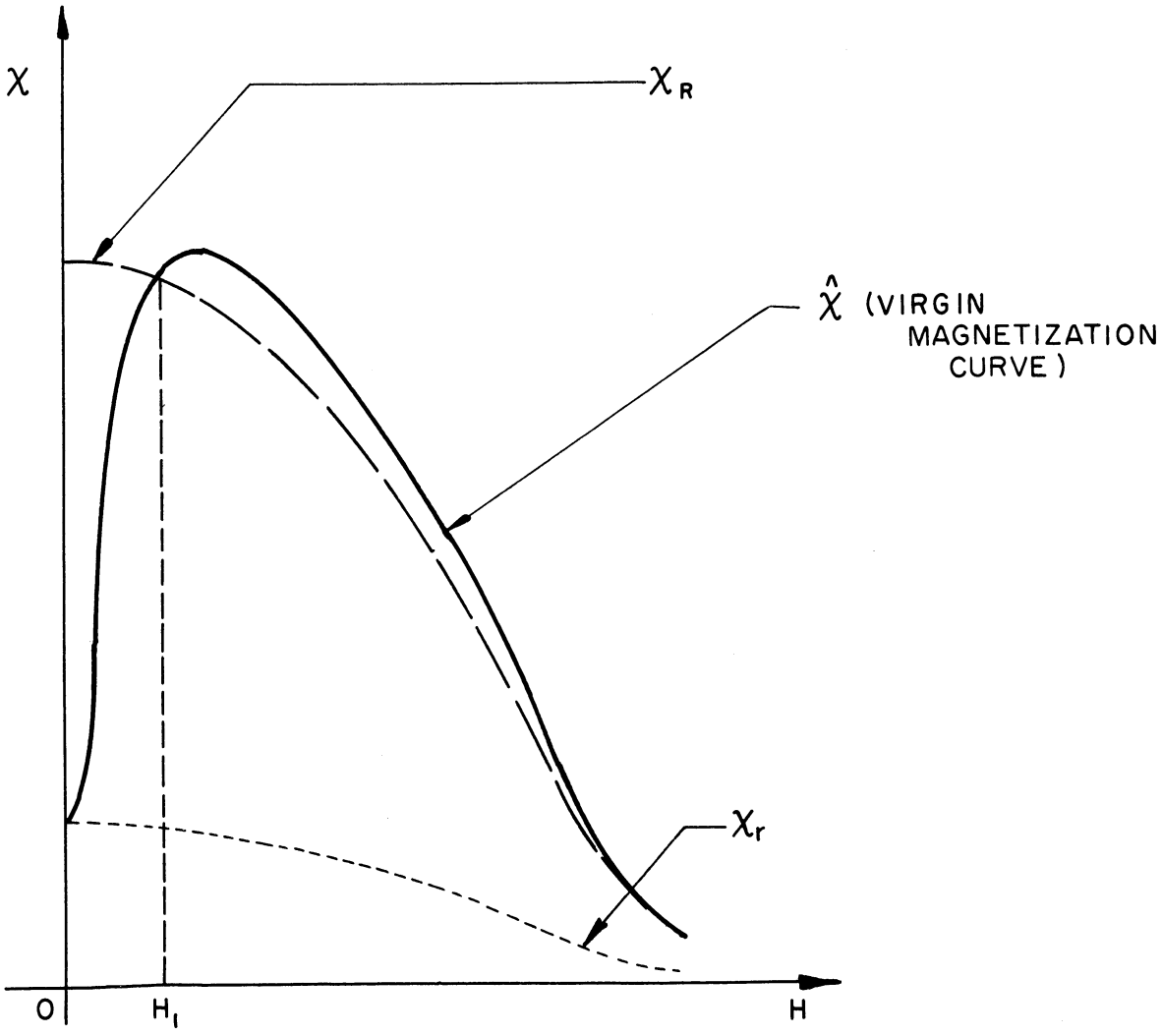

FIG C.I

VARIATION OF χ WITH H

(χ IN SAME DIRECTION AS H)

——— SLOPE OF THE VIRGIN MAGNETIZATION CURVE

— — — SLOPE OF THE QUASI-REVERSIBLE MAGNETIZATION CURVE

- - - - - - - - REVERSIBLE SUSCEPTIBILITY

where η is proportional to the applied field. Similar equations hold for assumed anisotropies, given by:

$$f_j = \frac{\exp(\eta \cdot \gamma_j)}{\sum_j^k \exp(\eta \cdot \gamma_j)} \qquad (C\text{-}2)$$

γ_j is a unit vector in the j-direction. Consider the case of a specific wall. Start from the demagnetized state where $f_j = \frac{1}{k}$ and a_{ij}^{σ} is the area of a particular wall separating domains oriented in the directions γ_i and γ_j respectively and x^{σ} is the spatial coordinate of the σ th wall relative to an equilibrium position. The sum over sigma is a sum over all walls of type ij, that is separating domains oriented in the i and the j direction, in unit volume. Now consider, using statistical arguments, the irreversible trapping of domain walls in metastable positions by potential holes. Each hole is to be characterized by a single number, loosely called its "depth", d. A wall encountering such a hole will be trapped if the total net force of the field plus reversible forces on the wall is less than d, but will break free irreversibly if this force exceeds d. Actually these potential minima must surely, for finite wall areas, have a finite radius of curvature. However, for purposes of this discussion consider them to be infinitely sharp "snags" i.e., a wall is held rigidly when trapped by a potential hole. A wall thus held would contribute nothing to the susceptibility. Consider a field to be applied, from the original position the resulting f_j must be given by

$$f_j = \frac{1}{k} + \sum_i^k \sum_{\sigma} a_{ij}^{\sigma} x^{\sigma} . \qquad (C\text{-}3)$$

Without snags, x^{σ} would be a function for a given wall only of the pressure p_{ij} which the applied field exerts, given by

$$p_{ij} = M_s \left[\vec{H} \cdot (\gamma_i - \gamma_j)\right] \mu_o$$

The wall would seek a position for which the reversible pressure just balanced this pressure.

When snags are present walls will become trapped in them, and x^σ will no longer be a simple function of pressure. We can express the average x^σ for a large number of walls in terms of a size distribution of these snags by arguments of the nature of a "mean free path" discussion. (See Fig. C2).

The number of snags per unit volume whose depth lies between d and d + Δd be given by ξ (d)Δd. Let there be an initial state in which there is a field H_o present, and all the walls occupy positions x_o determined only by this field and the reversible forces, i.e., no walls are snagged in metastable positions. When the field is changed to H_1, there will be a net force on each wall which will diminish again to zero when the wall reaches a new equilibrium position x_1. As a wall of area a moves over an interval dx, it sweeps over a volume adx. If this volume contains a snag "deeper" than the net force of the field plus reversible forces at that place, then the wall will be caught and held there.

Of all the walls in unit volume, let us select for attention the group consisting of all walls of class ij with area between a_{ij} and $a_{ij} + da_{ij}$. By choosing the coordinates so that x_o is zero for each wall, then in first approximation the final "reversible" position x_1 of every wall of this select group is equal to the average value $\bar{x}_1$, and the net force g(x) of field plus reversible force at each value of x for every wall is equal to some $\bar{g}(x)$ averaged over all the walls. The subscript ij will be assumed understood.

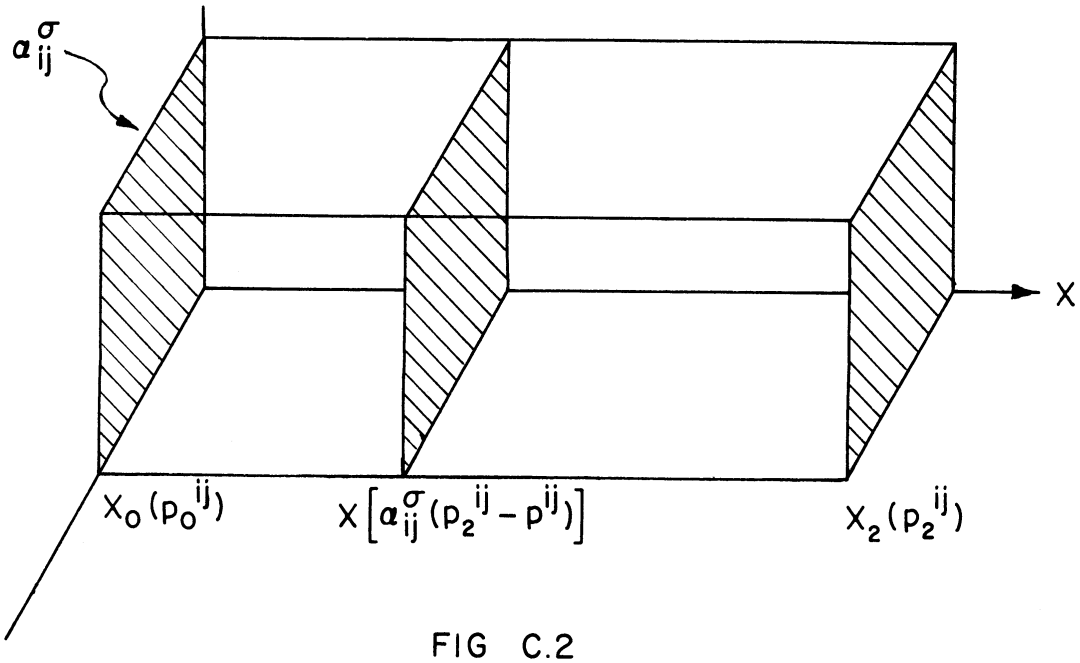

FIG C.2

SPATIAL CO-ORDINATE OF A DOMAIN WALL

Let N_o be the number of walls in this group, and N(x) the number not yet caught after moving a distance x from x_o. Then clearly

$$dN(x) = - N(x)\, a_{ij} dx \int_{g(x)}^{\infty} \xi\,(d)\Delta d$$

$$N(x) = N_o \exp \left[- a_{ij} \int_o^x dx' \int_{g(x)}^{\infty} \xi\,(d)\Delta d \right] .$$

The fraction of the original group of walls that becomes snagged in the interval x to x + dx is then

$$\psi\,(x)dx = \left| dN(x) \right| \quad N_o = \left(\exp \left[- a_{ij} \int_o^x dx' \right.\right.$$

$$\left.\left. \int_{g(x)'}^{\infty} \xi\,(d)\Delta d \right] a_{ij} \int_{g(x)}^{\infty} \xi\,(d)\Delta d \right) dx,$$

and the average position at which the walls of the group considered become snagged and stopped is

$$\bar{x} = \int_o^{\bar{x}_1} x\, \psi\,(x)\, dx . \qquad \text{(C-4)}$$

The result, whether or not the result of hysteresis can be expressed as an effective field, can be seen from the form of Eq. C-4. To the same approximation as that contained in Eq. C-4, the quantity x to be used in Eq. C-3 for the strictly reversible case is exactly the average "final reversible" coordinate $\bar{x}_1$ that appears as the upper limit in Eq. C-4. Now $\bar{x}_1$ must have a certain (perhaps quite complicated) dependence on the relative directions of γ_i, γ_j and the applied field H that is consistent with the existence of Eq. C-1 for the reversible case. Without any detailed analysis it is clear that $\bar{x}$ has additional

dependence on these directions arising in the expression for $\psi(x)$. So the distribution in numbers of atoms oriented in the various possible directions, in the presence of "snags" and metastable wall positions, is different from that implied by an expression of the form of Eq. C-1. Thus it is not possible to precisely define any simple vector "history field H_h" that accurately allows a description of the system solely in terms of Eq. C-1.

APPENDIX D

DERIVATION OF $f(\theta)\, d\theta$

D.1 General Formulation

The necessity for using statistical techniques for analyzing the ferromagnetic problem of the variation of the reversible susceptibility of ferromagnetic material with the magnetization level was discussed in the last of Chapter 2 and in Section 4.1. The difficulties involved were also mentioned. The basic difficulty is that if an attempt is made to carry over the usual techniques of statistical mechanics to the problem of formulating the probability of a particular magnetic moment being oriented in a particular direction, the usual disorder because of thermal agitation is negligible compared with the other forces involved. However, other randomizing effects do enter but in such a way that the energy of a particular atomic moment is not independent of its coordinates.

Let us start by considering the total energy of a system consisting of a ferromagnetic or ferrimagnetic polycrystalline nonoriented material. The energy will be divided into three rather distinctly different types: the magnetostatic energy, the exchange energy, and the magnetoelastic energy. Each type will be composed of a term proportional to the total number of atomic moments along some particular direction (a volume energy term) plus a term proportional to some type of surface area (a surface energy term).

Herein the magnetostatic energy will signify the mutual energy between the magnetization and the applied field as well as the energy be-

cause of effective magnetic poles and nonzero demagnetizing factors. The energy between the applied field and the magnetic moment contained by atoms aligned in a specified direction is proportional to the number of atoms so aligned. In addition each grain will contain an energy proportional to its demagnetizing factor which will depend upon the crystalline orientation of nearest-neighbor grains and also, though not independently, upon the angle between magnetic moments in neighboring grains. Our model assures that the orientation is random but not necessarily the angle between moments.

The exchange energy is considered to arise because of overlapping of wave functions associated with neighboring atoms. This energy is assumed to be a function only of the angle between neighboring atomic moments. At a later stage in the development of a distribution function it will be assumed that the material is arrayed in domains so that the exchange energy is constant except in a domain wall. It would therefore contain a constant volume term and a surface term proportional to the total domain wall area.

The magnetoelastic energy is considered to consist of both the anisotropy energy and the magnetostrictive energy. If it is assumed that each moment of the system remains arrayed along some "easy" crystallographic direction, then the anisotropy energy can and will be considered constant. In addition, the magnetostrictive energy will contain a term local to each crystallite with its associated pattern of arrayed magnetic moments. The result will be effective magnetic poles depending upon the strains induced by moments producing changes in size of neighboring domains. Once again this will depend upon both the relative crystalline orientation of nearest neighbor grains and the angle between their magnetic moments.

In the formulation of $f(\theta)\, d\theta$ proposed by Brown[11], the smallest unit was the domain. He chose all domains to be of fixed and equal volume. His justification for such a model was that the important relationships involved are the energy relationships which must vary but little from one model to another. For purposes of this paper it is convenient to take as the smallest unit of the system the atomic moment of the atomic constituents of the system.

The surface energy arising from the magnetostatic term and from the magnetoelastic term will produce fluctuations in the energy carried by the atomic moments from spot to spot in the crystal. The system is a static system so that each particular moment occupies a fixed energy, but the energy per moment must vary in some random fashion throughout the material. Any measurement on the system must asure a system average resulting from this random variation in local forces.

Since sufficient information does not exist to calculate the precise state inside the ferromagnet, it will be assumed here on the basis of the arguments of the preceeding paragraph that the randomized forces act to array the atomic moments in their most probable configuration. This is, of course, the role assigned to thermal agitation in a more conventional system such as a paramagnetic gas in thermal equilibrium. In the present system it is assumed that all temperature effects are adequately described by incorporating into the system such temperature-dependent parameters as the saturation moment, the anisotropy and the magnetostriction.

If there are N magnetic atoms per unit volume, and if γ is any specific direction in the crystal, then the number of atoms per unit volume with magnetization vectors lying in the γ-direction is $N\gamma$. Thus,

$$N = \sum_{\gamma} N_{\gamma} \qquad \text{(D-1)}$$

The number of ways that are macroscopically indistinguishable in which magnetization vectors can be distributed among a lattice of N atoms so that N_γ have their vectors lying in the γ direction is:

$$W = \frac{N!}{\prod(N_\gamma!)} \qquad \text{(D-2)}$$

By use of Stirling's approximation,

$$\ell n\, W = N \ell nN - \sum_{\gamma} N_\gamma \ell n N_\gamma . \qquad \text{(D-3)}$$

The surface magnetostatic and magnetoelastic energies are assumed to require that Eq. D-3 be stable with respect to variation in N_γ, which will adequately describe their effect. The volume magnetostatic energy remains and is given by:

$$V_1 = \sum_{\gamma} N_\gamma A H_t \cos\Theta \qquad \text{(D-4)}$$

where A is a constant, H_t is the total field and Θ is the angle between the direction γ and the field H_t. The exchange energy is given by:

$$V_2 = \sum_{\gamma} \sum_{nn} N_\gamma A_e \left[1 - (\Delta\Theta_\gamma)^2 \right] \qquad \text{(D-5)}$$

where $(\Delta\Theta_\gamma)$ is the angle between nearest neighbor atomic moments, A_e is the exchange interaction and $\sum_{nn}$ represents a sum over all nearest neighbor atomic moments.

Equations D-1, D-3, D-4 and D-5 must be stable with respect to variations in N_γ, the number of atomic moments oriented in the γ-direction.

D.2 Mathematical Development

Proceeding to take variations with respect to N_γ of Eqs. D-1, D-3, D-4 and D-5, and using the technique of Lagrange multipliers gives:

$$\sum_\gamma \delta N_\gamma \left[- \ell n N_\gamma + AH_t \cos\theta + \sum_{nn} BA_e - \sum_{nn} N_\gamma BA_e \frac{\partial(\Delta\theta_\gamma)^2}{\partial N_\gamma} + C \right] = 0 \qquad \text{(D-6)}$$

$$N_\gamma = \exp \left[AH_t \cos\theta + D - \sum_{nn} N_\gamma BA_e \frac{\partial(\Delta\theta_\gamma)^2}{\partial N_\gamma} \right]$$

where A, B, C are constants. Thus the normallized volume with its magnetic moment oriented in the γ-direction is given by:

$$f_\gamma = \frac{\exp\left(AN_t \cos - \sum_{nn} N_\gamma BA_e \frac{\partial(\Delta\theta_\gamma)^2}{\partial N_\gamma} \right)}{\sum \exp\left(AH_t \cos\theta - \sum_{nn} N_\gamma BA_e \frac{\partial(\Delta\theta_\gamma)^2}{\partial N_\gamma} \right)} .$$

The second term in the exponential is nonzero only if neighboring moments are not aligned. At this point let us introduce domain theory into the development by requiring that all moments be aligned except at the domain boundaries, and further require that the total domain wall area be constant. Thus the second term is constant and f_γ becomes:

$$f_\gamma = \frac{e^{AH \cos\theta_\gamma}}{\sum_\gamma e^{AH \cos\theta_\gamma}} \qquad \text{(D-7)}$$

where θ_γ is the angle between the field H and the γ-direction.

The magnetic moment per crystallite is the sum of the component of each atomic spin in the direction of the field; thus:

$$M = M_s \frac{\sum_\gamma \cos\theta_\gamma \exp (AH \cos\theta_\gamma)}{\sum_\gamma \exp (AH \cos\theta_\gamma)} \qquad \text{(D-8)}$$

To get the moment for a nonoriented polycrystalline material it is necessary to integrate Eq. D-8 over the unit sphere. The result is an integrated relationship between H and M about a specified point, so long as those variations do not result in altering the total wall area in the material. Thus any reversible susceptibility should be calculable from Eq. D-8. When the wall energy is altered its effect will be determined by its dependence upon N_γ. This is not known. However, about each point Eq. D-8 must be valid. Thus a determination of the operating point by a determination of the magnetization will, within the accuracy of this derivation, allow the calculation of other phenomena depending upon the form of Eq. D-6 as functions of the magnetization.

The preceeding paragraph infers that the result of different total wall area can be treated as an effective history field.

APPENDIX E

THE DERIVATION OF THE MAGNETIC MOMENT AND THE REVERSIBLE SUSCEPTIBILITIES IN THE PRESENCE OF INFINITE ANISOTROPY FIELDS

E.1 The Derivation of the Magnetic Moment[30]

Appendix D considers the fraction of material $f(\theta)\, d\theta$ which carries a magnetic moment oriented between θ and $\theta + d\theta$ as a function of the variable η, where η is proportional to H_t, i.e., $\eta = A(H_b - NM + H_r)$ where A is a constant. When a magnetic field is applied to the material it is considered that all of the material remains aligned along some "easy" crystallographic direction. It is to be assumed that the crystallites are nonoriented and that the magnetization can be obtained by averaging over a polycrystal in which each atomic moment can be oriented only along certain specified directions.

[100] Orientation. Consider the direction cosines of the applied field with respect to the crystalline axes to be ℓ_i. Then the direction cosines of the field with respect to the moment will be $\pm\, \ell_i$. The magnetic moment per crystallite, M_k, is given by M_s times the weighted-average value of the cosine as a function of η. Thus:

$$M_k = M_s \frac{\sum (\ell_i\, e^{\eta \ell_i} - \ell_i e^{-\eta \ell_i})}{\sum (e^{\eta \ell_i} + e^{-\eta \ell_i})} = M_s \frac{\sum \ell_i \sinh \eta \ell_i}{\sum \cosh \eta \ell_i} \qquad \text{(E-1)}$$

for each crystallite.

Averaging over the nonoriented crystallites gives:

$$M = M_s \int \frac{d\Omega}{4\pi} \frac{\sum \ell_i \sinh \eta\, \ell_i}{\sum \cosh \eta\, \ell_i} = M_s\, G(\eta)\ . \qquad \text{(E-2)}$$

The integral of Eq. E-2 has been evaluated by Brown.[30] For small values of η it is approximated by the series

$$G(\eta) = \frac{\eta}{3} - \frac{\eta^3}{45} + \frac{2\eta^5}{945} - \frac{2\eta^7}{8505} + \frac{8\eta^9}{280,665} - \cdots \qquad \text{(E-3)}$$

For large values of η,

$$G(\eta) = 0.8312 - \frac{1.367}{\eta^2} - \frac{0.8816}{\eta^3} - \frac{4.419}{\eta^5} + \cdots \qquad \text{(E-4)}$$

[111] Orientation. The direction cosine of the magnetic moment with respect to each crystalline axis is $\pm 1/\sqrt{3}$ for this case. Thus the direction cosine of the moment with respect to the applied field is given by $\sum_i (1/\sqrt{3})\, p_i \ell_i$, where the p_i are ± 1, and the ℓ_i are the direction cosines of the applied field with respect to the crystalline axes. Thus the magnetization per crystallite, M_k, is given by:

$$\frac{M_k}{M_s} = \frac{\frac{1}{\sqrt{3}} \sum_p \sum_i p_i \ell_i \exp\left(\frac{\eta}{\sqrt{3}} \sum_i p_i \ell_i\right)}{\sum_p \exp\left(\frac{\eta}{\sqrt{3}} \sum_i p_i \ell_i\right)} . \qquad \text{(E-5)}$$

The sum over p indicates the sum over all eight possible combinations of three plus or minus ones. To evaluate E-5 note that the denominator can be written as $8\prod_i \cosh \frac{\eta}{\sqrt{3}} \ell_i$ and that the numerator can be written:

$$\frac{1}{\sqrt{3}} \sum_p \sum_i p_i \ell_i \, e^{\frac{\eta}{\sqrt{3}} \sum_i p_i \ell_i} = \sum_p \sum_k \ell_k \frac{\partial}{\partial \eta \ell_k} \left(\exp\left[\frac{\eta}{\sqrt{3}} \sum_i p_i \ell_i\right]\right) \qquad \text{(E-6)}$$

$$= \frac{8}{\sqrt{3}} \sum_i \ell_i \sinh \frac{\eta}{\sqrt{3}} \ell_i \prod'_k \cosh \frac{\eta}{\sqrt{3}} \ell_k .$$

where the prime indicates that the product does not include i. Thus the moment per crystallite is given by:

$$\frac{M}{M_s} = \frac{1}{\sqrt{3}} \sum_i \ell_i \tanh \frac{\eta}{\sqrt{3}} \ell_i \qquad \text{(E-7)}$$

Averaging over the nonoriented polycrystal gives:

$$\frac{M}{M_s} = E(\eta) = \frac{1}{\sqrt{3}} \sum_i \int \frac{d\Omega}{4\pi} \ell_i \tanh \frac{\eta}{\sqrt{3}} \ell_i \, . \qquad \text{(E-8)}$$

Simplifying Eq. E-8 gives:

$$E(\eta) = \frac{3\sqrt{3}}{\eta} \int_0^{\eta/\sqrt{3}} u \tanh u \, d u \, . \qquad \text{(E-9)}$$

The integral E-9 has been evaluated by Brown.[30] For small values of η it can be expanded as:

$$E(\eta) = \frac{\eta}{3} - \frac{\eta 3}{45} + \frac{2\eta^5}{945} - \frac{17\,\eta^7}{76{,}545} + \frac{62\,\eta^9}{2{,}525{,}985} - \ldots \qquad \text{(E-10)}$$

For large values of η it can be expanded as:

$$E(\eta) = .8667 - \frac{3\sqrt{3}}{2\eta^2} \left[\frac{\pi^2}{12} - \left(\frac{2}{\sqrt{3}} \eta + 1 \right) u + \left(\frac{4}{\sqrt{3}} \eta + 1 \right) \frac{u^2}{2^2} - \left(\frac{6\eta}{\sqrt{3}} + 1 \right) \frac{u^3}{3^2} + \ldots \right] \qquad \text{(E-11)}$$

where

$$u = e^{-\frac{2\eta}{\sqrt{3}}} \, .$$

Powers of u^2 have been neglected.

Note that the largest possible value of M_s is larger for the [111] orientation than for the [100] orientation. This can be understood as arising from there being a larger number of possible directions of orientation for the [111] case.

Isotropic Material. The isotropic case must be considered as isotropic not from the standpoint of zero anisotropy but from the standpoint of an infinite number of possible orientations as opposed to the six and eight in the two preceeding paragraphs. For this case the moment is given by:

$$\frac{M}{M_s} = \frac{\int_0^{\pi} d\theta \sin\theta \cos\theta \, e^{\eta\cos\theta}}{\int_0^{\pi} d\theta \sin\theta \, e^{\eta\cos\theta}} = \frac{\frac{1}{\eta}(e^{\eta} + e^{-\eta}) - \frac{1}{\eta^2}(e^{\eta} - e^{-\eta})}{\frac{1}{\eta}(e^{\eta} - e^{-\eta})} \qquad \text{(E-12)}$$

$$\frac{M}{M_s} = L(\eta) = (\text{ctnh}\ \eta - \frac{1}{\eta}) \qquad \text{(E-13)}$$

To compare with the two preceding paragraphs, the expansions for small and large values of η are given by:

$$L(\eta) = \frac{\eta}{3} - \frac{\eta 3}{45} + \frac{2\eta 5}{945} - \frac{\eta 7}{4725} + \frac{2\eta 9}{93,555} - \ldots \qquad \text{(E-14)}$$

for small values of η, and by:

$$L(\eta) = 1 - \frac{1}{\eta} + 2(e^{-2\eta} + e^{-4\eta} + e^{-6\eta} + \ldots) \qquad \text{(E-15)}$$

for large values of η.

Note that the limiting M for large η is M_s as is to be expected when an infinite number of possible directions of orientation exist. For small values of η the series for all three types are identical to the seventh power of η.

E.2 The Parallel Field Reversible Susceptibility.[30] Wall Movement.

Mathematical functions for the magnetization in terms of the variable η are derived in Section E.1. It is desired to derive express-

ions for the susceptibility in terms of the same variable so it can then be eliminated between the two functions. The functions of Section E.1 were derived assuming that the material remained at all times oriented along some particular easy direction, i.e. the effective anisotropy fields were infinite. If the field is decreased slightly in the opposite direction from that which brought it to the point M,H the effective history field should remain constant. Thus the only change in the field H' will be felt through the change in the applied measuring field H_r. Thus the derivative of the magnetization function will give the parallel reversible susceptibility for the case of magnetization by wall movement. So,[12]

$$\chi^{w}_{rp} = \frac{\partial M}{\partial H_r} = \frac{dM}{d\eta}\frac{d\eta}{dH_r} = AM_s \frac{d\,F(\eta)}{d\eta} \qquad \text{(E-16)}$$

since $$\eta = A(H_b + H_r + H_h - NM). \qquad \text{(E-17)}$$

H_b represents the biasing field, H_r the applied reversible field and H_h the effective history field. The function $F(\eta)$ indicates one of the three functions $G(\eta)$, $E(\eta)$, or $L(\eta)$ as the anisotropy condition might warrant.

If the initial susceptibility χ^{w}_{o} is defined to be that value of the reversible susceptibility present when the magnetization is zero, and since the value of $\frac{dF(\eta)}{d\eta}$ for $\eta = 0$ is $1/3$, for any of the three functions derived in Section E.1,

$$\chi^{w}_{o} = \frac{1}{3} AM_s \qquad \text{(E-18)}$$

and $$\chi^{w}_{rp} = 3\,\chi^{w}_{o}\,\frac{d\,F(\eta)}{d\eta}\,. \qquad \text{(E-19)}$$

The subscript r on χ indicates the reversible susceptibility, the sub-

script p indicates parallel fields and the superscript w indicates wall motion.

E.3 The Transverse Field Reversible Susceptibility. Wall Movement.

This case differs from Section E.2 by the field H_r being oriented normal to the field H_b as opposed to antiparallel. The total magnetization must remain parallel with total field. Thus (see Figure 5):

$$\chi_{rt}^{w} = \frac{\partial M}{\partial H_r} = \frac{M}{H_t} = M_s \frac{F(\eta)}{\eta/A} = 3\chi_o^{w} \frac{F(\eta)}{\eta} . \qquad \text{(E-20)}$$

As before, the function $F(\eta)$ will be $G(\eta)$, $E(\eta)$, or $L(\eta)$ as the anisotropy conditions might warrant.

APPENDIX F

EVALUATION OF THE TRANSFORMATION MATRICES α AND α^{-1}

A matrix describing the transformation from one set of axes to another rotated at an arbitrary angle to the first is given in terms of the Euler angles as[31,33]:

$$A = \begin{pmatrix} \cos\psi\cos\phi - \cos\theta\sin\phi\sin\psi & \cos\psi\sin\phi + \cos\theta\cos\phi\sin\psi & \sin\psi\sin\theta \\ -\sin\psi\cos\phi - \cos\theta\sin\phi\cos\psi & -\sin\psi\sin\phi + \cos\theta\cos\phi\cos\psi & \cos\psi\sin\theta \\ \sin\theta\sin\phi & -\sin\theta\cos\phi & \cos\theta \end{pmatrix} \quad \text{(F-1)}$$

This matrix is for coordinates described in terms of x, y, and z. We wish to transform to a system described in terms of the coordinates x + iy, x - iy, and z. That is, we wish to solve for a matric C defined by:

$$C\,(x, y, z)' = (x + iy, x - iy, z)' \quad \text{(F-2)}$$

Solving for C from Eq. F-2:

$$C = \begin{pmatrix} 1 & i & 0 \\ 1 & -i & 0 \\ 0 & 0 & 0 \end{pmatrix} \quad \text{and } C^{-1} = \begin{pmatrix} \frac{1}{2} & \frac{1}{2} & 0 \\ -\frac{i}{2} & \frac{i}{2} & 0 \\ 0 & 0 & 1 \end{pmatrix} \quad \text{(F-3)}$$

To solve for the transformation matrix α in the new coordinate system, let q' and k' represent two coordinate systems based upon x,y,z and let q and k represent the same two coordinate systems based upon ($x + iy = x_+$, $x - iy = x_-$, z). From the definition of C, for any matrix Y, $CY_{q'} = Y_q$ and $CY_{k'} = Y_k$; so also $C^{-1}Y_q = Y_{q'}$. Now $AC^{-1}Y_q = AY_{q'} = Y_{k'}$, the last

equality by definition of the Euler matrix. Continuing by multiplying through by C, $CAC^{-1}Y_q = CAY_{q'} = CY_{k'} = Y_k$. Thus, if $AY_{q'} = Y_{k'}$, then $\alpha Y_q = Y_k$, where:

$$\alpha = CAC^{-1} \tag{F-4}$$

The algebra is considerable in the solution of Eq. F-4 for the matrix α. The result is

$$\alpha = \begin{pmatrix} a^2 & -b^2 & -2ab \\ -b^{*2} & a^{*2} & -2a^*b^* \\ ab^* & a^*b & aa^* - bb^* \end{pmatrix} \tag{F-5}$$

where

$$\begin{aligned} a &= \cos(\theta/2) \exp\left[-\frac{i}{2}(\phi + \psi)\right] \\ b &= -i \sin(\theta/2) \exp\left[\frac{i}{2}(\phi - \psi)\right] \end{aligned} \tag{F-6}$$

the asterisk (*) represents the complex conjugate.

It is also necessary to find the inverse matrix α^{-1}. To do this note that $\alpha = CAC^{-1}$ and, upon taking the inverse, $\alpha^{-1} = CA^{-1}C^{-1}$. One property of an orthogonal matrix is that its inverse is equal to its transpose or $A^{-1} = A'$, where the prime indicates the transpose operation. Continuing, $\alpha^{-1} = CA'C^{-1}$, but $A = C^{-1}\alpha C$ so $A' = C'\,\alpha'(C^{-1})'$. Thus $\alpha^{-1} = CC'\,\alpha'(C^{-1})'C^{-1} = CC'\,\alpha'(C')^{-1}C^{-1}$, so:

$$\alpha^{-1} = CC'\alpha'(CC')^{-1} \tag{F-7}$$

Solving for CC' and $(CC')^{-1}$ from Eq. F-3:

$$CC' = \begin{pmatrix} 0 & 2 & 0 \\ 2 & 0 & 0 \\ 0 & 0 & 1 \end{pmatrix} ; \quad (CC')^{-1} = \begin{pmatrix} 0 & \frac{1}{2} & 0 \\ \frac{1}{2} & 0 & 0 \\ 0 & 0 & 0 \end{pmatrix} \qquad \text{(F-8)}$$

Upon combining Eqs. F-5, F-6, and F-7 and working out the algebra,

$$\alpha^{-1} = \begin{pmatrix} a^{*2} & -b^2 & 2ab^* \\ -b^{*2} & a^2 & 2ab^* \\ -a^*b^* & -ab & aa^* - bb^* \end{pmatrix} . \qquad \text{(F-9)}$$

APPENDIX G

THE REVERSIBLE SUSCEPTIBILITY ASSUMING DOMAIN ROTATION

G.1 Development of the χ Matrix[34]

Expressions for the χ in terms of χ_+, χ_- and χ_z were developed in Appendix B and are given by Eq. B-2. In matrix notation, if k denotes a reference system based upon the individual crystallites,

$$\chi_k = \begin{pmatrix} \chi_+ & 0 & 0 \\ 0 & \chi_- & 0 \\ 0 & 0 & 0 \end{pmatrix} \qquad \text{(G-1)}$$

From Eq. 24, the susceptibility χ_q in a coordinate system based upon the gross sample is given by $a\chi_k a^{-1}$. The product $a\chi_k a^{-1}$ (from Eqs. F-5, F-9, and G-1) is given by:

$$\chi_q = \begin{pmatrix} (aa^*)^2\chi_+ + (bb^*)^2\chi_- & -b^2a^2(\chi_+ + \chi_-) & 2ab(aa^*\chi_+ - bb^*\chi_-) \\ -a^{*2}b^{*2}(\chi_+ + \chi_-) & (bb^*)^2\chi_+ + (aa^*)^2\chi_- & 2a^*b^*(-bb^*\chi_+ + aa^*\chi_-) \\ a^*b^*(aa^*\chi_+ - bb^*\chi_-) & -ab(bb^*\chi_+ - aa^*\chi_-) & 2aa^*bb^*(\chi_+ + \chi_-) \end{pmatrix} \qquad \text{(G-2)}$$

This is the general equation for the susceptibility of a polycrystal assuming only the Landau-Lifshitz differential equation.

G.2 The Reversible Susceptibility per Crystallite with Parallel Fields

For parallel fields the field matrix can be written as $H = (\,0\ 0\ H_r)'$. Multiplying H on the left by χ_q and taking the ratio M_z/H_r as the observed susceptibility, χ^r_{rp}, gives

$$\chi^r_{rp} = 2aa^*bb^*(\chi_+ + \chi_-) \qquad \text{(G-3)}$$

Substituting a and b from Eq. F-6 into Eq. G-3 gives:

$$\chi^r_{rp} = 2\cos^2(\theta/2)\sin^2(\theta/2)(\chi_+ + \chi_-) = (1/2)\sin^2\theta(\chi_+ + \chi_-) \qquad \text{(G-4)}$$

$$\chi^r_{rp} = \frac{1}{2}(1 - \cos^2\theta)(\chi_+ + \chi_-)$$

G.3 The Reversible Susceptibility per Crystallite with Transverse Fields

For transverse fields the field matrix can be written as

$(H) = (H_r \;\; 0 \;\; 0)'$. Multiplying H on the left by χ_q and taking the ratio M_x/H_r,

$$\chi^r_{rt} = \frac{1}{2}(\chi_{11} + \chi_{12} + \chi_{21} + \chi_{22}) \qquad \text{(G-5)}$$

where the χ's represent the components of the matrix χ_q. The result of combining Eqs. G-5, G-2 and F-6 gives:

$$\chi^r_{rt} = \frac{1}{2}(\chi_+ + \chi_-)\left[1 + \frac{1}{4}\sin^2\theta\,(e^{2i\psi} + e^{-2i\psi} - 2)\right]$$

or

$$\chi^r_{rt} = \frac{1}{4}(\chi_+ + \chi_-)\left[1 + \cos^2\theta + \sin^2\theta\cos 2\psi\right] \qquad \text{(G-6)}$$

APPENDIX H

THE EVALUATION OF THE AVERAGE χ^r_{rp} AND χ^r_{rt}

The equations for the susceptibility to be expected as a function of the angle θ between the z-axis of the macroscopic sample and the z-axis of the domain and as a function of the angle ψ in the x-y plane of the crystallite are given in Eqs. G-4 and G-6 of Appendix G. The only remaining problem is to average these equations over a polycrystal considering the possible orientations of the magnetic moment. This, in essence, assumes that the anisotropy fields are of the proper magnitude so that all of the material, in the presence of purely static fields, is oriented along easy directions. However, when an alternating low frequency signal is applied the resultant susceptibility arises because of the rotation of the moments of the domains against the noninfinite anisotropy fields.

By symmetry the third term of Eq. G-6 must average to zero over the polycrystal. It is therefore necessary only to average the terms $(1 - \cos^2\theta)$ and $(1 + \cos^2\theta)$ over the polycrystal. Define $\chi^r_o = \frac{1}{3}(\chi_+ + \chi_-)$.

[100] Orientation. Since both susceptibilities involve averaging the weighted value of $\cos^2\theta$ first over a single crystal, then over a polycrystal, it is necessary to solve for this averaged value; then each of the susceptibilities follow trivially. Referring to the definition of Section E.1 the weighted average value for the $\cos^2\theta$ for a given crystallite over all six possible orientations in the crystallite is given by:

$$\sum_{\theta} f(\theta) \cos^2\theta = \frac{\sum_i \ell_i^2 \left(e^{\eta \ell_i} + e^{-\eta \ell_i}\right)}{\sum_i \left(e^{\eta \ell_i} + e^{-\eta \ell_i}\right)} \qquad \text{(H-1)}$$

The sum over θ represents a sum over all possible orientations. Averaged over a nonoriented polycrystal:

$$\int \frac{d\Omega}{4\pi} \sum_{\theta} f(\theta) \cos^2\theta = \int \frac{d\Omega \sum \ell_i^2 \cosh \eta \ell_i}{4\pi \sum \cosh \eta \ell_i} = \frac{1}{3} + \frac{2}{3} H(\eta) \qquad \text{(H-2)}$$

The function $H(\eta)$ is defined by Eq. H-2. This function was encountered by Brown during his work on magnetostriction[30] and was evaluated by him. It cannot be expressed in an integrated closed form. Combining Eq. H-2 with the expression for χ_o^r, χ_{rp}^r and χ_{rt}^r gives:

$$\chi_{rp}^r = \chi_o^r \left[1 - H(\eta)\right] \qquad \text{(H-3)}$$

$$\chi_{rt}^r = \chi_o^r \left[1 + \frac{H(\eta)}{2}\right] \qquad \text{(H-4)}$$

when $M = M_s G(\eta)$. (See E-2).

As given by Brown for low values of η,

$$H(\eta) = \frac{\eta^2}{15} - \frac{2\eta^4}{315} + \frac{9\eta^6}{17{,}010} - \frac{4\eta^8}{93{,}555} + \ldots \qquad \text{(H-5)}$$

and for values of η high enough so that $e^{-\eta}$ can be neglected;

$$H(\eta) = 0.5513 - 2.721/\eta^2 - 1.527/\eta^3 + 6.266/\eta^4 + \ldots \qquad \text{(H-6)}$$

The values of the susceptibility and magnetization are listed in Table 4, and are illustrated in Figs. 8 and 9.

[111] Orientation. As was the case for [100] orientation, the problem is the evaluation of the average value of $\cos^2\theta$ weighted by the averaging function $f(\theta)$. This is seen to be, for a particular crystallite:

$$\sum_{\theta} f(\theta)\cos^2\theta = \frac{\frac{1}{3}\sum_{p}\left(\sum_{k} p_k \ell_k\right)^2 \exp\frac{\eta}{\sqrt{3}}\sum_{i} p_i \ell_i}{\sum_{p} \exp\frac{\eta}{\sqrt{3}}\sum_{i} p_i \ell_i} \qquad \text{(H-7)}$$

The denominator can also be written as:

$$\Sigma \exp\left(\frac{\eta}{\sqrt{3}}\sum_{i} p_i \ell_i\right) = 8\Pi_k \cosh\frac{\eta}{\sqrt{3}}\ell_k \qquad \text{(H-8)}$$

(See Section E.1)

To evaluate the numerator note that:

$$\sum_{p}\left(\sum_{k}\ell_k\frac{\partial}{\partial\eta\ell_k}\right)^2 \exp\left(\frac{\eta}{\sqrt{3}}\sum_{i} p_i\ell_i\right) = \frac{1}{3}\sum_{p}\left(\sum_{k} p_k\ell_k\right)^2 \exp\left(\frac{\eta}{\sqrt{3}}\sum_{i} p_i\ell_i\right)$$

$$+\frac{1}{\sqrt{3}\eta}\sum_{p}\sum_{k}(p_k\ell_k)\exp\left(\frac{\eta}{\sqrt{3}}\sum_{i} p_i\ell_i\right)$$

so that

$$\sum_{\theta} f(\theta)\cos^2\theta = \frac{\sum_{p}\left(\Sigma\,\ell_k\frac{\partial}{\partial\eta\ell_k}\right)^2 \exp\left(\frac{\eta}{\sqrt{3}}\sum_{i} p_i\ell_i\right) - \frac{1}{\sqrt{3}\eta}\sum_{p}\sum_{k} p_k\ell_k \exp\left(\frac{\eta}{\sqrt{3}}\sum_{i} p_i\ell_i\right)}{\Sigma \exp\left(\frac{\eta}{\sqrt{3}}\sum_{i} p_i\ell_i\right)} \qquad \text{(H-9)}$$

The first term in the numerator, upon evaluating, using Eq. H-8, becomes:

$$\frac{8}{\sqrt{3}\eta}\sum_{i}\ell_i \sinh\frac{\eta}{\sqrt{3}}\ell_i \prod_{k}{}' \cosh\frac{\eta}{\sqrt{3}}\ell_k + \frac{8}{3}\prod_{k}\cosh\frac{\eta}{\sqrt{3}}\ell_k$$

$$+\frac{16}{\sqrt{3}}\Sigma\cosh\frac{\eta}{\sqrt{3}}\ell_i \prod_{k}{}'\ell_k \sinh\frac{\eta}{\sqrt{3}}\ell_k$$

The second term in the numerator of Eq. H-9 was evaluated in Section E.1 for the calculation of the magnetic moment as a function of the variable η. It is seen to be:

$$-\frac{8}{\sqrt{3}\eta} \sum_i \ell_i \sinh \frac{\eta}{\sqrt{3}} \ell_i \prod_k{}' \cosh \frac{\eta}{\sqrt{3}} \ell_k$$

Thus Eq. H-9 simplifies to:

$$\sum_\theta f(\theta) \cos\theta = \frac{1}{3} + \frac{2}{3} \sum_i \sum_{\substack{j \\ i \neq j}} \ell_i \ell_j \tanh \frac{\eta}{\sqrt{3}} \ell_i \tanh \frac{\eta}{\sqrt{3}} \ell_j \quad \text{(H-10)}$$

Averaging over a nonoriented polycrystal gives:

$$\int \frac{d\Omega}{4\pi} \sum_\theta f(\theta) \cos^2\theta = \frac{1}{3} + \frac{2}{3} \int \frac{d\Omega}{4\pi} \sum_i \sum_j \ell_i \ell_j \tanh \frac{\eta}{\sqrt{3}} \ell_i \tanh \frac{\eta}{\sqrt{3}} \ell_j$$

$$= \frac{1}{3} + \frac{2}{3} R(\eta) \; . \quad \text{(H-11)}$$

The function $R(\eta)$ is defined by Eq. H-11. It was encountered by Brown[30] during his work on magnetostriction and has been evaluated by him. Substituting into the form for the susceptibilities,

$$\chi^r_{rp} = \chi^r_o \left[1 - R(\eta)\right] \quad \text{(H-12)}$$

$$\chi^r_{rt} = \chi^r_o \left[1 + \frac{R(\eta)}{2}\right] \quad \text{(H-13)}$$

where $M = M_s E(\eta)$. (See Section E.1)

As given by Brown for the low values of η,

$$R(\eta) = \frac{\eta^2}{15} - \frac{2\eta^4}{315} + \frac{\eta^6}{1701} - \frac{46\eta^8}{841,995} + \ldots . \quad \text{(H-14)}$$

and for large values of η,

$$R(\eta) = 0.6367 - \frac{4.712}{\eta^2} + \frac{15.12}{\eta^4} - \ldots \qquad \text{(H-15)}$$

Tabular values of the susceptibilities are given in Table 4 and are depicted graphically in Figs. 8 and 9.

Isotropic Orientation. As was the case when considering the susceptibilities for wall motion, the condition of isotropy is here considered not to mean zero effective anisotropy but rather passing to the limit of the number of easy directions in the crystal, each of which has a large enough effective anisotropy field to keep the material aligned in any easy direction in the presence of static fields.

Thus when an alternating field is applied, the effective rotational susceptibility is not infinite as would otherwise be expected, but is some finite value determined by the anisotropy field.

The quantity of interest here is the expression:

$$\sum_{\theta} f(\theta) \cos^2\theta = \frac{\int_0^{\pi} d\theta \sin\theta \cos^2\theta \, e^{\eta \cos\theta}}{\int_0^{\pi} d\theta \sin\theta \, e^{\eta \cos\theta}} \qquad \text{(H-16)}$$

Eq. H-16 can be directly integrated to:

$$\sum_{\theta} f(\theta) \cos^2\theta = 1 - \frac{2L(\eta)}{\eta} . \qquad \text{(H-17)}$$

where $L(\eta)$ is the Langevin function, as defined in Section E.1. The resulting susceptibility equations are:

$$\chi^r_{rp} = 3\chi^r_o \frac{L(\eta)}{\eta} \qquad \text{(H-18)}$$

$$\chi^r_{rt} = \frac{3}{2}\chi^r_o \left[1 - \frac{L(\eta)}{\eta}\right] \qquad \text{(H-19)}$$

where $M = M_s L(\eta)$.

Values of the susceptibilities are listed tabularly in Table 4 and are depicted in Figs. 8, 9 and 10.

To make Eqs. H-18 and H-19 look more like their counterparts for the assumed anisotropies, Eqs. H-3, H-4, H-12 and H-13, define a function $S(\eta)$ by the equations

$$\chi^r_{rp} = \chi^r_o \left[1 - S(\eta)\right] \tag{H-20}$$

$$\chi^r_{rt} = \chi^r_o \left[1 + \frac{S(\eta)}{2}\right] \tag{H-21}$$

Then the expansion for $S(\eta)$ for small values of η is given by:

$$S(\eta) = \frac{\eta^2}{15} - \frac{2\eta^4}{315} + \frac{\eta^6}{1571} - \frac{2\eta^8}{31,185} + \cdots\cdots \tag{H-22}$$

For large values of η:

$$S(\eta) = 1 - \frac{3}{\eta} + \frac{3}{\eta^2} \tag{H-23}$$

Note that Eqs. H-5, H-14 and H-22 are identical to the sixth power of η.

H.2 A Discussion of χ^r_o and of Q^r_o.

The initial susceptibility as computed from 1/3 the sum of χ_+ and χ_- is given by:

$$\chi^r_i = \frac{2\gamma\mu_o M_s}{3} \left[\frac{\gamma\mu_o H'(1 + \epsilon^2) + j\,\omega\,\epsilon}{(\gamma\mu_o H')^2\,(1 + \epsilon^2) - \omega^2 + j\,2\omega_1\,\epsilon(\gamma\mu_o H')}\right] \tag{H-24}$$

H' was defined in Section 3.2 and ϵ in Appendix B. At the low-frequency limit:

$$\chi^r_o = \frac{2M_s}{3H'} \tag{H-25}$$

The magnetic Q, or the ratio of the real to the imaginary part of the susceptibility is given by (from Eq. H-24):

$$Q_o^r = \frac{\gamma\mu_o H'}{\omega\epsilon}\left[\frac{\omega_1^2(1+\epsilon^2)^2 + \omega^2(\epsilon^2 - 1)}{\omega_1^2(1+\epsilon^2) + \omega^2}\right] \qquad \text{(H-26)}$$

The low-frequency limit of the Q is thus:

$$Q_o^r = \frac{\gamma\mu_o H'}{\omega\epsilon}\ (1+\epsilon^2) \qquad \text{(H-27)}$$

Upon comparing the expressions for the initial susceptibility and Q, both depend upon the total field H'. Thus they can be considered constant only so long as the applied field H_b is much smaller than the anisotropy field H_{an}. However the product given by:

$$\chi_o^r Q_o^r = \frac{2\gamma\mu_o M_s}{3\omega\epsilon}\ (1+\epsilon^2) \qquad \text{(H-28)}$$

does not contain H' and should obey the averaging equations of section H.1 to larger values of applied field than should the susceptibility alone. Deviations would occur through the field dependence of ϵ.

BIBLIOGRAPHY

1. Mayer, J. E. and Mayer, M. G., Statistical Mechanics, p. 342-352, John Wiley and Sons, New York, 1940.

2. Becker, R. and Döring, W., Ferromagnetismus, p. 12-21 and p. 83-98, Edwards Bros., Ann Arbor, 1943.

3. Bizett, H., Squire, C. F. and Tsai, B., "Le Point de Transition λ de la Susceptibilité Magnétique de Protoxyde de Manganése MnO," Compt. Rend. 207, 449-452 (1938).

4. Bozorth, R. M., Ferromagnetism, D. Van Nostrand, New York, 1951.

5. Slater, J. C., Quantum Theory of Matter, McGraw-Hill, New York, 1951.

6. Kittel, C., "Physical Theory of Ferromagnetic Domains," Rev. Mod. Phys. 21, 541-583 (1949).

7. Néel, L., "Propriétés Magnétiques des Ferrites; Ferrimagnétisme et Antiferromagnétisme," Ann. Physique 3, 137-198 (1948).

8. Döring, W., "Über die Trägheit der Wande Zwischen Weischen Bezirken," Z. fur Naturforschung 3a, 373-379 (1948).

9. Landau, L. and Lifshitz, E., "On the Theory of the Dispersion of Magnetic Permeability in Ferromagnetic Bodies," Physik. Zeits. Sowjetunion 8, 153-169 (1935).

10. Khinchin, A. I., Mathematical Foundations of Statistical Mechanics, p. 52-55, Dover Publications, New York, 1949.

11. Brown, W. F., Jr., "Physical Theory of Ferromagnetics Under Stress," Phys. Rev. 52, 325-334 (1937).

12. Brown, W. F., Jr., "Physical Theory of Ferromagnetics Under Stress," Part III: The Reversible Susceptibility," Phys. Rev. 54, 279-287 (1938).

13. Wangsness, R. K., "Susceptibility Tensor and the Faraday Effect in Ferrimagnetics," Phys. Rev. 95, 339-345 (1954).

14. Tebble, R. S., and Corner, W. D., "Investigations on the Reversible Susceptibility of Ferromagnetics," Proc. Phys. Soc. 63B, 1005-1016 (1950).

15. Reference 4, p. 577 and 821.

16. Kittel, C., "On the Theory of Ferromagnetic Resonance Absorption," Phys. Rev. 73, 155-161 (1948).

17. Becker, R., "La Dynamique de la Pario de Block et la Perméabilité en Haute Fréquence," J. Phys. Rad. 12, 332-338 (1951).

18. Kersten, M., "Über den Einfluss des Elastischen Spannungszustandes auf die Grösse der Anfangspermeabilität," Z. tech. Physik. 12, 665-669 (1931).

19. McIsaac, Paul R., "A Study of the Initial Permeability of Ferromagnetic Metals at High Frequencies," Thesis, University of Michigan, 1954.

20. Becker, R., "Elastische Spannungen und Magnetische Eigenschaften," Physik. Z. 33, 905-913 (1932).

21. Snoek, J. L., "Dispersion and Absorption in Magnetic Ferrites at Frequencies Above one Mc/s." Physica 14, 207-218 (1948).

22. Polder, D. and Smith, J., "Resonance Phenomena in Ferrites," Rev. Mod. Phys. 25, 89-90 (1953).

23. Rado, G. T., Wright, H. W. and Emerson, W. H., "Ferromagnetism at Very High Frequencies. III. Two Mechanisms of Dispersion in a Ferrite," Phys. Rev. 80, 273-280 (1950).

24. Rado, G. T., "Magnetic Spectra of Ferrites," Rev. Mod. Phys. 25, 81-89 (1953).

25. Birks, J. B., "The Properties of Ferromagnetic Compounds at Centimetre Wavelengths," Proc. Phys. Soc. (London) B63, 65-74 (1950).

26. von Hippel, A., Westphal, W. B. and Miles, P. A., "Dielectric Spectroscopy of Ferromagnetic Semiconductors," Tech. Report No. 97, Laboratory for Insulation Research, M.I.T., July, 1955.

27. Went, J. J. and Wijn, H. P. J., "The Magnetization Process in Ferrites," Phys. Rev. 82, 269-270 (1951).

28. Wijn, H. P. J., Gevers, M. and van der Burgt, C. M., "Note on the High Frequency Dispersion in Nickel-Zinc Ferrites," Rev. Mod. Phys. 25, 91-92 (1953).

29. Brown, W. F., Jr., "Theory of Reversible Magnetization in Ferromagnets," Phys. Rev. 55, 568-578 (1939).

30. Brown, W. F., Jr., "Domain Theory of Ferromagnetics Under Stress; Part II: Magnetostriction of Polycrystalline Material," Phys. Rev. 53, 482-491 (1938).

31. Park, David, "Magnetic Rotation Phenomena in a Polycrystalline Ferrite II," Phys. Rev. 98, 438-441 (1955).

32. Grimes, D. M. and Martin, D. W., "Reversible Susceptibility of Ferromagnetics," Phys. Rev. 96, 889-896 (1954).

33. Goldstein, H., Classical Mechanics, Addison-Wesley, Cambridge, 1950, p. 109.

34. Grimes, D. M., "Reversible Susceptibility Assuming Domain Rotation," Bull. Am. Phys. Soc. 1, 25 (1956).

35. Bozorth, R. M., Tilden, E. F., and Williams, A. J., "Anisotropy and Magnetostriction of Some Ferrites," Phys. Rev. 99, 1788-1798 (1955).

36. Gans, R., "Die Gleichung der Kurve Die Reversiblen Suszeptibilität," Phys. Z. 12, 1053-1054 (1911).

37. Goodenough, J. B., "Theory of Domain Creation and Coercive Force in Polycrystalline Ferromagnetics," Phys. Rev. 95, 917-932 (1954).

38. Elliott, J. F., Legvold, S. and Spedding, F. H., "Some Magnetic Properties of Gadolinium Metal," Phys. Rev. 91, 28-30 (1953).

39. Kittel, C., Introduction to Solid State Physics, John Wiley and Sons, New York, 1953.

40. Elliott, J. F., Legvold, S. and Spedding, F. H., "Some Magnetic Properties of Dy Metal," Phys. Rev. 94, 1143-1145 (1954).

DISTRIBUTION LIST

1 Copy	Director, Electronic Research Laboratory Stanford University Stanford, California Attn: Dean Fred Terman
1 Copy	Commanding General Army Electronic Proving Ground Fort Huachuca, Arizona Attn: Director, Electronic Warfare Department
1 Copy	Chief, Research and Development Division Department of the Army Washington 25, D. C. Attn: SIGEB
1 Copy	Chief, Plans and Operations Division Office of the Chief Signal Officer Washington 25, D. C. Attn: SIGEW
1 Copy	Countermeasures Laboratory Gilfillan Brothers, Inc. 1815 Venice Blvd. Los Angeles 6, California
1 Copy	Commanding Officer White Sands Signal Corps Agency White Sands Proving Ground Las Cruces, New Mexico Attn: SIGWS-CM
1 Copy	Commanding Officer Signal Corps Electronics Research Unit 9560th TSU Mountain View, California
1 Copy	Mr. Peter H. Haas Mine Fuze Division Diamond Ordnance Fuze Laboratories Washington 25, D. C.
1 Copy	Dr. J. K. Galt Bell Telephone Laboratories, Inc. Murray Hill, New Jersey
1 Copy	Dr. R. M. Bozorth Bell Telephone Laboratories, Inc. Murray Hill, New Jersey

1 Copy	Dr. G. T. Rado Naval Research Laboratory Washington 25, D. C.
60 Copies	Transportation Officer, SCEL Evans Signal Laboratory Building No. 42, Belmar, New Jersey FOR - SCEL Accountable Officer Inspect at Destination File No. 22824-PH-54-91(1701)
1 Copy	H. W. Welch, Jr. Engineering Research Institute University of Michigan Ann Arbor, Michigan
1 Copy	J. A. Boyd Engineering Research Institute University of Michigan Ann Arbor, Michigan
1 Copy	Document Room Willow Run Laboratories University of Michigan Willow Run, Michigan
11 Copies	Electronic Defense Group Project File University of Michigan Ann Arbor, Michigan
1 Copy	Engineering Research Institute Project File University of Michigan Ann Arbor, Michigan